Telomere Damage Induces Internal Loops that Generate Telomeric Circles

Thesis

IFOM / The Open University PhD Programme in Fundamentals of Cancer Biology

TELOMERE DAMAGE INDUCES INTERNAL LOOPS THAT GENERATE TELOMERIC CIRCLES

Giulia Mazzucco

OU personal identifier: F5817854

Director of Studies: Ylli Doksani

External Supervisor: Simon Boulton

December 2020

Table of contents

Abstract..... 4

Introduction..... 6

1. **Telomeres and the end protection..... 7**

1.1 Mammalian DNA damage response and repair pathways..... 7

1.1.1 ATR pathway..... 8

1.1.2 ATM pathway..... 10

1.1.3 DNA Double Strand Breaks (DSBs) DNA repair pathways..... 12

1.2 Telomere structure..... 17

1.3 Shelterin and chromosome end-protection functions..... 19

1.4 Consequences of telomere dysfunction in senescence, ageing and tumorigenesis..... 22

1.4.1 Telomere erosion due to the end replication problem: dysfunctional telomeres contribution to ageing and tumor suppression..... 25

1.4.2 Dysfunctional telomeres contribution in genome instability and tumorigenesis..... 26

1.4.3 DNA damage and telomere replication can cause rapid telomere loss..... 29

2. Extrachromosomal telomeric DNA..... 32

2.1 Alternative Lengthening of Telomeres (ALT)..... 40

2.1.1 C-circles..... 46

2.2 Method for extrachromosomal telomeric circles detection..... 46

Results..... 53

A two-step procedure for the purification of mammalian telomeric DNA..... 54

Electron microscopy analysis of telomere-enriched samples..... 60

Intramolecular loops (i-loops) enriched at telomeric DNA..... 64

I-loops represent the most frequent structures detected at ALT telomeres..... 73

I-loops formation is induced by single-strand damage at telomeric DNA..... 79

The formation of i-loops requires branch migration..... 86

I-loops are a substrate for the generation of telomeric circles..... 88

Discussion and Future plans..... 93

Material and methods..... 108

References..... 120

ABSTRACT

Telomeres are essential in preventing the recognition of chromosome ends by the DNA damage response (DDR), thereby permitting the maintenance of linear chromosomes. Extrachromosomal telomeric circles are important players in telomere maintenance, but little is known about their origin. We developed a new procedure for the purification of mammalian telomeric repeats in order to study telomere structures by Electron Microscopy (EM). Using this approach, we detected the expected telomeric features (i.e. t-loops) but we also found accumulation of internal loops (i-loops) at telomeric repeats that occur in the proximity of nicks and single-stranded DNA gaps. We showed that i-loops are induced by single-stranded damage at normal telomeres and represent the majority of the telomeric structures that accumulate in ALT (Alternative Lengthening of Telomeres) tumor cells, which are characterized by DNA damage accumulation at telomeric repeats. We also demonstrated that telomeric molecules containing i-loops can become a source of extrachromosomal telomeric circles. We propose that i-loops can form through strand exchange events at sites of damage, a process which is facilitated by the high sequence homology at telomeric repeats. This leads to the formation of intramolecular Holliday junctions that can be resolved to generate circular molecules made of telomeric DNA and resulting in a net loss of telomeric repeats. We propose that damage-induced i-loops are common intermediates in telomere maintenance that link telomere damage to the accumulation of extrachromosomal telomeric circles and to telomere erosion.

INTRODUCTION

1.TELOMERES AND CHROMOSOMES END PROTECTION

Telomeres are the terminal part of linear chromosomes and are essential for their maintenance. The concept of telomeres came from cytological data showing that natural chromosome ends are resistant to fusion reactions that otherwise occur at DNA ends generated by double-strand DNA breaks (DSB) (McClintock 1941). Linear chromosomes, in fact, lead to an important biological problem: their ends must be distinguished from internal chromosome breaks to avoid aberrant activation of DNA damage signaling and consequent DNA repair processes that would result in arrest of proliferation and chromosome fusions. Chromosomes alterations could lead to problems in chromosome segregation in the next mitosis, such as breakages that requires further repair. Repeated cycles of these events result in massive genome instability and eventually cell death. Therefore, telomeres have evolved to ensure that the natural ends of chromosomes are not mistaken for sites of DNA damage.

1.1 Mammalian DNA damage response and repair pathways

The major regulators of the mammalian DNA damage response are ataxia telangiectasia mutated (ATM) and ATM and Rad3-related (ATR) kinases, two serine /threonine kinases members of the phosphatidylinositol 3-kinase-like family of protein kinase (PIKKs) family. They are activated depending on the type of structures that are present on the site of damage, while ATM responds to DNA ends generated at DSBs, ATR pathway is activated in the presence of extended single-stranded DNA tracts that can form during replication stress or after exonucleolytic resection of 5'-ends of DSBs. Following recognition of damaged sites ATM and ATR kinases trigger a phosphorylation cascade starting with Chk2 and Chk1, respectively, culminating in activation of the tumor suppressor protein p53 and thus cell-cycle checkpoint activation (Figure 1,2) (Sanchez et al. 1997; Matsuoka, Huang,

and Elledge 1998). DDR activation can lead to transient cell-cycle arrest to allow for repair of the damage, or in the case of more excessive or irreparable damage, a permanent cell cycle arrest (cellular senescence) and programmed cell death (apoptosis) (Tibbetts et al. 1999; Shieh et al. 2000; Vousden and Lane 2007).

1.1.1 ATR pathway

ATR signaling starts with the binding of the Replication Protein A (RPA) to the exposed 3'-single-stranded DNA of the lesion (Zou and Elledge 2003) (Figure 1). The ATR-interacting protein (ATRIP) recruits ATR, forming heterodimers that directly bind the RPA/ssDNA and promote ATR recruitment to the damaged site (Cortez et al. 2001; Zou and Elledge 2003). However, damage-site localization is not sufficient for ATR activation but it also requires interaction with TOPB1 (DNA topoisomerase II binding protein 1) which is recruited by the 9-1-1 (Rad9-Rad1-Hus1) complex (Bermudez et al. 2003; Kumagai et al. 2006; Delacroix et al. 2007). Once activated at the site of the damage, ATR begins a phosphorylation cascade which involves phosphorylation of Chk1 and other downstream targets, leading to a slowdown of replication rate and limiting origin firing (Matsuoka et al. 2007; Tercero and Diffley 2001).

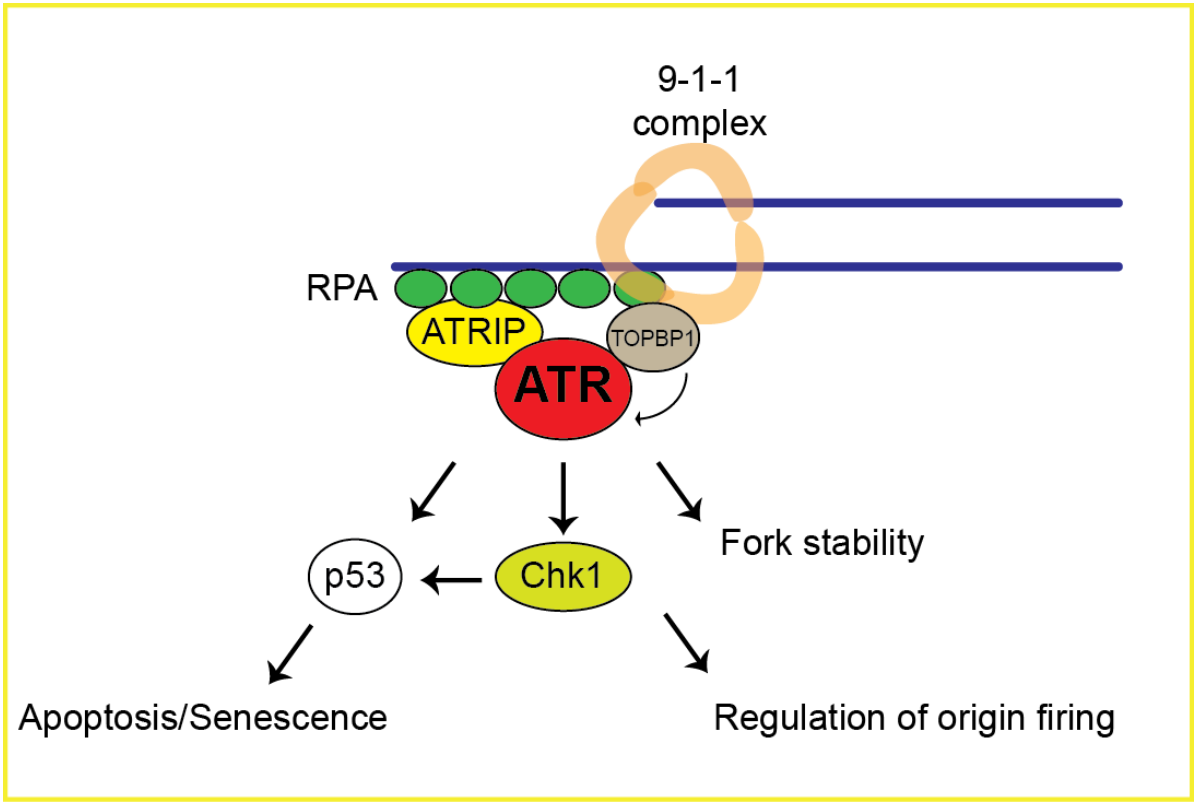

Figure 1. Simplified mammalian ATR pathway

The ATR pathway starts with the binding of RPA proteins at the exposed ssDNA leading to the recruitment of ATR in complex with ATRIP. But ATR activation also requires its interaction with TOPBP1, which is recruited at the lesion via the 9-1-1 complex. At the level of stalled forks, ATR can prevent their collapse. Once activated, ATR starts a phosphorylation cascade that involves Chk1 and leads to cell cycle arrest and a regulation of origin firing. One of the substrates of the ATR signaling is also p53 able to promote the apoptotic or senescence pathways.

1.1.2 ATM pathway

DSBs occur when both strands of the DNA molecule are broken in close proximity. In mammals, the MRN (Mre11-Rad50-Nbs1) complex is the major DSBs sensor in the ATM response. The MRN complex performs multiple functions the site of the damage, since it tethers the broken DNA ends, it is essential for the recruitment and the activation of ATM at the site of the lesion and it performs nucleolytic processing of DNA ends required for DNA repair (de Jager et al. 2001; Hopfner et al. 2002; Seifert et al. 2016; Williams, Lees-Miller, and Tainer 2010; Uziel et al. 2003; Lee and Paull 2005; Stewart et al. 1999). One of the earliest consequences of ATM activation is the phosphorylation of the histone-variant H2AX at the DSB site generating γH2AX (p-Ser139) which acts as signal for DNA damage signaling (Figure 2). γH2AX is then bound by the Mediator of DNA damage Checkpoint 1 (MDC1) which increases the local ATM activation and H2AX phosphorylation. Through a positive feedback loop, involving MDC1 and other signaling proteins the DNA damage signal is rapidly spread in cis to the chromatin surrounding the DSB (Burma et al. 2001; Bonner et al. 2008; Rogakou et al. 1998). The ATM-dependent phosphorylation cascade leads to activation of p53 which plays a central role in mediating the final outcome: cell-cycle arrest and DNA repair, apoptosis or senescence (Helton and Chen 2007).

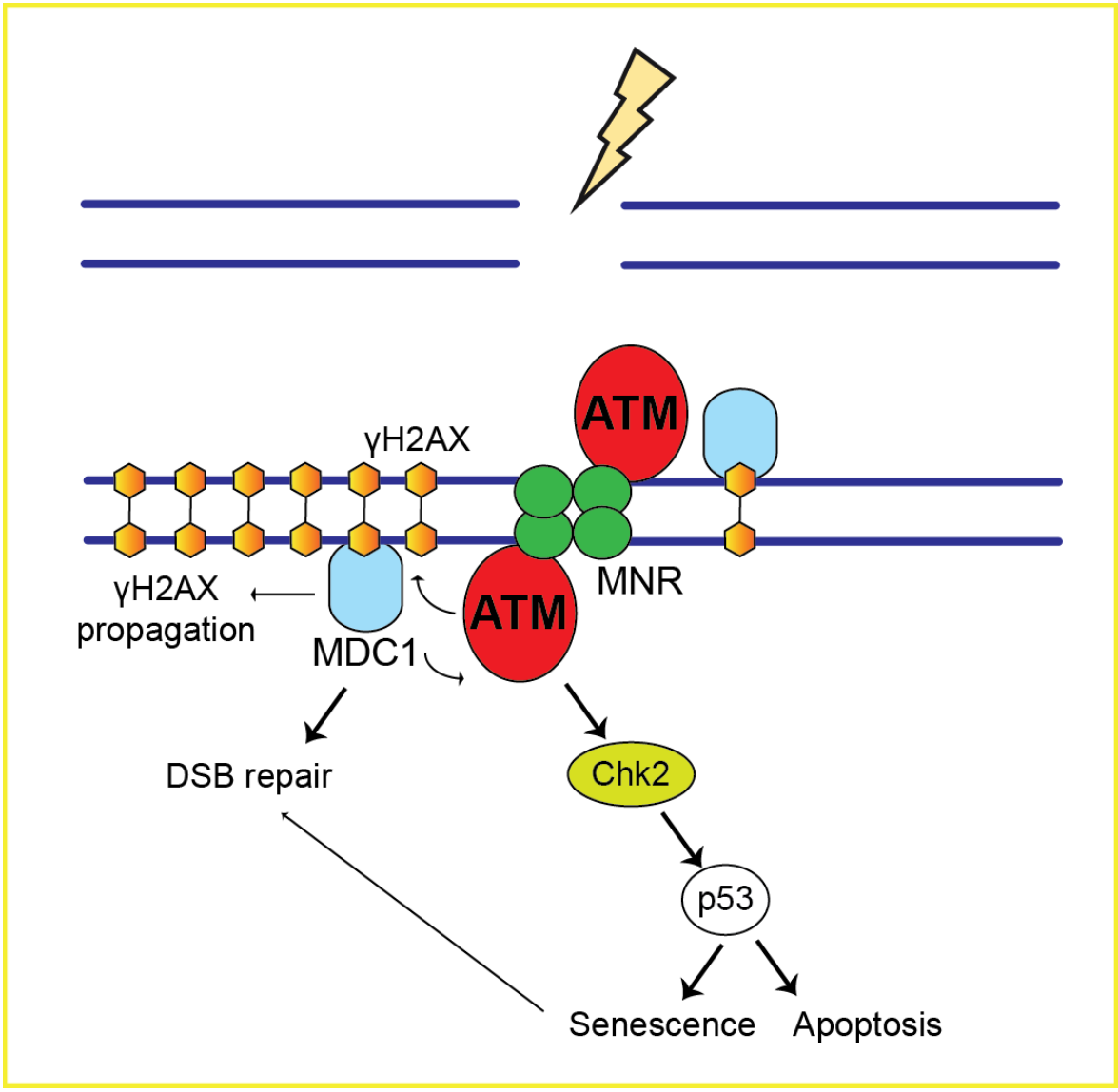

Figure 2. Simplified mammalian ATM pathway

Double stranded breaks (DSB) are sensed and bound by the MRN complex, which recruits and activates ATM at the site of damage. ATM phosphorylates the histone H2AX producing γH2AX that is recognized by MDC1 that further stimulates ATM activation leading to γH2AX signal propagation. ATM phosphorylates Chk2 leading to p53 activation which mediates either cell cycle arrest, favoring DNA repair, or apoptosis.

1.1.3 DNA Double Strand Breaks (DSBs) DNA repair pathways

Mammalian cells have two main pathways to repair DSBs: Non-homologous end-joining (NHEJ) and Homologous recombination (HR). NHEJ includes two different mechanisms, the classical (c-NHEJ) that occurs throughout the cell cycle and the alternative (alt-NHEJ) that operates in S/G2. (Figure 3) (Rothkamm et al. 2003). The classical NHEJ starts with the binding of the Ku70/80 heterodimer to the broken DNA ends that works as scaffold for the recruitment of the other factors including DNA Ligase IV which ligates the DNA termini (Deriano and Roth 2013). Although c-NHEJ ligation cans result in small deletions or insertions such changes do not significantly alter global genome integrity and most repair events occur accurately and free of such mutations (Chiruvella, Liang, and Wilson 2013). Alt-NHEJ was more recently discovered and involves recognition of DSBs by poly adenosine diphosphate ribose polymerase 1 (PARP1). Differently from the c-NHEJ, a-NHEJ results in microhomology-mediated ligation rather than blunt-end ligation. In a-NHEJ microhomology is generated by MRN- and CtIP-dependent end resection and ligation seems to occur through the action of DNA ligase III, but there is evidence that DNA ligase I may also have a role (Lee-Theilen et al. 2011; Rass et al. 2009; Xie, Kwok, and Scully 2009; Simsek et al. 2011; Simsek and Jasin 2010). A-NHEJ repair is generally less accurate than c-NHEJ resulting in insertions, deletion or chromosome translocations (Frit et al. 2014) (Frit et al., 2014. DNA Repair). In S/G2 phase Ku70/80 inhibits alt-NHEJ by competing with PARP1 for DSB binding (Paddock et al. 2011). Both NHEJ pathways can occur at dysfunctional telomeres that are no longer able to protect chromosome ends from the DDR (van Steensel, Smogorzewska, and de Lange 1998; Sfeir and de Lange 2012). Inappropriate repair of chromosome ends by NHEJ results in fused dicentric chromosomes that are unstable in mitosis and can initiate breakage-fusion-bridge (BFB) cycles thereby leading to genomic instability (described below) (Gisselsson et al. 2000).

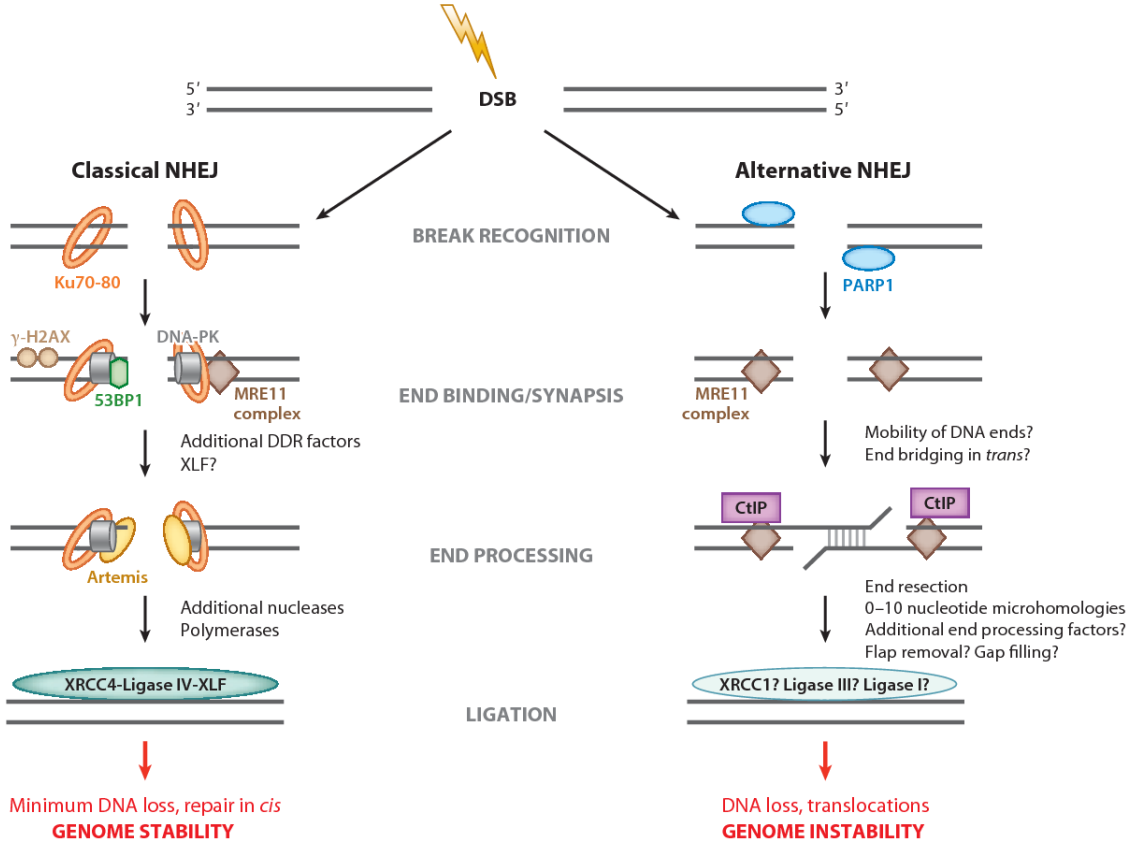

Figure 3. Classical and alternative nonhomologous end-joining (NHEJ) pathway

Left, classical NHEJ: Ku70/80 binds to the broken ends and recruits the other factors like DNA PK which allows localization of factors necessary for end-ligation at the site of the damage (Neal and Meek 2011). ATM signaling activates 53BP1 which protects end from nucleases promoting c-NHEJ (Bothmer et al. 2011; Bothmer et al. 2010). If required, additional enzymes, such as Artemis, intervene to prepare DNA ends for ligation. Last ligation step involves DNA Ligase IV that is stabilized and assisted by XRCC4 and XLF (Grawunder et al. 1997; Riballo et al. 2009)

Right: alternative NHEJ: PARP1 is responsible for break recognition. The Mre11 complex and CtIP process DNA ends, in order to create stretches of 2 to 20 nucleotides and allowing microhomology-mediated end joining.

From (Deriano and Roth 2013).

Homologous recombination (HR) pathways allow for error-free repair of DSBs since they employ a homologous template to repair. Sister chromatid are the most common donor sequence in HR, although the homologue chromosome can also be used as homology donors (Johnson and Jasin 2001). Briefly, the first step during HR is resection of the 5'-ends of DSBs, revealing a 3' single-stranded protruding end which is then coated by RPA. Rad51 then displaces RPA, to form a nucleoprotein filament that conducts homology search. Rad51-coated single-stranded DNA promotes strand invasion into the homologous donor region leading to the generation of heteroduplex DNA and a displacement loop (D-loop). The 3'-end from the broken filament is then used then to prime DNA synthesis which is templated by the donor duplex (Figure 4 A). The repair can proceed in three different ways. In one case, the second DSB end can be captured to stabilize the D-loop generating a double Holliday Junction (dHJ) (Figure 4 B) (Szostak et al. 1983). Holliday Junctions can be resolved in two ways leading to crossover or non-crossover products, or dissolved generating only non-crossover molecules. Resolution of HJs involves SLX1 and SLX4 nucleases that interact with MUS81 and EME1, forming the SLX-MUS complex, and the nuclease GEN1. These HJ dissolution involves the Bloom's syndrome helicase (BLM) and topoisomerase III alpha (TOP3α) that together with RecQ-mediated genome instability protein 1 (RMI1) and RMI2 form the BTR complex. (Andersen et al. 2009; Fekairi et al. 2009; Munoz et al. 2009; Svendsen et al. 2009; Castor et al. 2013; Garner et al. 2013; Wyatt et al. 2013; West et al. 2015; Ip et al. 2008; Rass et al. 2010). In synthesis-dependent strand-annealing (SDSA) (Figure 4 C), the invading strand from one end of the DSB is dissociated from the D-loop and anneals with the other side (complementary strand) of the DSB (Nassif et al. 1994). In the break-induced replication (BIR) (Figure 4 D) the invading strand is extended indefinitely to the end of the doner chromosome, resulting in a migrating D-loop, resembling a one-sided

replication fork (Malkova, Ivanov, and Haber 1996). All these mechanisms have to be suppressed at natural chromosome ends in order to preserve genome stability.

Differently from cNHEJ that occurs throughout the cell cycle, the HR pathway is active only in S/G2 phases of the cell cycle. Work in yeast has shown that resection of 5' ends and DSB repair by HR requires CDK1 activity (Ira et al. 2004). The same mechanism was later shown to work also in human cells (Jazayeri et al. 2006). It was later shown that CDK1/2, phosphorylates several key targets in the DSB response pathway that determine the repair pathway choice, including Nbs1 and Brca2 (Jazayeri et al. 2006). Similarly to DSBs, repair of deprotected telomeres is dependent on the cell cycle stage. Taz1 deletion was associated with massive telomere fusions when cells were arrested in G1 by Nitrogen starvation (Ferreira and Cooper 2001). Experiments with a TRF2 temperature-sensitive mutant showed that NHEJ-dependent telomere fusions occurred primarily in the G1 phase of the cell cycle. cNHEJ-mediated fusions in S/G2 were increased in roscovitine-treated cells, suggesting a Cdk1-dependent mechanism that counteracts cNHEJ in S/G2 ((Konishi and de Lange 2008).

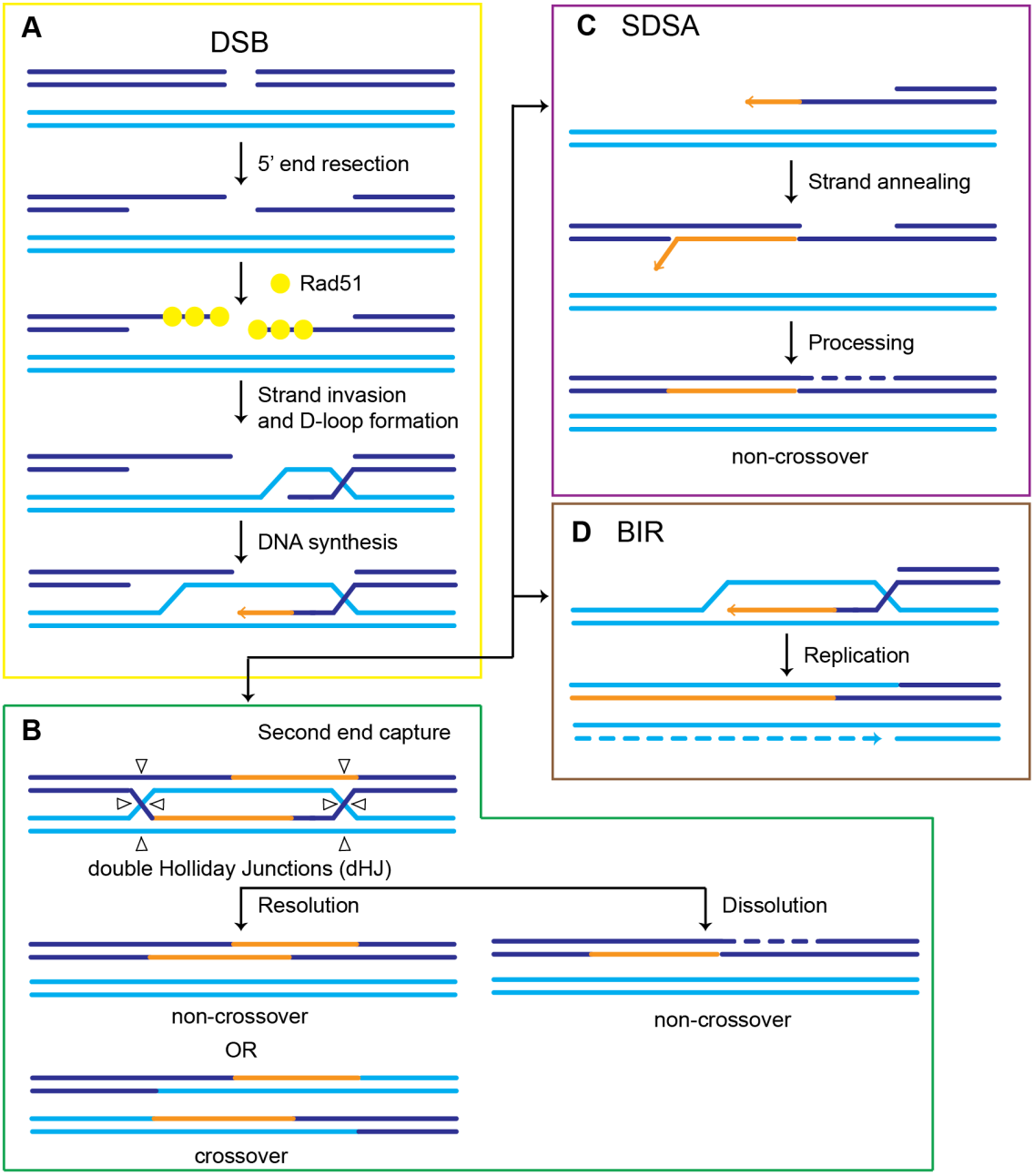

Figure 4. Homologous recombination pathways

Double-strand breaks ends undergo resection to generate 3'-overhang that are coated by Rad51 molecules and through strand invasion at homologous regions, form D-loop. DNA synthesis can occur using the overhang as primer (**A**). The second DSB end can be engaged to form double Holliday junctions (**B**) that can be resolved or dissolved, producing crossover or non-crossover products. The nascent strand could instead be displaced from the D-loop and, annealing with the other DSB protruding end, DNA synthesis can fill the gap (**C**). Another possibility is that, the second end is not available, therefore the 3' overhang invade a replication fork allowing the replication until the end of the molecule (**D**).

1.2 Telomere structure

The telomeric DNA of most eukaryotes is made of arrays of short tandem repeats that extends for several kilobases as double-stranded (ds) DNA ending with a 3'-G-rich single-stranded overhang (Figure 5 A). Like the majority of the eukaryotes, the telomeric motif in mammals is TTAGGG and length varies among different species, for examples human telomeres can range from 10 to 15 kilobases (kb) whereas mouse telomeres can reach from 20 to 50 kb (de Lange et al. 1990; Kipling and Cooke 1990). The terminal 3'-overhang is made of about 50-500 nucleotides and the last base is variable, appearing almost random in telomerase-negative cells (Sfeir et al. 2005). The 5'-end of human telomeres instead is characterized by a conserved sequence ATC-5', consistent with the active and regulated process of resection of the C-rich strand for the formation of the overhang after telomere replication. In order to to protect the end of the telomere the 3'-overhang is sequestered in a secondary structure called the t-loop (Figure 5 B). The t-loop is a telomeric structure formed by the invasion of the 3'-overhang into upstream double-stranded telomeric DNA, displacing the G-rich strand and pairing with the C-rich strand, thereby forming a displacement loop (D-loop) and resulting in a lariat-like structure (Griffith et al. 1999; Doksani and de Lange 2014) . It has been proposed that t-loops provide an architectural solution to the end protection problem, by sequestering the ends of linear chromosomes, thus preventing their recognition by the DNA damage response. The de Lange and Griffith labs reported the first images of t-loops in electron microscopy from human and mouse telomeres, but t-loops have been observed also in trypanosomes, ciliates, plants, C. elegans and in Kluyveromyces lactis (yeast) (Griffith et al. 1999; Munoz-Jordan et al. 2001; Murti and Prescott 1999; Cesare et al. 2003; Raices et al. 2008; Cesare et al. 2008). The length of the t-loop contour seemed to vary randomly with telomere length, suggesting that the position of the 3' overhang invasion is variable (Griffith et al.

1999; de Lange 2018). Actually, the size of the loop does not seem relevant for its function and actually varies between telomeres of the same cells as well as among organisms. T-loops can range from 0.3 kb in tryapanosomes to 30 kb in mice and 50 kb in peas (Munoz-Jordan et al. 2001; Griffith et al. 1999; Cesare et al. 2003). Although, t-loops have been observed in all cell cycles stages, the fraction of telomeres are organized in this structure is not yet known (Timashev and De Lange 2020).

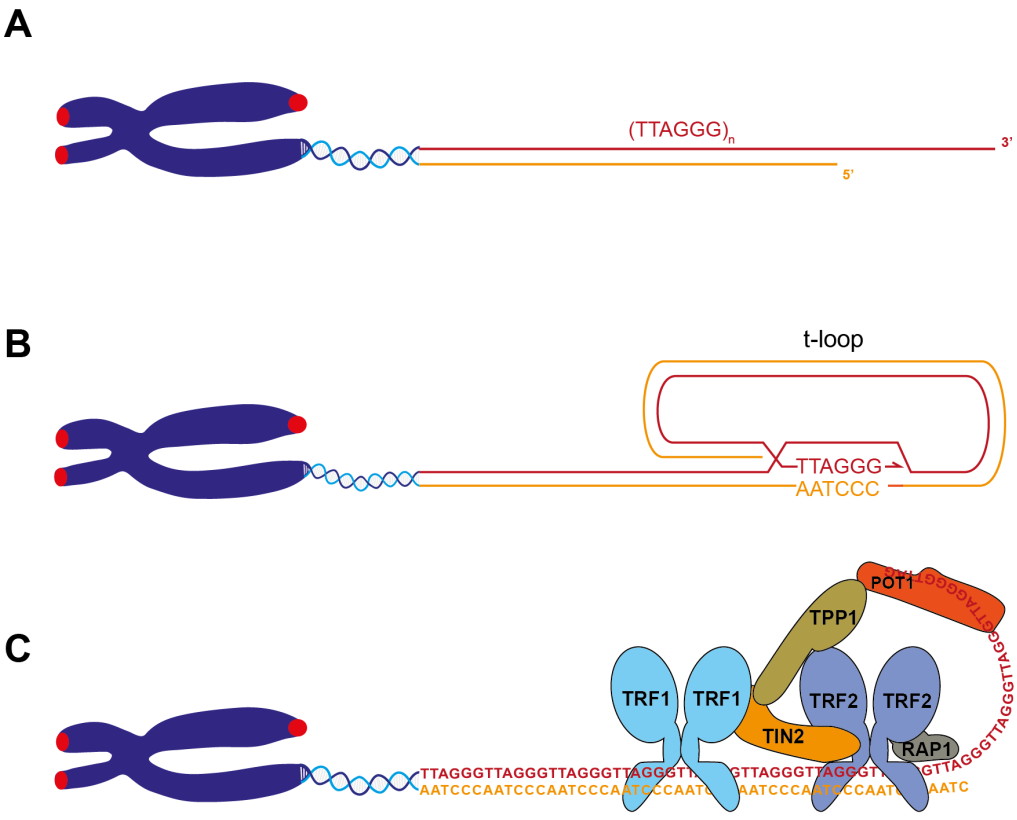

Figure 5. Telomeric structures and shelterin complex

A. Mammalian telomeres consists of long array of double-stranded TTAGGG repeats that terminates with a 3' single-stranded G-rich overhang.

B. Illustration of telomere in the t-loop configuration: the 3' telomeric overhang invade the double stranded tract, displacing the G-rich filament and pairing with the complementary C-rich strand.

C. Shelterin complex load on telomeric DNA: simplified illustration. Many complexes bind throughout telomeric DNA.

Modified from (Doksani 2019)

1.3 Shelterin and chromosome end-protection functions

Telomere's function is mediated by a six-protein complex named shelterin, that specifically recognizes and binds to telomeric repeats (de Lange 2005a) (Figure 5 C), and is essential in telomere metabolism. The first component of the shelterin complex to be identified was the Telomere Repeat Binding Factor 1 (TRF1), isolated in vitro due to its specific binding to the double-stranded TTAGGG repeats (Zhong et al. 1992; Chong et al. 1995). Telomere Repeat Binding Factor 2 (TRF2) was identified as paralog of TRF1s using databases and through two-hybrid screens of TRF1 and TRF2. TRF2 Interacting Nuclear protein 2 (TIN2) and Rap1 were also identified, respectively (Bilaud et al. 1997; Broccoli et al. 1997; Kim, Kaminker, and Campisi 1999; Li, Oestreich, and de Lange 2000). POT1 (Protection Of Telomeres 1) was identified while looking for sequence homology among proteins binding chromosome ends in unicellular eukaryotes (Baumann and Cech 2001). In rodents, the POT1 gene has undergone duplication leading to two closely related proteins, POT1a and POT1b (Hockemeyer et al. 2005; Wu et al. 2006). The interactions among different components of the shelterin complex have been established with co-immunoprecipitation, yeast two-hybrid analysis and structural studies (de Lange 2018). TRF1 and TRF2 bind to double-stranded telomeric repeats as homodimers but do not interact directly with each other (Bianchi et al. 1999; Broccoli et al. 1997; Fairall et al. 2001). TRF1 and TRF2 bind to TIN2 which interacts with TPP1 which in turn binds to POT1 that localizes at telomere overhang since specifically binds single-stranded telomeric repeats. Thus, TIN2 provides a bridge between shelterin, which binds double-stranded (TRF1 and TRF2) and single-stranded (POT1) telomeric DNA. Then, Rap1 interacts with TRF2 and depends on it for telomere localization (Li, Oestreich, and de Lange 2000). Isolating the shelterin components from nuclear cell extracts revealed that they can form a stable complex also in absence of telomeric DNA (Liu et al. 2004) (Ye et al. 2004). Each shelterin

component explicates different functions in telomere metabolism or in chromosome end protection. In the fission yeast *S. pombe* the deletion of TAZ1 (the orthologue of TRF1 and TRF2), leads to high frequency of telomere fork stalling and, due to the absence of telomerase, to massive loss of telomeric repeats (Miller, Rog, and Cooper 2006). Also in mammals, one essential role of the shelterin complex is to ensure efficient telomere replication. Indeed, TRF1 is essential for telomere replication in mouse and human cells as DNA combing analysis of TRF1-deleted cells show impairment in telomere replication with frequent fork stalling. This phenotype is also accompanied by activation of ATR signaling and accumulation of telomere abnormalities observed on metaphase spreads, such as fragility and sister telomere association (Sfeir et al. 2009; Martinez et al. 2009; Iwano et al. 2004).

TRF2 is essential for t-loop formation and its deletion leads to t-loop loss (Doksani et al. 2013). The purified protein is able to induce the invasion of the telomeric 3'-overhang into internal repeats leading to t-loop conformation at telomeric DNA (Griffith et al. 1999; Stansel, de Lange, and Griffith 2001; Amiard et al. 2007). Through the formation of the t-loops, chromosome ends are sequestered avoiding their recognition by the DNA damage sensor MRN complex, therefore TRF2 inhibits the activation of the ATM signaling and consequent c-NHEJ (Karlseder et al. 1999; van Steensel, Smogorzewska, and de Lange 1998; Celli and de Lange 2005; Denchi and de Lange 2007; Smogorzewska et al. 2002). In fact, TRF2 deletion results in ATM activation and massive chromosome fusions, a phenotype that is not observed in absence of other shelterin components (van Steensel, Smogorzewska, and de Lange 1998).

While TRF2-mediated t-loop formation sequesters the chromosome ends and prevents activation of ATM signaling, the shelterin component POT1 covers the single stranded telomeric overhang (or the displaced G-strand at the base of the t-loop) preventing loading of RPA and therefore activation of the ATR pathway

(Hockemeyer et al. 2005; Hockemeyer et al. 2006; Denchi and de Lange 2007). Moreover, it has been shown that POT1 plays an essential role in the regulation of telomere elongation and of the generation of the 3'-overhang (Hockemeyer et al. 2006; Wu et al. 2006). In mouse cells, the 3' overhang is generated by two exonucleases, Apollo and exonuclease 1 (EXO1) (Figure 6 a) (Dai et al. 2010; Wu, Takai, and de Lange 2012; Wang et al. 2012; Wu et al. 2010). An excessive resection of chromosome's ends during the generation of the 3' overhang could create a substrate for DNA damage response affecting chromosome end protection. For this reason, this process is carefully regulated by the shelterin components, TRF2 recruits Apollo, which activity is regulated than by POT1, that also recruits the CST complex to fill in long overhang generated by the exonucleases.

Shelterin components are abundant and constitutively expressed in order to cover all telomere length, likely reflecting their essential function in protecting chromosome ends (Takai et al. 2010). Apart from its direct roles in telomere maintenance, the shelterin complex recruits many accessory factors at telomeres, most of which are involved in cellular processes like the DNA repair, as for the Ku70/80, Apollo, Mre11 complex or in DNA replication (RTEL1, BLM, ORC, RecQ) (Hsu et al. 1999; Hsu et al. 2000; Lenain et al. 2006; van Overbeek and de Lange 2006; Zhu et al. 2000; Sarek et al. 2015; Zimmermann et al. 2014; Opresko et al. 2002; Deng et al. 2007).

1.4 Consequences of telomere shortening

Telomeric repeats are lost at each cell division resulting in a progressive loss of telomeric material until a critically short length is reached. Critically short telomeres lose their ability to protect chromosome ends from the DNA damage response, and are thus classified as dysfunctional. Persistent DNA damage response at dysfunctional telomeres ultimately leads cells into a permanent cell cycle arrest also known as cellular senescence (d'Adda di Fagagna et al. 2003; Takai, Smogorzewska, and de Lange 2003; Herbig et al. 2004; Rodier et al. 2009; Rodier et al. 2011) (Figure 6 B). Telomere erosion is due to the inability of the DNA replication machinery to fully replicate the lagging strand template, also known as the end replication problem (Harley, Futcher, and Greider 1990) (Figure 6 A). The semi-conservative DNA replication involves two different mechanism of DNA synthesis leading and lagging strand. In leading-strand synthesis, the polymerase moves in the same direction as the replication fork allowing a continuous strand replication until the end of the chromosome. In lagging-strand synthesis, DNA is synthesized in the opposite direction to the replication fork and requires RNA primers to initiate DNA synthesis: this results in DNA fragments, the Okazaki fragments, that are later ligated together once the RNA primers have been removed. This means that, at linear chromosomes, DNA synthesis of the lagging strand, will be incomplete due to the presence of an RNA primer for the last Okazaki fragment, thus resulting in loss of the terminal sequences in the daughter cell (Huffman et al. 2000). The rate of telomere erosion is also influenced by the 5'-end resection required for the generation of the 3'-overhang as well as by telomere damage (Huffman et al. 2000; von Zglinicki 2002).

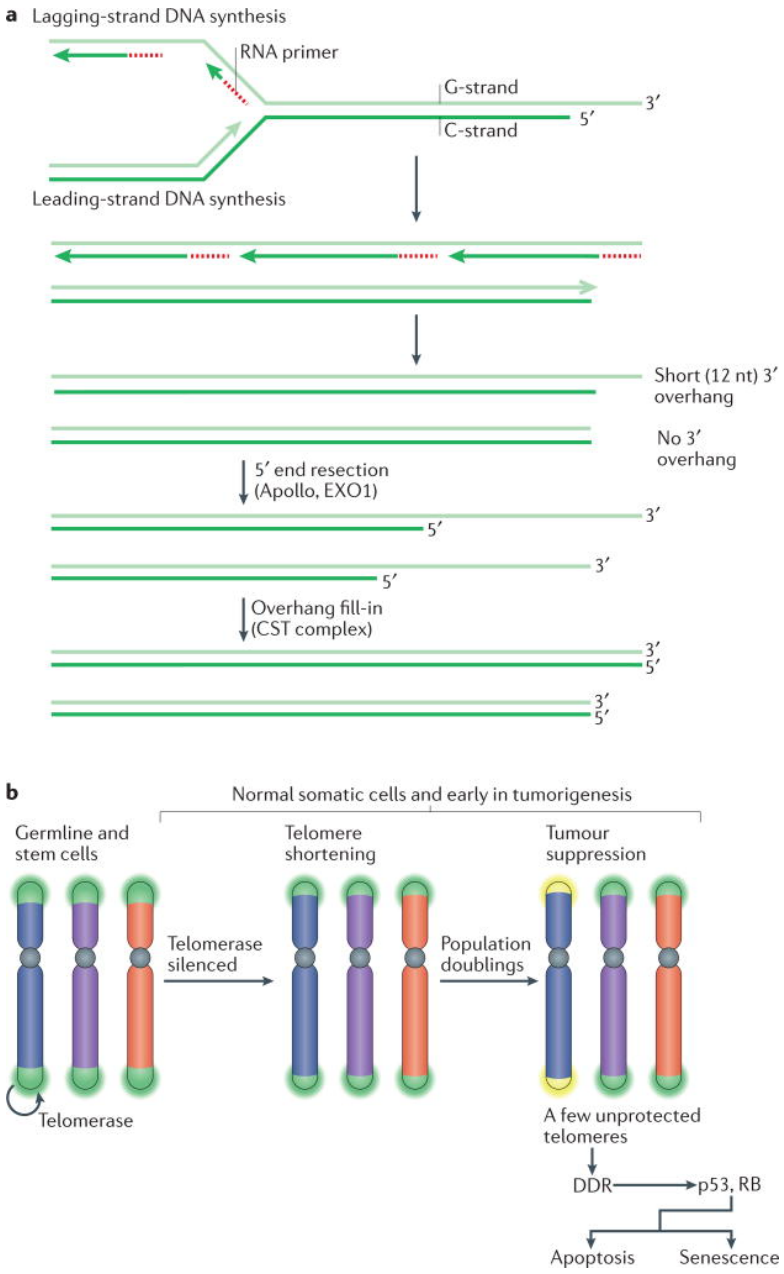

Figure 6. Telomere shortening as proliferative barrier

a. End-replication problem: telomere shortening due to the inability of the DNA replication machinery to fully replicate the lagging strand (RNA primer degradation creates a gap). Moreover, the shortening is enhanced by the 5' end resection required for the generation of the 3' G-rich overhang. In this process are involved Apollo nuclease and Exo1. The last create an excessive overhang that is filled out by the CST complex.

b. In germline and stem cells telomere shortening is counteracted by telomerase activity that is instead downregulated in somatic cells. As a result, telomeres undergo gradual shortening as described in (a). When telomeres become too short to ensure end protection, they are recognized by the DNA damage response (DDR) that induces senescence or apoptosis. Telomere-induced senescence is a tumor suppression pathway. If cell escape this proliferative barrier, telomere-mediated genome instability promotes tumorigenesis. *Image from (Maciejowski and de Lange 2017)*

Telomere erosion is involved in tissue ageing and ageing-related disease but also in tumorigenesis (Harley, Futcher, and Greider 1990; Blasco et al. 1997; Rudolph et al. 1999). The first experimental evidences that telomere shortening affects lifespan, derived from studies in mice deficient for telomerase, the reverse transcriptase that in germ lines and stem cells maintain telomere length by adding telomeric DNA repeats at the end of the chromosomes. These telomerase-deficient mice showed premature ageing phenotypes specifically in tissue with high cellular turnover potential (Blasco et al. 1997; Choudhury et al. 2007; Rudolph et al. 1999). Important information about telomere attrition derived from the study of the length distribution of individual telomeres in telomerase-negative fibroblast using a PCR-based approach, called single telomere length analysis (STELA), that allows for the accurate measurement of telomere length from individual chromosomes (Baird et al. 2003). Using this system, it was possible to distinguish between two different events: a gradual shortening of all telomeres that progress together with cell divisions and rapid changes that occur stochastically at different telomeres.

Intra-clonal and inter-clonal differences in the proliferative potential were observed in human fibroblast and yeast and could be explain with the stochastic and sudden loss of telomeric repeats at chromosome ends of some cells that consequently enter in senescence (Smith and Whitney 1980; Lundblad and Szostak 1989). It has been shown that in mammalian cells short telomeres trigger senescence and, that in telomerase-negative *S. cerevisiae* cells the generation of a single critically-short telomere accelerates senescence outcome (Hemann et al. 2001; Armanios et al. 2009; Abdallah et al. 2009). Together these evidences lead to the conclusion that the cell fate is dictated by the length of the shortest telomeres rather than the mean telomere length (Hemann et al. 2001).

1.4.1 Telomere erosion due to the end replication problem: dysfunctional telomeres contribution to ageing and tumor suppression.

Due to the end replication problem, in human cells telomeres shorten 50 to 100 bp per population doubling (Huffman et al. 2000). In germ line and stem cells, this gradual shortening is counteracted by telomerase reverse transcriptase which adds GGTTAG repeats to the 3' chromosome end. In human somatic cells, telomerase expression is downregulated throughout the development, therefore, somatic cells undergo a limited number of cell divisions until telomeres become critically short and lose their protective functions. Dysfunctional telomeres activate the DNA damage response which arrests cell proliferation, inducing senescence (Figure 6 B). This proliferative barrier could contribute to organismal ageing by limiting tissue regeneration. On the same time, telomere loss has also another important role as a tumor suppression mechanism avoid that cells with critically short telomeres enter cell division (telomere crisis, described below) and risk undergoing to massive chromosomal rearrangements. Indeed, most cancer cells acquire and maintain unlimited proliferation potential through the reactivation of the telomerase allowing for the bypass the senescence barrier (Greenberg et al. 1999; Qi et al. 2003; Feldser and Greider 2007; Lee et al. 1998). Actually, it is not the average but rather the shortest telomeres that limit cell survival, inducing replicative arrest, in absence to telomerase (Hemann et al. 2001). So, chromosome end protection is an important mechanism to protect cells from the risk of genome instability.

1.4.2 Dysfunctional telomeres contribution in genome instability and tumorigenesis

Apart from inducing senescence and driving tissue ageing, dysfunctional telomeres can have also an opposite role in tumorigenesis; being source of genome instability. In a cellular context where the senescence barrier is bypassed, such as after loss of p53 or RB tumor suppressor pathways, cells can enter division with dysfunctional telomeres and undergo a stage known as telomere crisis (Figure 7) (Artandi et al. 2000; Artandi and DePinho 2010; Maciejowski et al. 2015).

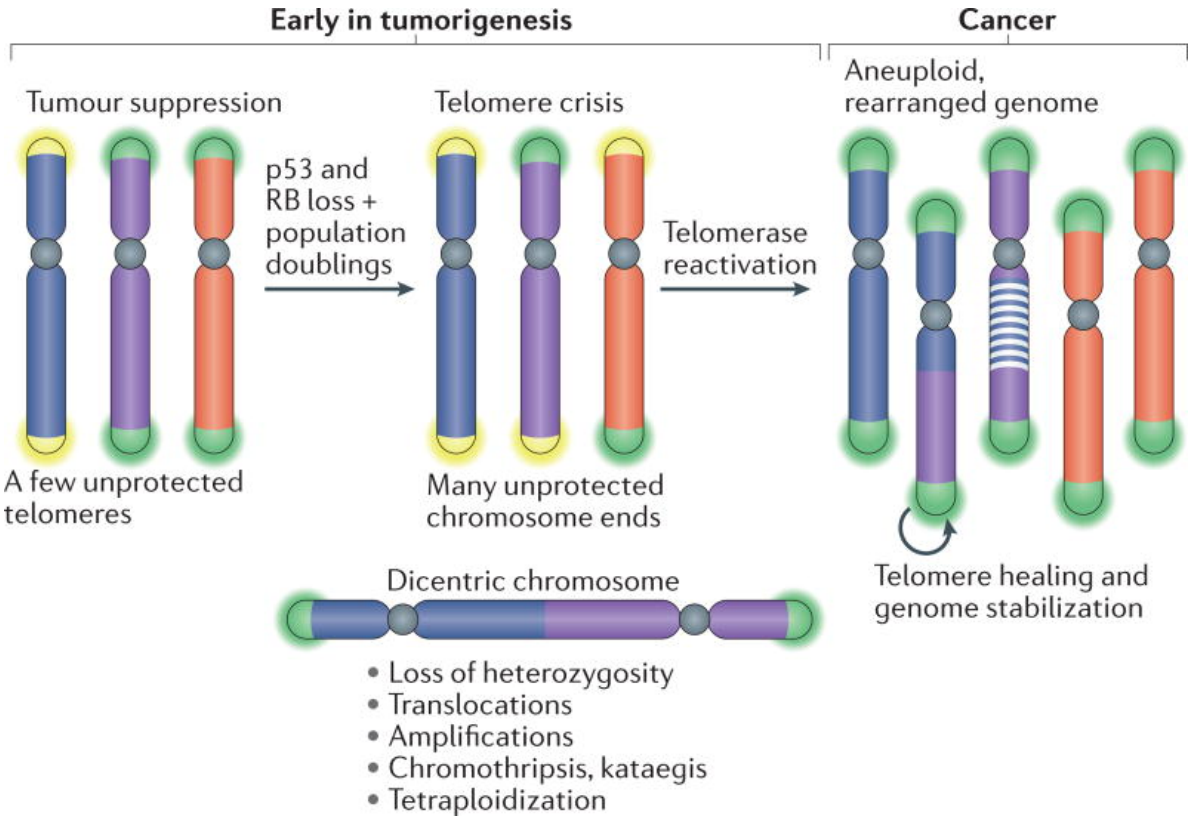

Figure 7. Telomere crisis

In case of dysfunctional telomeres, the loss of the p53 and RB tumor suppressor pathway allow cells to bypass the proliferative block and enter the cell cycle with critically short telomeres that will continue to shorten. When many telomeres become critically short, events of end-to-end fusion are promoted with the formation of dicentric chromosomes which leads to various forms of genome instability. Cancer transformation occurs when, after chromosomes rearrangement, telomerase activity is reactivated allowing cell proliferation. *Image from (Maciejowski and de Lange 2017).*

In this scenario, an accumulation of dysfunctional telomeres increases the probability that they fuse each other producing dicentric chromosomes. This scenario leads to the Breakage-Fusion-Bridge (BFB) cycle where dicentric chromosomes missegregate in mitosis undergoing breakage followed by a second fusion of the broken ends in daughter cells where the cycle can begin again (Gisselsson et al. 2000) (Figure 8). BFB was discovered by Barbara McClintock and can cause massive genome instability (McClintock 1939). BFB cycles can leads to different outcomes depending also on how fusion events occur, between different

chromosomes or, after DNA replication, between sister chromatids (Murnane 2006). They can be mainly grouped in three categories: loss of heterozygosity (LOH), non-reciprocal translocations and gene amplification. Chromosome rearrangements caused by telomere crisis are included in the cancer-relevant genome alterations that facilitate oncogenic progression, suggesting contribution of dysfunctional telomeres in oncogenesis (De Lange 2005b)

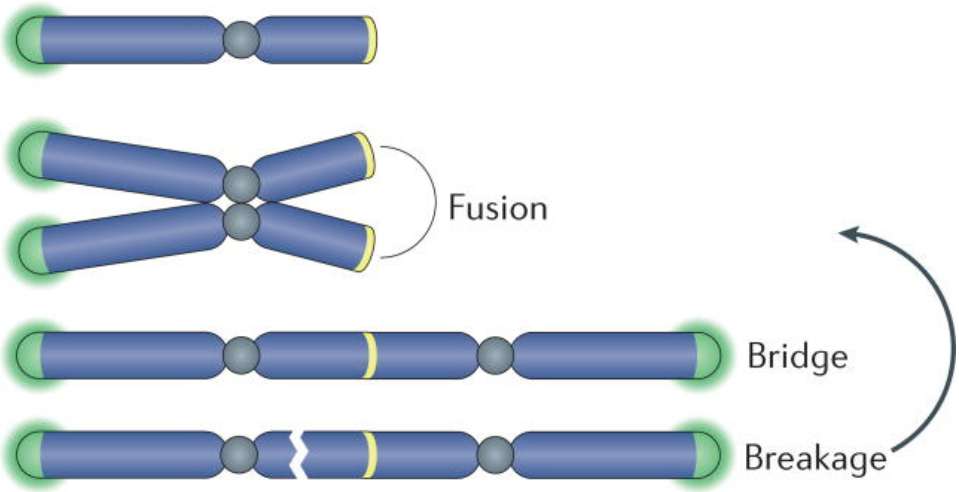

Figure 8. Breakage-fusion bridge cycle

Breakage-fusion bridge (BFB) cycle occurs starting from dicentric chromosomes generated by end-to-end fusion. During cell cycle, these chromosomes undergo to breakage due to mitotic spindle pulling, leading to other events of fusion that generate other dicentric chromosomes.

Image from (Maciejowski and de Lange 2017).

1.4.3 DNA damage and telomere replication can cause rapid telomere loss

In the context of somatic cells, where telomerase activity is absent, the only way for the cells to preserve telomeres from massive telomeric repeats loss and consequent genome instability, is to ensure proper telomere replication and telomere damage repair. DNA damage and particularly single-stranded damage at telomeric repeats have important roles in telomere erosion but the molecular mechanisms that translate telomere damage to telomere shortening are not well understood (Petersen, Saretzki, and von Zglinicki 1998; von Zglinicki 2000). Telomere damage for example can cause telomere loss by affecting telomere replication (von Zglinicki et al. 1995; Sitte, Saretzki, and von Zglinicki 1998; Munro et al. 2001). Telomeric replication forks move towards the chromosome end (terminal forks), differently from the internal regions, thus in case of collapse, these terminal replication forks cannot be rescued by nearby origins of replication, leading to loss of the distal fragment (Figure 9).

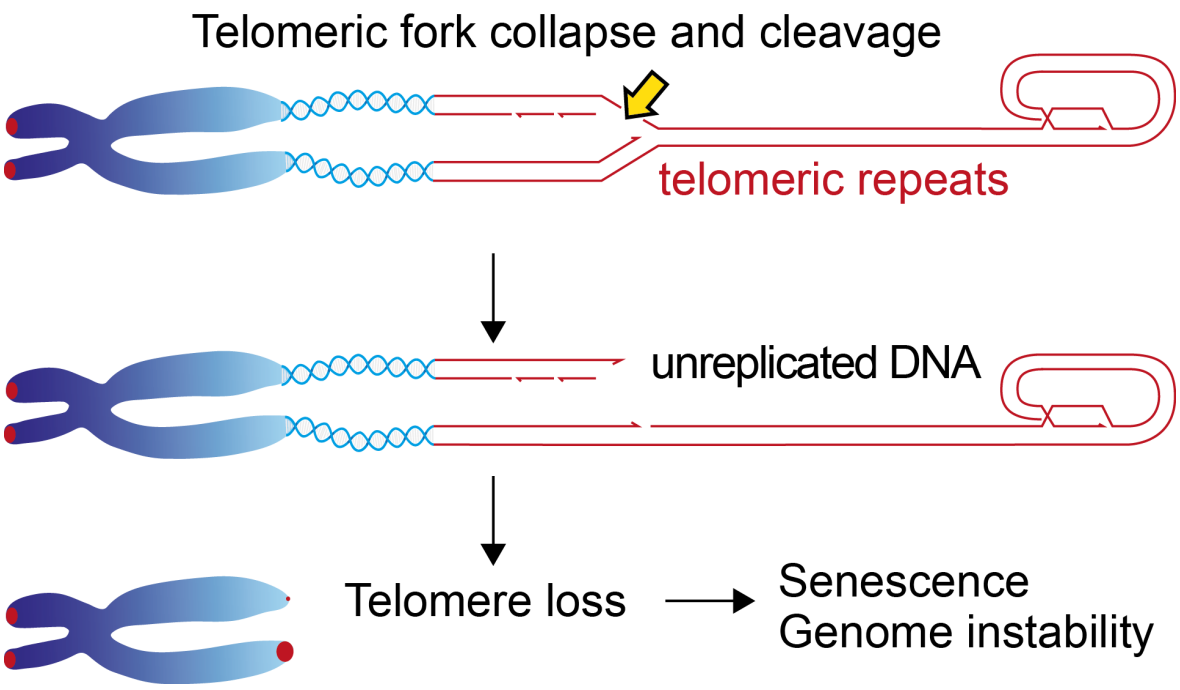

Figure 9. Telomere loss due to replication fork collapse

Illustration of telomeric (terminal) replication fork collapse that can lead to loss of telomeric repeats resulting in critically-short telomeres which can leads to senescence or contribute to genome instability.

Image from (Doksani 2019)

This means that any factors that may obstacle replication fork progression at telomeric repeats could be responsible for telomere shortening. This contest is worsened by the fact that telomeres behave like replication fragile sites and their replication is challenged by the repetitive nature of their sequence, inclined to form secondary structures like G-quartets, by the presence of the t-loop as well as by the ongoing transcription (TERRA) (Sfeir et al. 2009; Martinez et al. 2009) (Figure 10). For these reasons, telomeric replication has essential role in genome stability and is strictly assisted by specialized proteins. Actually, the shelterin complex recruits many accessories factors, with well-defined functions in replication stress response, to assist telomere replication, like RTEL1, the RecQ helicases WRN and BLM or SLX4 and Fanconi Anemia complexes, which could be directed towards specific structures that otherwise could interfere with telomere replication causing collapse

and loss of telomeric repeats (Vannier et al. 2012; Crabbe et al. 2004; Ding et al. 2004). There is another process that could leads to telomeric repeats loss, discussed below, the formation of circular extrachromosomal telomeric DNA.

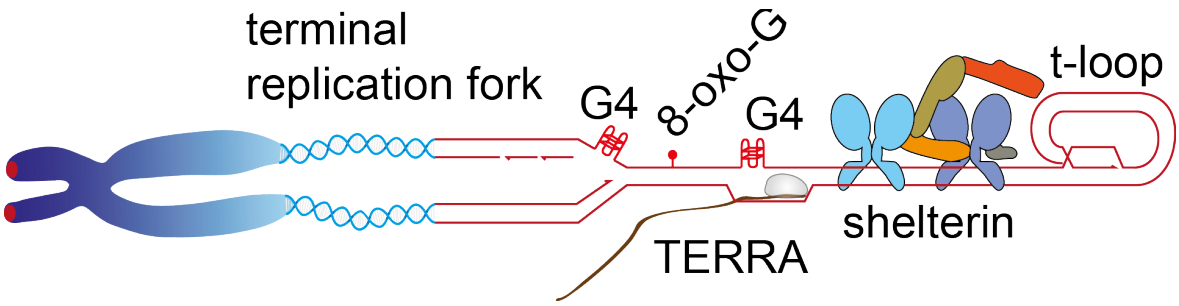

Figure 10. Telomere are hard to replicate

Telomere replication can be challenged by different factors and telomeres behave like replication fragile sites. The G-rich filament is prone to form G4 secondary structures and is mor susceptible to oxidative stress (8-oxo-G). Moreover, telomeric DNA is continuously transcribed (TERRA), tightly bound by the shelterin complex and the t-loop if not properly processed can interfere with the replication fork progression.

Image from (Doksani 2019).

2. EXTRACHROMOSOMAL TELOMERIC CIRCLES

Extrachromosomal telomeric circles have been found in wide variety of organisms, such as yeast, the plant *Arabidopsis thaliana*, the nematode *Caenorhabditis elegans*, in *Xenopus laevis* embryonic cells and also in mammalian ALT cells (Tomaska et al. 2000; Nosek et al. 2005; Cesare et al. 2008; Groff-Vindman et al. 2005; Zellinger et al. 2007; Raices et al. 2008; Cohen and Mechali 2002; Cesare and Griffith 2004; Nabetani and Ishikawa 2009; Wang, Smogorzewska, and de Lange 2004). The discovery and the investigation of telomeric circles started in the eighties with the study of the linear mitochondrial genome of the yeast *C. parapsilosis* (Kovac, Lazowska, and Slonimski 1984). Their mitochondrial DNA (mtDNA) have ends that resemble nuclear telomeres, since it terminates with a 738-bp tandem repeat unit that form an array of up to 12 units and has a single-stranded overhang (Nosek et al. 1995). Moreover, the overhang is bound by a mitochondrial telomere binding protein (mtTBP) (Tomaska, Nosek, and Fukuhara 1997). Further *in vivo* studies of the mtDNA of *C. parapsilosis* lead to the identification of extrachromosomal DNA fragments made of the tandem repeats of the mtDNA terminal regions (Tomaska et al. 2000). Two-dimensional agarose gel electrophoresis (2D-gel), a technique for the separation of DNA structures described in detail later, revealed that the electrophoretic migration of these fragments is compatible with a circular DNA structure. To further investigate this aspect, the extrachromosomal DNA circles were enriched by alkaline lysis, technique used for the isolation of small bacterial plasmid, from purified mitochondria of *C. parapsilosis*, and analyzed by electron microscopy. EM revealed the presence of short and stiff linear molecules, thicker than normal linear DNA, often with small balls at the ends (Figure 11, arrows). This rods-like conformation represents tightly supercoiled DNA molecules. In fact, introducing nicks through a mild DNase I treatment before EM analysis, lead to a higher proportion of relaxed molecules that appeared as open

DNA circles (Figure 11). Size distribution analysis showed that these circles have dimensions corresponding to integral multiples of 738 bp, confirming they are entirely made of the terminal region of the mitochondrial genome.

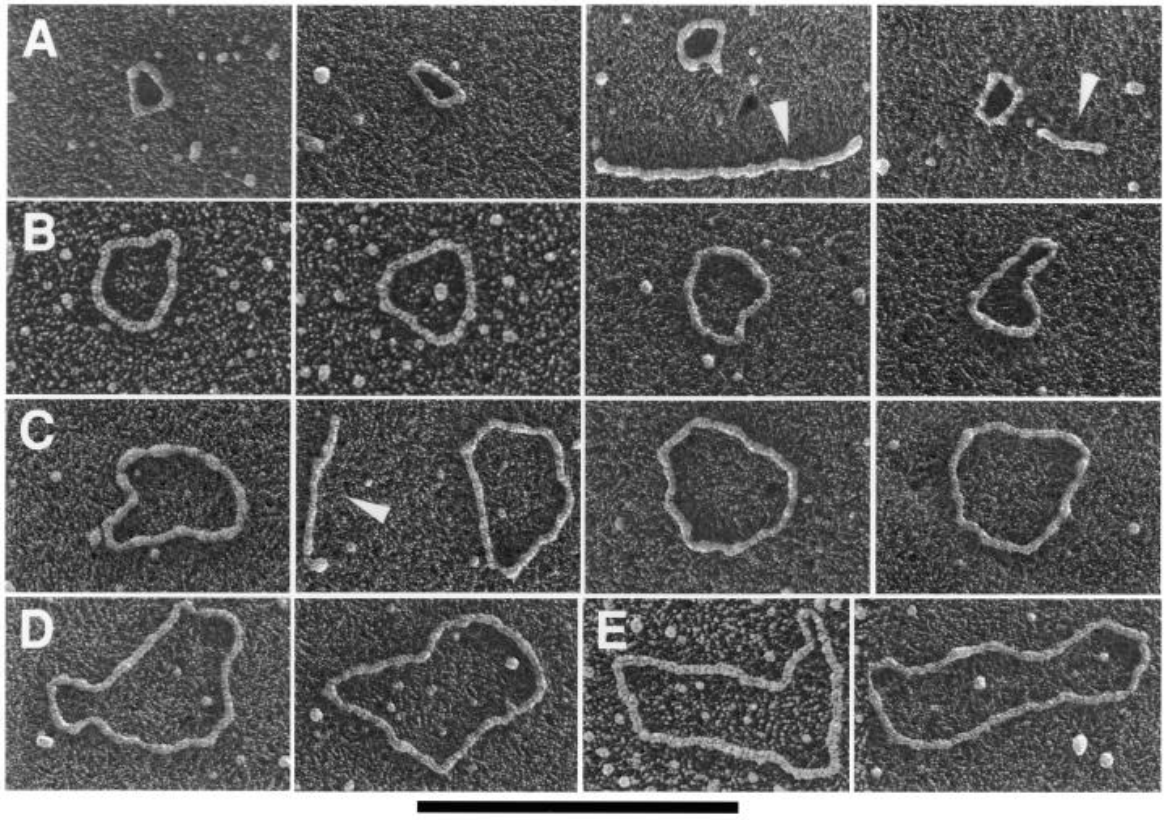

Figure 11. Mitochondrial telomeric circles of *C.parapsilosis*

Telomeric circles isolated by alkaline lysis from purified *C.parapsilosis* mitochondria and prepared for EM. Arrows indicate supercoiled molecules, that appeared as short linear molecules thicker than normal linear DNA, often with small balls at the ends. Mild DNaseI treatment increased the presence of circular molecules that allowed a more precise length measurement. Black bar on the bottom represents 0.5 μm.

Image from (Tomaska et al. 2000).

The same kind of analysis was conducted with similar results also in other yeast species (*C. metapsilosis*, *P. philodendra* and *C. salmanticensis*) all containing mtDNA in linear conformation with terminal arrays of tandemly repeated sequences (Tomaska et al. 2000; Nosek et al. 2005). Originally, these circular molecules were regarded as byproducts of genome instability, but later it was demonstrated that, instead, t-circles have active roles in telomere maintenance (Tomaska et al. 2000) (Regev et al. 1998). It has been reported that mtDNA circles of yeast provide substrates for rolling circle-dependent amplification, being therefore involved in telomere elongation through recombination (Nosek et al. 2005). A rolling circle dependency for mtDNA telomere maintenance was confirmed by a screening of yeast mutants lacking mitochondrial circles made of telomere-like tandem repeats. They resulted to have circular molecules but formed by end-to-end fusion of the original linear mitochondrial genome. This result suggested that the only mechanisms for mitochondrial telomere maintenance was the one depending on the presence of telomeric circles probably involving recombinational mode for telomere elongation (Kosa et al. 2006; Rycovska et al. 2004). The strongest evidence of a direct role of telomeric circles in telomere maintenance came from studies of the yeast *Kluyveromyces lactis.* Synthetic telomeric circles were introduced in *K. lactis* cells with disrupted telomerase RNA gene (*ter1*Δ) and uncapped telomeres (Natarajan, Groff-Vindman, and McEachern 2003; Natarajan and McEachern 2002). Telomeres after transformation resulted to be elongated and their sequencing revealed frequent presence of repeating patterns. Since the provided telomeric circles lacked a replication origin and cells lacks active telomerase, the most probable explanation for both telomere elongation and acquisition of a sequence pattern would be recombination events. Studies on the *tert1-16T K. lactis* mutant, where telomerase add at chromosome ends a telomeric repeat variant that is poorly recognized by the Rap1 protein, reported that telomeres resulted deprotected and

abnormally elongated (Natarajan, Groff-Vindman, and McEachern 2003; Natarajan and McEachern 2002). Long telomeres in this setting facilitated telomeric DNA purification and electron microscopy analysis. *tert1-16T* telomeres showed t-loop conformations and the presence of free circular molecules. The amount of both t-loops and telomeric circles significantly decreased both with overexpression of the Rap1, complementing the uncapping phenotype, and by the deletion of the rad52 gene, essential for homologous recombination (Cesare et al. 2008). These experiments suggest that telomeric circles allowed telomere elongation through a roll-and-spread mechanism, where extrachromosomal telomeric circles are the template for rolling circle amplification and the resulting long arrays of telomeric repeats can be incorporated into telomeres through homologous recombination-dependent events (Cesare and Griffith 2004; Natarajan and McEachern 2002) (Figure 12). This mechanisms of roll and spread is supported also by the presence of extrachromosomal telomeric circles and the detection of DNA molecules that resemble rolling circle replication intermediates visualized in electron microscopy of both *K. lactis* genomic DNA and *C. parapsilosis* mitochondrial DNA preparations (Groff-Vindman et al. 2005) (Nosek et al. 2005).

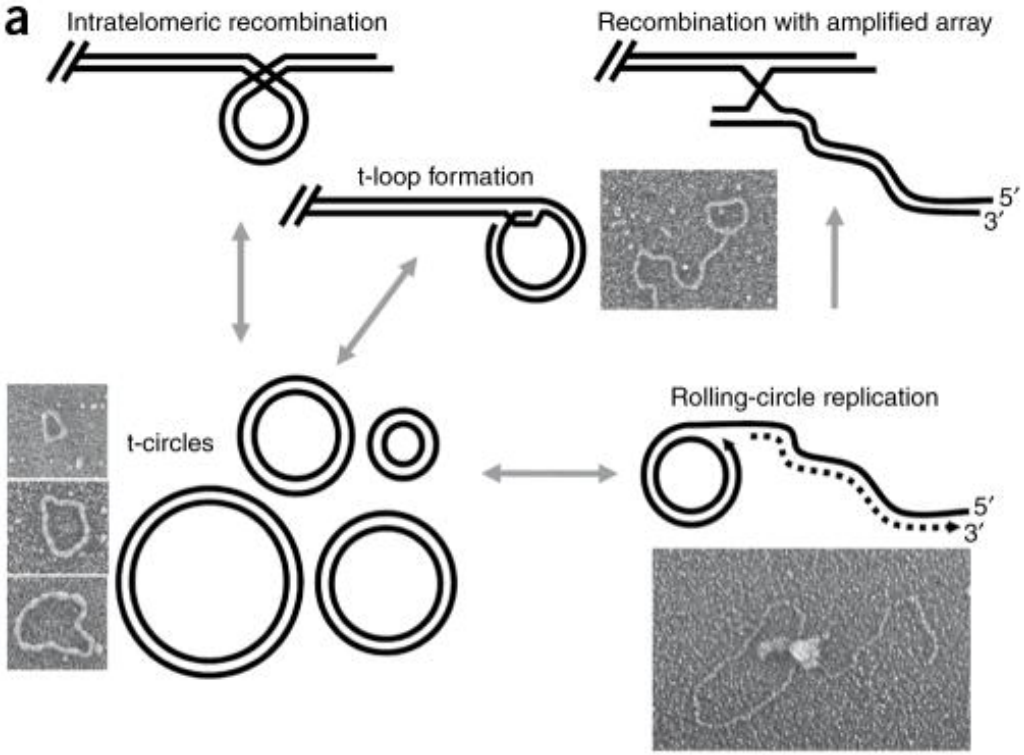

Figure 12. Model for t-loops and t-circles in telomere maintenance.

a. Model for telomere maintenance of mitochondrial DNA in yeast *C. parapsilosis.* The t-loop is formed by strand invasion of the 3'-overhang into double-stranded telomeric region. T-circles can be formed by intramolecular recombination of the repetitive sequence or by t-loop excision. The extrachromosomal circles can be amplified through rolling-circle replication, forming structures characterized by a loop which junction is recognized by single-stranded binding protein and a tail. The resulting long filament made of telomeric repeats can recombine and extend chromosome ends. The main structures, proposed to be involved in this pathway for mitochondrial telomere maintenance, were observed in electron microscopy.

Image modified from (Tomaska et al. 2009).

In mammals, telomeric circles have been identified in tumor cell lines where telomerase is not active and telomeres are maintained by processes that involves recombination events, known as alternative lengthening of telomeres (ALT) (Nabetani and Ishikawa 2009; Wang, Smogorzewska, and de Lange 2004; Cohen and Lavi 1996; Cesare and Reddel 2010). However, accumulation of telomeric circles was reported also in stem cells and in telomerase-positive human cell lines, when telomeres were artificially elongated (Pickett et al. 2009; Rivera et al. 2017). A model proposed for the formation of telomeric circles is the resolution of the t-loop junction by recombination enzymes, resulting in the formation of extrachromosomal circular molecules and truncated telomeres (Wang, Smogorzewska, and de Lange 2004) (Figure 13). This model derived from experiments with the TRF2 mutant $TRF2^{\Delta B}$, which lacks the N-terminal basic domain, but is able to properly bind telomeric DNA. The expression of the $TRF2^{\Delta B}$ induced in several human and mouse cell lines a rapid and stochastic loss of telomeric repeats from individual telomeres (Schmutz et al. 2017). In addition, the expression of $TRF2^{\Delta B}$ leads to accumulation of telomeric circles which size distribution reflects the size range of telomeres. The deletions of telomeric repeats in $TRF2^{\Delta B}$-expressing cells requires proteins involved in homologous recombination, NBS1 that is part of the MRN complex, and XRCC3, that is also associated to Holliday Junction (HJ) resolvase activity (Brenneman et al. 2002; Pierce et al. 1999; Liu et al. 2004). Based on these data, and considering that TRF2 is responsible for the stability and maintenance of t-loop, it was suggested that limited branch migration at level of the t-loop junction can generate a Holliday junction, that is not fully protected by TRF2, and can be resolved by HJ resolvases. The result would be t-loop excision, generating telomeric circles, containing nicks in both strands, with consequent rapid loss of telomeric repeats (Wang, Smogorzewska, and de Lange 2004; Schmutz et al. 2017).

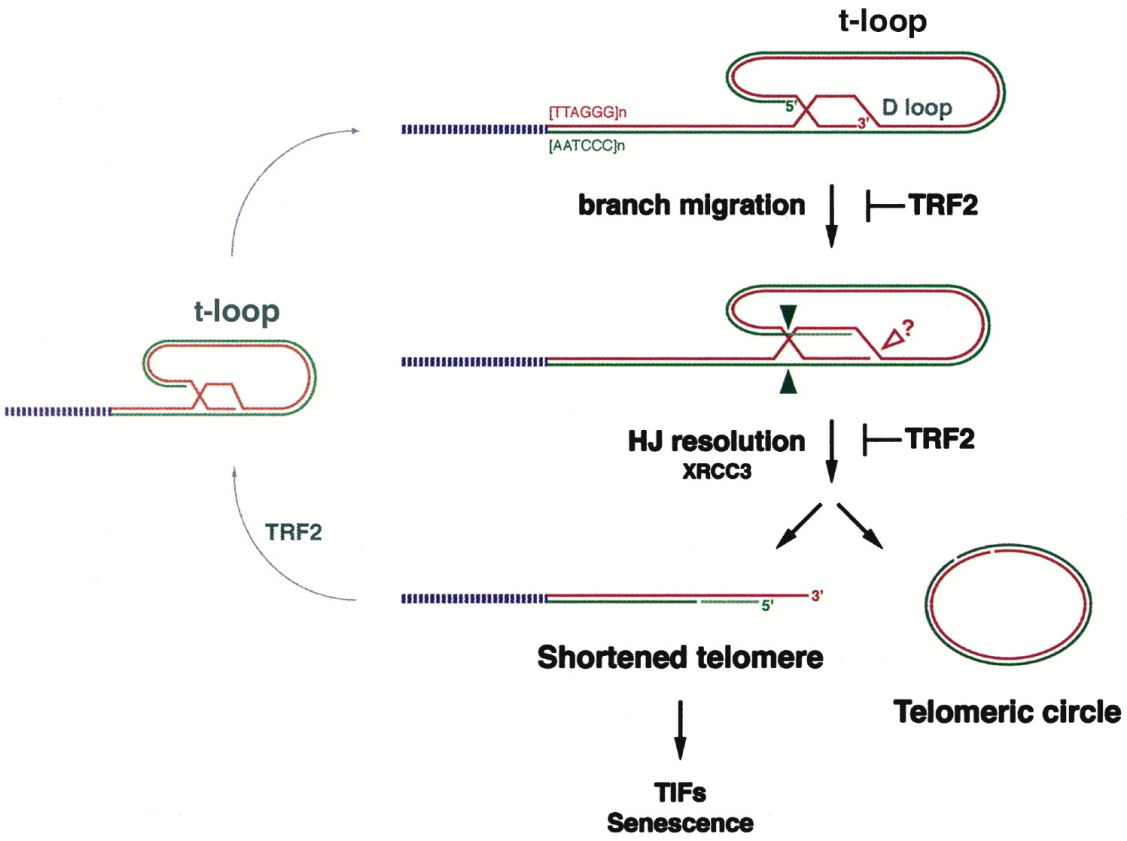

Figure 13. Model for t-loop excision.

From the top: branch migration of the t-loop junction (D-loop) results in the formation of Holliday junction. Here, HR-related protein (XRCC3 HJ resolvases) cut at the level of the HJ (green arrows) and a nuclease activity (red open arrow) at the level of the D-loop. The results are the formation of relaxed telomeric circle (containing two nicks, one on each strand) and telomere loss. The shortened telomeres might form a new t-loop but if the deletion was too extended, telomere can become dysfunctional activating the DNA damage response and induces senescence. The basic domain of TRF2 result essential to inhibits t-loop excision.

Image from (Wang, Smogorzewska, and de Lange 2004).

Since telomeric circles can generate spontaneously in a variety of human cells, it has been proposed that the HR-mediated excision of t-loops, could contribute to the stochastic shortening of human telomeres. The t-loop excision model has several aspects in common with the telomere rapid deletion (TRD) process described in yeast, where elongated telomeres experience rapid deletion (Bucholc, Park, and Lustig 2001; Li and Lustig 1996; Lustig 2003). Both mechanisms involve intratelomeric homologous recombination events and require the activity of components of the MRN complex for telomere loss. Moreover, the final products are the formation of circular molecules containing telomeric DNA and consequent telomeric repeats loss. These processes could provide a connection between the accumulation of telomeric circles and telomere erosion. However, the fact that normal cells with long telomeres as well as a long list of mutants, apparently unrelated to t-loop metabolism, accumulate extrachromosomal telomeric circles, suggests that there are also other mechanisms that can generate telomeric circles (Pickett et al. 2009; Wang et al. 2009; Gu et al. 2012; O'Sullivan et al. 2014; Li et al. 2017; Tomaska et al. 2009). For example, telomeric circles have been reported in mutants of genes involved in DNA metabolism and telomere maintenance such as human somatic cells depleted for the Ku86 gene, involved in nonhomologous end joining (NHEJ) and telomere maintenance, or in mutant for the origin recognition complex (ORC) which coordinates DNA replication at most chromosome sites but localizes at telomeres via interaction with TRF2 (Wang et al. 2009; Deng et al. 2007).

2.1 Alternative Lengthening of Telomeres (ALT)

Malignant transformation depends on extensive cell proliferation that is achieved by counteracting telomere shortening and avoiding senescence (Reddel 2000). Around 85% of human cancers increase the expression of telomerase that in somatic cells is downregulated throughout the development (Shay and Bacchetti 1997). In the remaining 15% of cancers, telomerase activity is not detected and telomere length is maintained by mechanisms referred to as Alternative Lengthening of Telomeres (ALT) (Bryan et al. 1997; Henson et al. 2005; Costa et al. 2006; Dilley and Greenberg 2015). ALT telomeres retain the canonical telomeric features, as they are made of the same repetitive motif array that extend as double-stranded, ending with G-rich overhang involved in the t-loop formation and is covered by Shelterin complex. Nevertheless, they have some peculiar features. Compared to telomerase-positive or non-tumor counterparts, ALT cells display increased telomere length heterogeneity and the presence of ALT-associated PML bodies (APBs), where telomeric DNA localizes in peculiar PML nuclear bodies (Yeager et al. 1999). The also display more frequent telomere recombination events, such as telomere-sister chromatid exchange (T-SCE) that results in crossover products that could derive from DSB repair (Bryan et al. 1997; Bryan et al. 1995; Grobelny, Godwin, and Broccoli 2000; Bechter, Shay, and Wright 2004; Dunham et al. 2000; Londono-Vallejo et al. 2004; Bailey, Goodwin, and Cornforth 2004). The increased frequency of recombination at telomeres is not associated with a general genome-wide upregulation of HR and is not caused by loss of functions, alteration or variation in the expression levels of shelterin components (Bechter, Shay, and Wright 2004; Lovejoy et al. 2012). The most common mutation that characterizes ALT cells is on the ATRX/DAXX chromatin remodeling complex; the loss of ATRX is not sufficient to induce ALT, but its complementation suppresses some ALT phenotypes (Lovejoy et al. 2012; Heaphy et al. 2011; Napier et al. 2015). Another peculiar aspect is that

ALT telomeres accumulate nicks and single-stranded gaps (Nabetani and Ishikawa 2009). This accumulation could cause replication stress and DSBs formation promoting DNA repair and recombination events This aspect suggests that ALT development may involve a selection of cells that experience telomere damage. The origins of the damage in ALT telomeres are not clear but could be produced by metabolic products, such as reactive oxygen species that preferentially cut G-rich sequences (von Zglinicki 2002; Henle and Linn 1997). One of the most consistent features of ALT cells is the presence of extrachromosomal telomeric circles, double-stranded (t-circles) or partially single-stranded (C-circles) (Wang, Smogorzewska, and de Lange 2004; Cesare and Griffith 2004; Henson et al. 2009). ALT mechanism was first described in *S. cerevisiae* cells inactivated for telomerase activity that survive using HR-dependent telomere maintenance pathways, but it has been observed in other yeast species like *K. lactis* (Lundblad and Blackburn 1993*)*. The survivor cells of *S. cerevisiae*, the one that continue to proliferate, were classified in type I and type II based on their different dependency on HR proteins. In the type I cells, telomere maintenance is dependent on RAD51 and RAD52 but not on RAD50, whereas in type II cells RAD50 and RAD52 are required but not RAD51. Yeast RAD50 is part of the MRX complex whose counterpart in mammals is the MRN (MRE11-RAD50-NBS1) complex. RAD50 and NSB1 have been reported to be important for ALT cells therefore was suggested that human ALT cells are analogous of the type II yeast survivors (Jiang et al. 2005; Potts and Yu 2007). In human cells, the first evidence about ALT mechanisms derived from the observation that in telomerase-negative cells telomere length was maintained for many population doublings and often underwent to rapid shortening or lengthening events, likely as a result of recombination (Bryan et al. 1995; Rogan et al. 1995; Murnane et al. 1994). Several studies have since reported physical evidences of recombination at human ALT telomeres. For example, (Dunham et al. 2000) showed

that a DNA cassette inserted into a single telomere was copied to other telomeric sequences in ALT cells, but not in telomerase-positive cells. ALT cells also showed complex rearrangements resulting in the presence of non-canonical repeats in the telomeric regions (Varley et al. 2002). Further, supporting the involvement of HR-based telomere elongation, telomere maintenance in mammalian ALT cells is impaired in cells mutated for HR factors such as Brca2, FANCD2, FANCA, SMC5/6 BLM and Rad52 (Verma et al. 2019; Zhang et al. 2019; Min, Wright, and Shay 2017). Although is generally accepted that telomere elongation involves DNA recombination, the molecular mechanisms of ALT remain unclear. The models proposed involved homologous-recombination dependent mechanisms that involve DNA replication, in common with BIR. Basically, the high sequence homology can favor strand invasion of a short telomeres into another telomere of the same cells which is then used as a template for telomere elongation. In one model it is proposed that ALT telomeres are lengthened by recombination-mediated synthesis of new telomeric repeats using existing telomeres from adjacent chromosome as template (Dunham et al. 2000; Henson et al. 2002) (Figure 14). In this scenario, the terminal 3' overhang from one telomere can invade another telomere at any level and use its sequence as template for elongation. Replication could proceed until the end of the chromosome and, depending on the point of strand invasion, could lead to excessive lengthening. These events are consistent with the previous observation of the spreading of a single DNA cassette to multiple telomeres in ALT cells and telomeric rearrangements that lead to unequal exchange and could favor the heterogeneity that characterize ALT telomeres (Dunham et al. 2000; Varley et al. 2002).

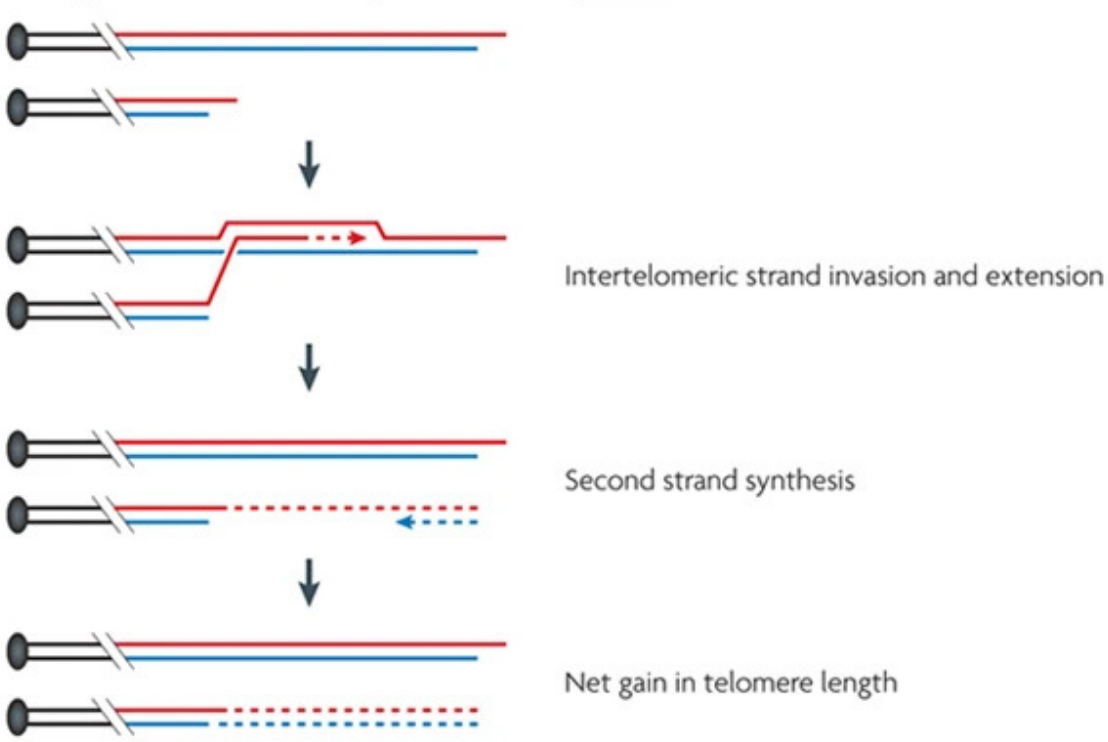

Figure 14. Model for ALT telomere maintenance

Homologous recombination-dependent DNA replication proposed as model for ALT telomere maintenance. Telomere lengthening occurs through DNA replication, mediated by homologous recombination, using as template the telomeric sequence of adjacent chromosomes. Due to the high level of homology, strand invasion can occur at any point of the donor telomeres and replication proceed until the end of the chromosome, causing net gain of telomeric repeats.

Image from (Cesare and Reddel 2010).

However, there is some evidence that in ALT cells it is not necessary to use telomeric DNA from another chromosome for telomere elongation (Muntoni et al. 2009). Therefore, another model proposes that telomeric DNA can use intra-molecular DNA synthesis, meaning that a short telomere can use itself as template through the formation of secondary structures like t-loops, or perform elongation during DNA replication, using its sister chromatid as a template (Figure 15 a, b). It cannot be excluded that extrachromosomal linear telomeric fragments can be used as template (Figure 15 c) as well as the extrachromosomal telomeric circles (Figure 15 d), which accumulate in ALT cells, and could be used as template for rolling-circle mediated telomere extension (Henson et al. 2002). The involvement of circular forms in telomere elongation is consistent with the “roll and spread” mechanisms described in yeast. Furthermore, C-circles (partially single-stranded circles) are excellent substrates for rolling circle in vitro (described later). It has been proposed that after the annealing of telomeric G-rich strand to single stranded C-rich-strand of C-circle, DNA synthesis by rolling circle replication could promote rapid elongation of telomeres also in vivo in ALT cells (Tomaska et al. 2009; Henson et al. 2009; Cesare and Griffith 2004; Wang, Smogorzewska, and de Lange 2004). However, direct experimental evidence that telomeric circles are employed as substrates for amplification of telomeric arrays in mammalian cells is lacking.

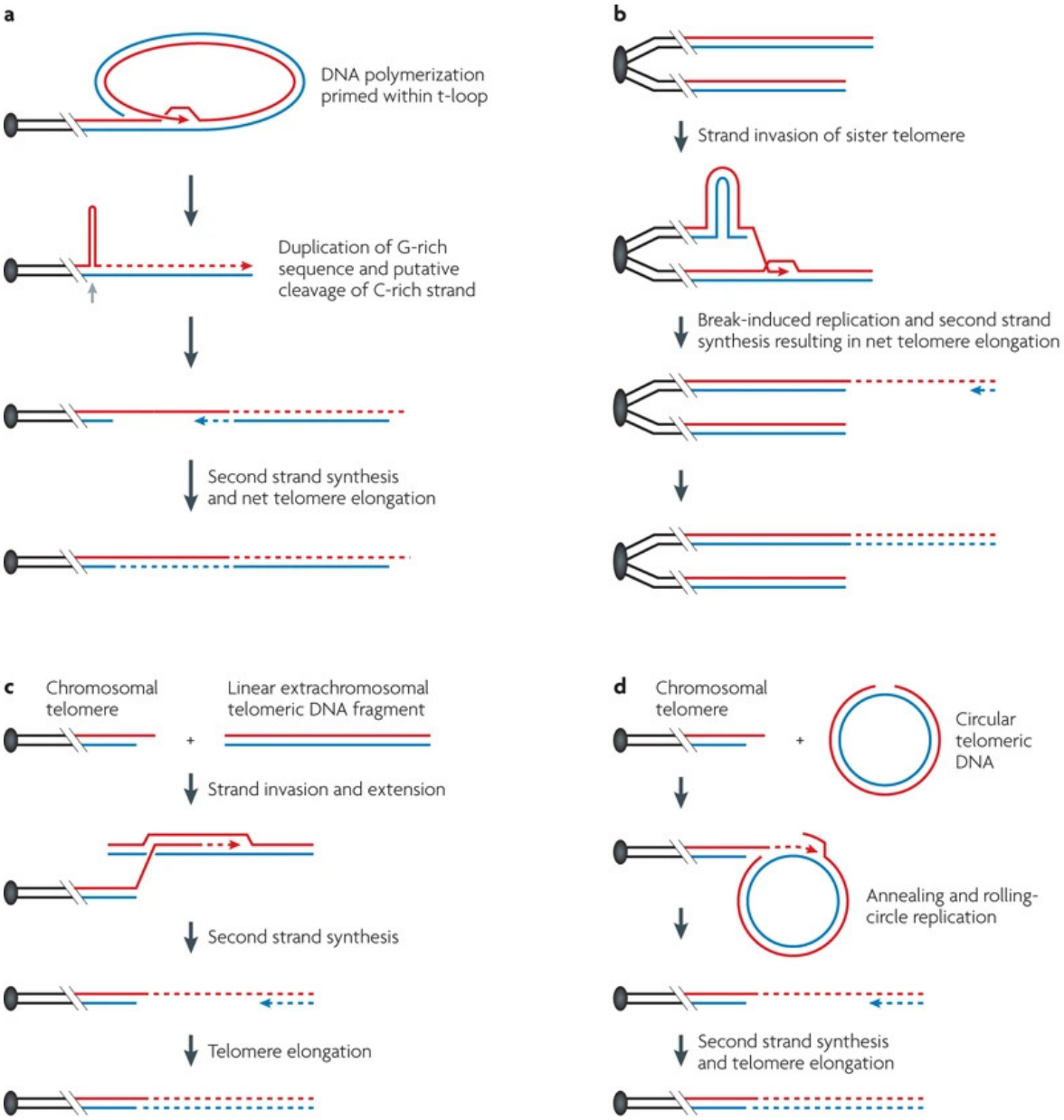

Figure 15. Alternative copy template for ALT telomere elongation.

Alternatively, to the model proposed in Figure 14, where DNA template for telomere elongation is another telomere, it has been proposed that the copy template could be the same molecule (a, b) using t-loop of sister chromatid, or extrachromosomal telomeric molecules (c, d), linear of circular (like C-circles).

Image from (Cesare and Reddel 2010).

2.1.1 C-circles

C-circles are circular telomeric DNA molecules with an intact and covalently closed C-rich strand and gapped G-rich strand. Their origin is not clear yet and they are several-fold more abundant in ALT cells than telomerase-positive cells or non-immortalized cell lines. ALT cell lines, can lack some or most of ALT features but nevertheless contain abundant C-circles. Therefore, differently from t-circles (the double-stranded telomeric circles), C-circles are a peculiar feature of ALT cells and their accumulation seems to be proportional to the ALT activity (Henson et al. 2009). In two clones of spontaneously immortalized fibroblasts, overexpressing of a fusion protein that sequesters the MRE11-RAD50-NBS1 complex leads to ALT inhibition. In these ALT-inhibited cells C-circles levels dropped and, interestingly, there was a difference also between the two clones. The clone with lower C-circles had also less ALT activity detected as accumulation APBs and telomere attrition. This means that C-circles are more specific for ALT mechanisms compared to t-circles. ALT cells also contain G-circles (G-strand intact, C-strand with gap) but they are around 100-fold less abundant than C-circles (Henson et al. 2009).

2.2 Methods for extrachromosomal telomeric circles detection

Two-dimensional agarose gel electrophoresis

Two-dimensional agarose gel electrophoresis (2D-gels) is a technique which allows for the separation of molecules according to their size and structures. Briefly, DNA undergoes to size-dependent separation in a first dimension electrophoresis run, followed by a second dimension where molecules migrate depending on their molecular complexity, with slower migration of more extensively branched DNA molecules. Then DNA could be either transferred by Southern blotting to nylon membrane or detected directly with in-gel hybridization using the probe of interest (Villwock and Aparicio 2014). This approach is widely used for replication studies

where is essential to separate linear DNA molecules form branched ones (Bell and Byers 1983; Brewer and Fangman 1987; Nawotka and Huberman 1988; Friedman and Brewer 1995; Lopes et al. 2001). Previous studies have shown also that 2D gel is efficient in the separation of circular structures from linear molecules, since covalently closed and nicked circles migrate slowly compared to linear molecules of equal length (Oppenheim 1981). (Cohen and Lavi 1996) using as model for circular DNA, a heterogeneous population of defective SV40 circular genomes, demonstrated that 2D gels is efficient also for the separation of different circular species. They characterized the different conformation of the molecules producing the 2D signals in their system, extracting the DNA from each 2D spot and analyzing it by electron microscopy. With this approach they also demonstrated that 2D gel allows us to distinguish between supercoiled and non-supercoiled molecules, as supercoiled molecule remain intact throughout the analysis, whereas non-supercoiled that underwent nicking during the preparation of the second dimension therefore migrate there as relaxed forms. All these aspects make 2D gel analysis a suitable approach for the identification of different types of DNA conformations, in fact in addition to replication studies, it has been used also for the characterization of mammalian telomere structures, including the extrachromosomal telomeric circles (Wang, Smogorzewska, and de Lange 2004; Cesare and Griffith 2004; Nabetani and Ishikawa 2009). The advantages to use this approach to study telomere structure are the possibility to specifically probe telomeric DNA and to quite easily monitor structure accumulation of different preparations in parallel (i.e. different cell lines, treatments, time points). In fact, this approach was important for the discovery of the extrachromosomal telomeric circles and for the monitoring of their formation in specific context like ALT cells. Through 2D gel analysis the accumulation of extrachromosomal telomeric circles was reported in TRF2$^{\Delta B}$-expressing cells suggesting that their distribution reflect the size range of telomeres.

These results support the model for the telomeric circle formation as excision of unprotected t-loop (Wang, Smogorzewska, and de Lange 2004). Moreover, 2D gel analysis was also used to define the telomeric nature of the extrachromosomal circular molecules found by electron microscopy to accumulate in a variety of ALT positive cells lines (Cesare and Griffith 2004).

Detection of extrachromosomal telomeric circles by the rolling circle amplification assay.

The rolling circle assay was developed in *Arabidopsis* since telomeric circles were not easily detected in 2D-gels, probably due to the short length of telomeric repeats that further decreases in the observed mutants (Zellinger et al. 2007). It consists in the rolling circle amplification (RCA) of telomeric circles starting from a provided telomeric-specific oligonucleotide that anneals after DNA denaturation. The amplification is performed by the Phi29 polymerase which is a highly processive enzyme, with strand displacement activity (Blanco and Salas 1996). This reaction generates long, single-stranded telomeric DNA molecules that results in a high molecular weight signal accumulating on the top of agarose gel, detected after southern blot and hybridization with a probe that specifically recognize telomeric repeats (Figure 16 A, B). The specificity of the reaction was verified by treating the DNA with exonuclease V before incubation for RCA. This exonuclease degrades double-stranded molecules with exposed extremities, therefore in the linear conformation. After the ExoV treatment, the high molecular weight products derived from Phi29 amplification were resistant, differently form the linear DNA that was no longer detectable, confirming the circular nature of the amplification substrate (Figure 16 B). This approach has been widely used in the field (Li et al. 2017; Margalef et al. 2018).

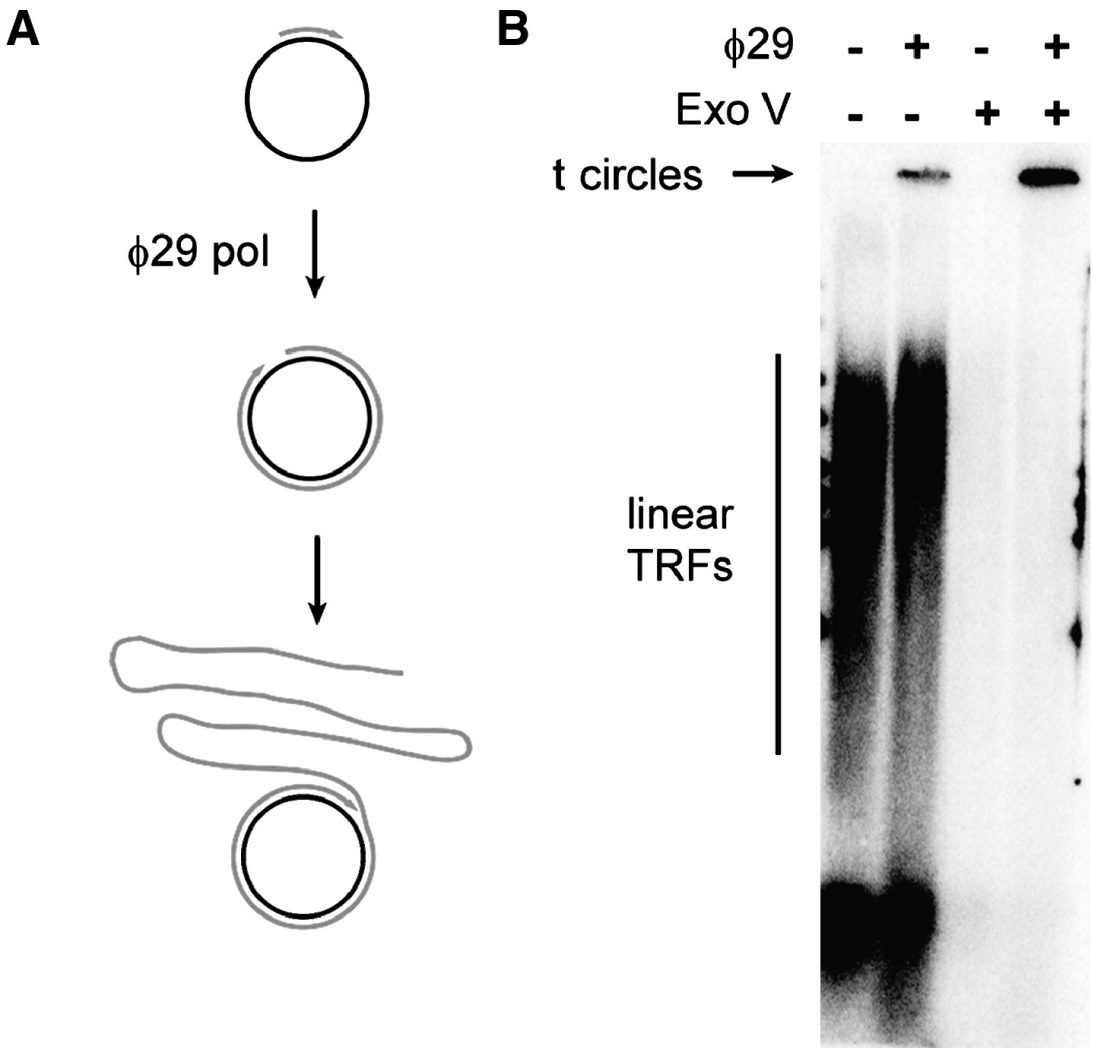

Figure 16. Telomeric circle detection by rolling circle amplification.

A. Schematic representation of the rolling circle amplification of the telomeric-specific primer by Phi29 polymerase from circular template.

B. Telomeric signal of the products after telomeric circle assay. DNA from Arabidopsis cells was subjected to telomeric circle amplification directly or after ExoV treatment and in presence or absence of Phi29 polymerase. The reaction products were separated in alkaline gel electrophoresis, transferred on membrane and hybridized with a TTAGGG telomeric probe.

Image from (Zellinger et al. 2007).

Rolling circle amplification assay for the detection of C-circles: the C-circle assay.

The C-circle assay (CCA) has become a standard method to measure the presence of ALT mechanisms, since it is a rapid and quantitative assay that detects changes in ALT activity (Henson et al. 2009; Bryan et al. 1995; Henson and Reddel 2010). This method is based on the rolling circle amplification of telomeric C-circles partially double-stranded by the highly processive DNA polymerase Phi29 (Dean et al. 2001). In this case, a DNA primer is not added to the reaction since the partially single-stranded G-rich strand can provide a 3'-end for elongation. This process produces a long filament of G-rich single-stranded telomeric DNA which migrate minimally from the gel in electrophoresis (Figure 17 a,b). The Phi29 polymerase has been reported to generate rolling circles products bigger than 70 kb (Dean et al. 2001). The specificity for C-circles is supported by the fact that omitting dCTP from the reaction did not affect the amplification of the C-circles (consistent with the fact that the amplified strand does not contain Cytidine residues) (Henson et al. 2009). Moreover, it was also demonstrated the partially double-stranded nature of the amplified circles, since the CCA products are not detected if the input material is first digested with Kamchatka crab duplex specific nuclease (DSN), an endonuclease that has highly specificity for double-stranded DNA being inactive towards single-stranded DNA (Anisimova et al. 2006) (Figure 17 b). This nuclease was used to set up a method for direct measurement of overhang length (Zhao et al. 2008). Moreover, the treatment of ALT-positive genomic DNA with exonuclease λ, I and V, results in the degradation of most of the linear telomeric DNA but did not decrease the CC-assay products, demonstrating that they derived from the amplification of circular molecules (Figure 17 c,d) (Henson et al. 2009). However, in ALT cells there are also telomeric circular molecules that derive from t-loops

excision by HR. These telomeric circles, following the model, are mainly double stranded but likely nicked on both strands, thus should not be a major substrate for RCA therefore do not contribute to CCA products (Cesare and Griffith, 2004. Mol Cell Biol; Wang et al., 2004. Cell). This was demonstrated promoting t-circles formation overexpressing telomerase activity in ALT-negative Hela cells, that lead to over-elongated telomeres (Pickett et al. 2009). As results, despite the presence of t-circles, CCA products were not significantly different in the Hela overexpressing telomerase compared to the Hela controls cells and anyway, resulted 400-fold lower than the ALT positive control. Therefore, CCA is unaffected by the presence of ALT independent t-circle formation underling the specificity of this assay in detecting ALT phenotypes, based on the accumulation of C-circle.

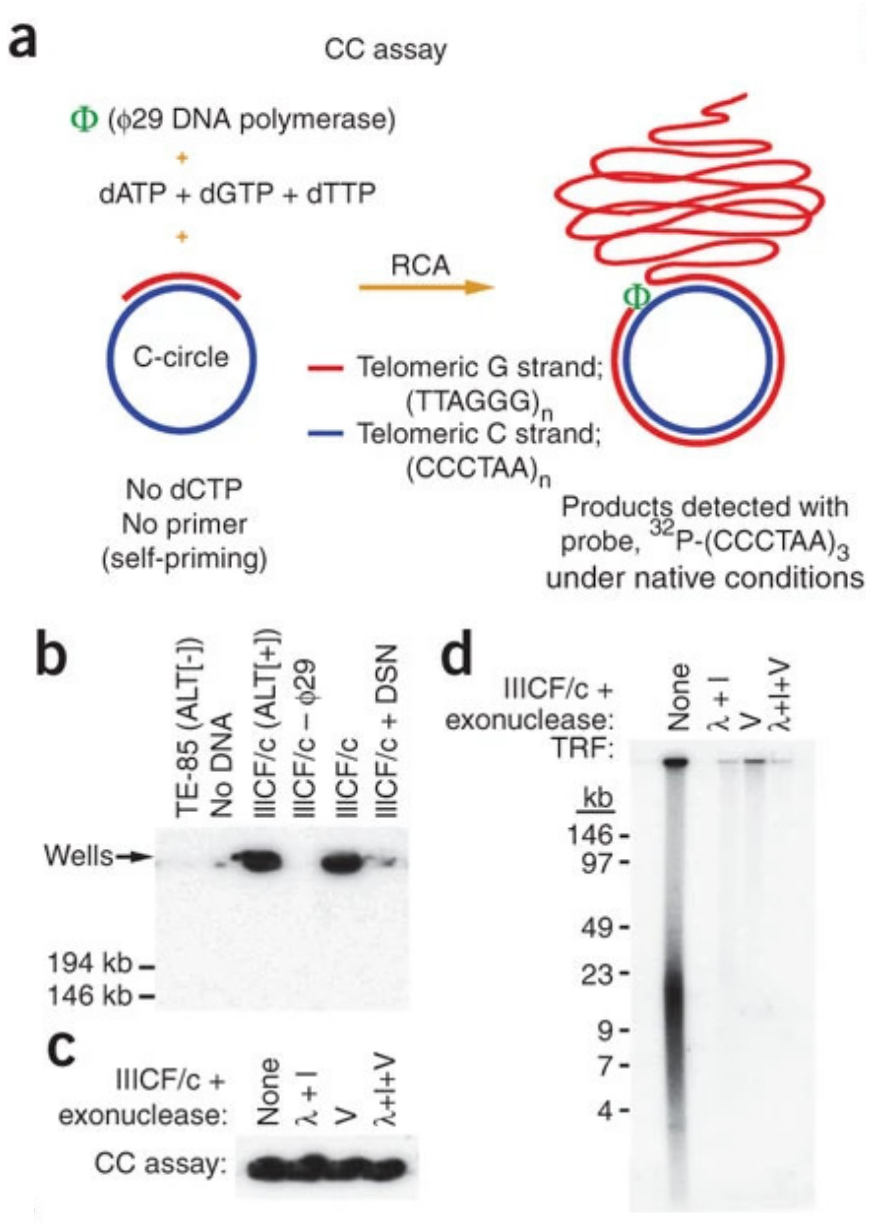

Figure 17. C-circle assay.

a. Schematic representation of the C-circle assay (CCA).

b. 30 ng of genomic DNA from both ALT$^+$ cells (IIICF/c) and ALT$^-$ cells (TE-85) was process for CCA in the indicated conditions. The HMW G-rich strand, that minimally migrates from the wells was not detected when the template DNA or the Phi29 was omitted from the reaction and when DNA was pre-treated with DSN nuclease, which digest specifically double-stranded DNA.

c. Genomic DNA from ALT$^+$ cells (IIICF/c) after restriction digestion, was treated with exonucleases λ, I and V and was subjected to CCA (c) or separation in agarose gel (d). The linear DNA signal is no more detected after treatment whereas CCA products resulted unaffected.

Image from (Henson et al. 2009)

RESULTS

Structural transitions are involved in several aspects of telomere metabolism, like chromosome end protection function through the formation of the t-loop, telomere replication and recombination events. Our lab was interested in monitoring telomere structure by electron microscopy (EM), an approach widely used to characterize replication and recombination intermediates genome-wide. However, in EM, labelling for specific DNA sequences is not efficient and telomeric DNA is low represented compared to the overall genome. For example, considering the size of the mouse diploid genome of 5.6×10^9 bp and an average telomere length of 50Kb mouse telomeric repeats represent less than the 0.1% of all genomic DNA. Therefore, in order to specifically study telomeric DNA by EM, telomeric repeats need to be highly enriched. For this purpose, we developed a new procedure for the purification of telomeric DNA from mammalian cells.

A two-step procedure for the purification of mammalian telomeric DNA

The principle for the enrichment of telomeric DNA is based on the fact that TTAGGG repeats lack restriction sites and therefore after extensive digestion with frequently-cutting restriction enzymes they can be separated from the bulk DNA by size fractionation (de Lange et al. 1990). This strategy has been used in the past for the imaging of the t-loop structure both in isolated DNA and in telomeric chromatin (Griffith et al. 1999; Cesare et al. 2003; Nikitina and Woodcock 2004). The standard procedure consisted in a single step of enrichment in which large amounts of human or mouse genomic DNA are digested, reducing most non-telomeric fragments to less than 1 kb. Following digestion, samples were subjected to size exclusion chromatography to separate larger molecules that do not contain restriction sites (~ 10 kb) from smaller genomic fragments. In these experiments, most of the telomeric signal eluted in the first excluded fractions, while the small fragments from the bulk DNA eluted later (Griffith et al. 1999; Cesare et al. 2003; Nikitina and Woodcock

2004). While the first fractions were certainly rich in telomeric repeats, their absolute frequency (i.e. the ratio between telomeric and non-telomeric DNA) in those fractions was not reported. Moreover, gel filtration chromatography is more suitable for the separation of globular structures rather than long DNA filaments, making this approach quite unreliable in its ability to enrich for telomeres and limiting its application. We therefore developed an improved protocol based on the same principle of digestion with frequent cutters, but consisting in two rounds of enrichment and an alternative approaches for size fractionation (Mazzucco et al. 2020). The first round of the enrichment consists of the digestion of 2.5 mg of genomic DNA with two frequent cutters, HinfI and MspI, selected also based on the relative cost/unit. The most efficient and widely-used system to separate DNA fragments by size is agarose gel electrophoresis, but its limited capacity (~30 µg/well) is not compatible with the large amount of starting material required for telomere enrichment. We therefore decided to use sucrose gradient centrifugation which is deal for our protocol since it allows for efficient resolution of high amounts of DNA, whoses sizes can range from less than 1 kb up to 60 kb, and it is gentle on DNA, essential to preserve native structures (Weis and Quertermous 2001). Digested DNA is therefore loaded on gradient of sucrose solutions (10%-20%-30%) and separated by ultracentrifugation, where restriction fragments deposit along the gradient according to their size, with smaller fragments collecting first in the lower sucrose concentrations, and larger fragments later in higher sucrose concentrations. After centrifugation different volumes of the gradient (fractions) were collected and an aliquot was loaded on an agarose gel. The fragmented, bulk DNA, deposits in the first two fractions where the sucrose concentration is lower, whereas long molecules are in the last fractions made of solution with higher concentration of sucrose (Figure 1A, top). In order to verify the distribution of the telomeric DNA in the gradient, the DNA form the agarose gel was transferred to a membrane and

hybridized with a radioactive probe that specifically recognizes telomeric repeats. Most of the telomeric DNA is retained among the fragments of the last fractions (Figure 1A, bottom). Pooling and concentrating those telomeres-containing fraction, we recovered around 200 µg of high molecular weight DNA. Considering the starting DNA amount (2.5 mg), at this step the enrichment for telomeres is estimated at around 10-fold. This is also confirmed by the dot blot analysis, where the telomeric signal intensity in 50 ng of DNA recovered from the sucrose gradient is similar to the telomeric signal intensity in 500 ng of bulk DNA (Figure 1C). However, since telomeres represent around the 0.1% of all genomic DNA, a 10-fold enrichment means that around 99% is non-telomeric DNA, making this sample not suitable for EM analysis. Therefore, we introduced a second round of the enrichment in order to further enrich for telomeric DNA in which high molecular weight DNA, which was recovered from the last sucrose gradient fractions of the first enrichment, is then digested with a mix of seven frequently-cutting restriction enzymes and separated in a preparative agarose gel. The final sample is recovered from the area of the preparative gel containing telomeric repeats (Figure 1B). In order to verify the levels of enrichment for telomeric DNA, I blotted defined amounts of DNA of each sample on a membrane in duplicate. One membrane was hybridized with a telomeric probe, the other with a probe recognizing the mouse long interspersed repeats (L1 repeats), which should be depleted from the enriched sample (Figure 1C). Telomeric repeats were enriched around 1000-fold in the final sample, whereas the signal for the L1 repeats is not detectable. Considering that mouse telomeric repeats represent around 0.1% of the whole genome, this means that our final samples should be made almost entirely of telomeric DNA. In order to verify the enrichment level in a more direct manner we combed DNA on glass coverslips before and after the enrichment procedure. All DNA fibers were detected with an antibody against single-stranded DNA and telomeric fibers were detected with a PNA probe. (Figure

1D). In the enriched sample around 80% of the molecules were recognized by the telomeric probe consistent with the enrichment values obtained in dot blots. In Figure 1 is reported the enrichment procedure performed starting from SV40-Mouse Embryonic Fibroblasts (SV40-LT MEFs) is pictured, however we also obtained similar results also with Hela1.3 cells, which are human cells with long telomeres (Figure 3A), and with U2OS ALT cells (Figure 3).

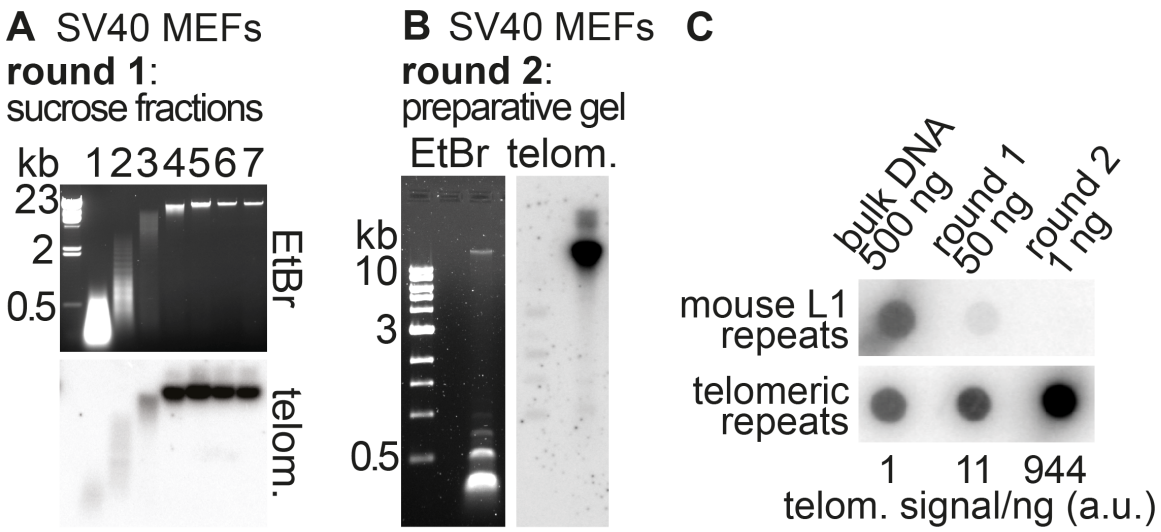

Figure 1. Purification of telomeric repeats from SV40-LT immortalized Mouse Embryonic Fibroblasts

A. First round of enrichment. Top: agarose gel showing the distribution of SV40-LT MEFs restriction fragments in sucrose gradient fractions. 2.5 mg of SV40-LT MEFs genomic DNA was digested with HinfI and MspI restriction enzymes and separated according to size by sucrose gradient ultracentrifugation. ~1/500 of each recovered fraction of the gradient was loaded on agarose gel. Bottom: telomeric DNA distribution among sucrose gradient fractions. The DNA from the agarose gel (top) was blotted on membrane and hybridized with a telomeric-specific probe. Telomeric repeats are found in the high molecular weight (HMW) fractions.

B. Second round of enrichment. Left: gel showing the second restriction digestion. HMW DNA of the last four sucrose gradient fractions in (A) were pooled and digested again with a mix of 7 restriction enzymes (see Materials and Methods). 1/100 vol of the digestion was run in the agarose gel shown. Right: Blot showing that the telomeric DNA remains in the HMW area of the gel after the second digestion step. The DNA from the agarose gel (left) was blotted on membrane and hybridized with a telomeric specific probe.

C. Dot-blot analysis showing the enrichment of telomeric DNA at each step of the protocol. The reported amounts of DNA are spotted on membrane and hybridized either with a probe specific for recognizing the TTAGGG repeats or a probe recognizing the mouse L1 interspersed repeats. The enrichment level was obtained as telomeric signal/ng of each sample relative to the one of the bulk DNA.

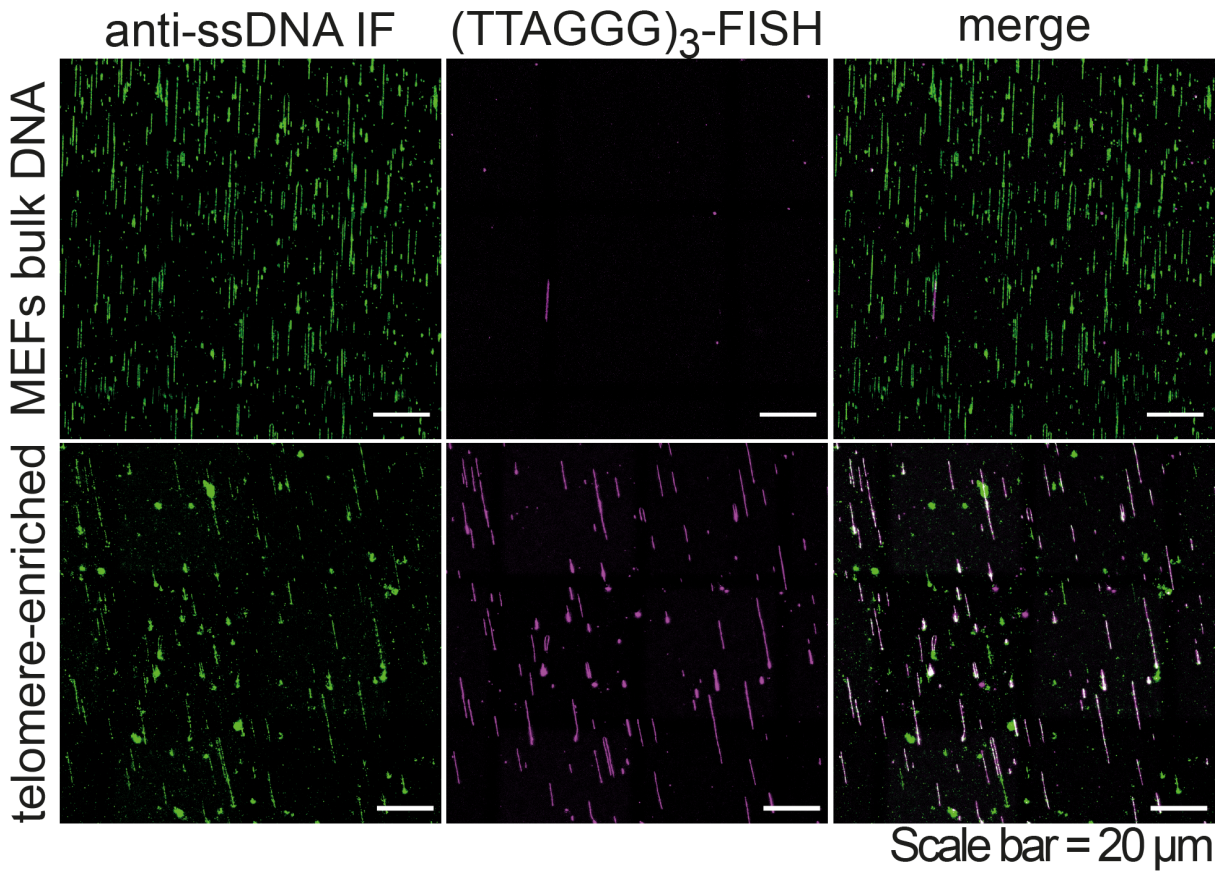

Figure 2. Single molecule analysis showing telomeric DNA enrichment level.
Bulk DNA and telomere-enriched sample were combed on silanized coverslips, denatured in situ and labeled with an antibody against single-stranded DNA (green) and with a Cy3-labeled telomeric (TTAGGG)3 PNA probe (magenta).

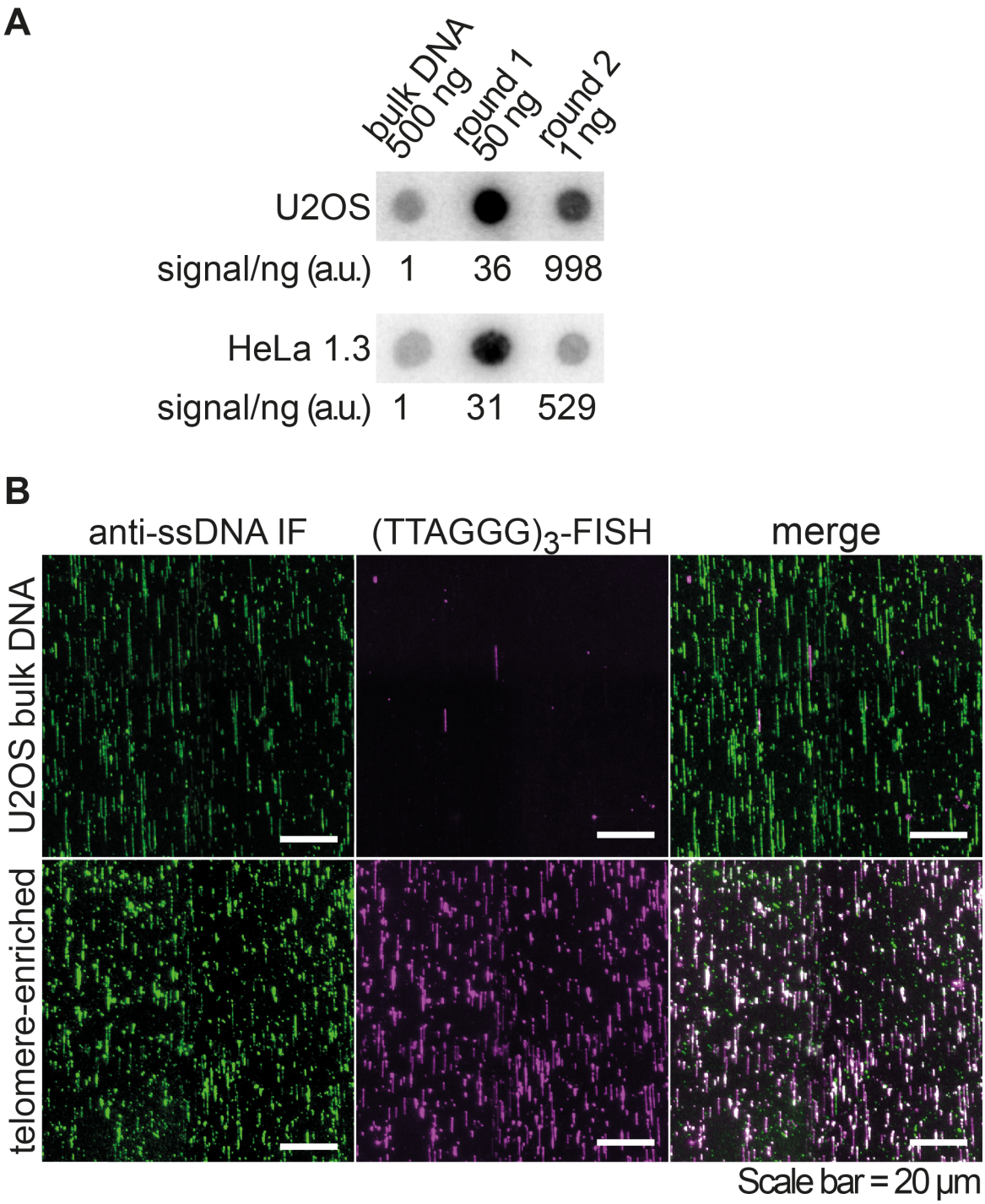

Figure 3. Enrichment of telomeric repeats from human cells.

A. Dot blots showing the enrichment of telomeric repeats of U2OS and Hela1.3. Genomic DNA was subjected to the telomere enrichment procedure shown in Figure 1. The reported amounts of DNA from each step are spotted on membrane and hybridized with a probe recognizing the TTAGGG repeats. The enrichment level was obtained as telomeric signal/ng of each sample relative to the one of the bulk DNA.

B. Single molecule analysis showing U2OS telomere enrichment. Bulk DNA and telomere-enriched sample were combed on silanized coverslips, denatured in situ and labeled with an antibody against single-stranded DNA and with a Cy3-labeled telomeric (TTAGGG)3 PNA probe.

Electron microscopy analysis of telomere-enriched samples

We applied the procedure described above to purify telomeric DNA from SV40-immortalized Mouse Embryonic Fibroblasts (SV40-LT MEFs) in order to analyze their structure by electron microscopy (EM). EM provides nm-scale resolution for the imaging of DNA structures and has been widely used in the past to describe the fine structure of key intermediates in DNA metabolism, such as DNA replication forks or nucleosome distribution, in different systems ranging from bacteriophages to mammalian cells (Inciarte, Salas, and Sogo 1980; Lucchini and Sogo 1995; Sogo et al. 1986). In order to preserve DNA structures by preventing branch-migration during DNA manipulation, prior to cell lysis and deproteinization steps we applied *in vivo* inter-strand crosslinking with psoralen (Lopes 2009). We performed four cycles of crosslinking with trimethylpsoralen (TMP) followed by irradiation with 365 nm light, where first TMP intercalates within duplex DNA and then it is photoactivated by 365 nm UV to generate covalent inter-strand linkage. Previous EM analysis of telomeres were done with the cytochrome C spreading method that involves thick coating of DNA molecules with a basic protein (CytC). Whereas, our samples were prepared with the "BAC method", collected on carbon-coated EM grids, stained with uranyl acetate and rotary shadowed with platinum (Lopes 2009) (see Material and Methods). The low molecular weight of the spreading agent (BAC), compared to protein-based methods, allows a better visualization of details of secondary structures and to appreciate differences in thickness between single-stranded and double-stranded DNA regions. Our telomere-enriched samples resulted to be suitable for EM analysis, generally clean and with a good contrast, indicative of clean DNA preparation. Molecule length range from 2 to 40 kb (Figure 4), compatible with telomere length, but it is likely affected also by unavoidable mechanical fragmentation of the genomic DNA during preparation. However, the consistent presence of long DNA fragments means that our protocol does not cause excessive

mechanical fragmentation of the DNA. During EM analysis of our samples we detected molecules with t-loops (Figure 5). T-loops are a conserved telomeric lariat structure that are generated through the invasion of the 3'-overhang into the double stranded telomeric DNA (Griffith et al. 1999). They have been visualized by electron microscopy, in telomeric-enriched DNA preparation as previously discussed, in mouse and human cells but also in trypanosomes, ciliates, plants, C. elegans and in Kluyveromyces lactis (yeast) (Griffith et al. 1999; Nikitina and Woodcock 2004; Munoz-Jordan et al. 2001; Murti and Prescott 1999; Cesare et al. 2003; Raices et al. 2008; Cesare et al. 2008). Counting the occurrence of t-loops in our preparation, as expected, we found higher incidence in the samples enriched for telomeric repeats compared to the bulk DNA (Figure 5B). In literature the t-loop frequency is reported to range from 15% to 40%, whereas our samples have t-loops frequency of around 5%. It is possible that t-loop visualization in EM is limited by the density of psoralen-crosslinking. T-loops are formed by the strand invasion of the 3'-overhang that in mammalian cells is around 50-500 nt (Palm and de Lange 2008). If an inter-strand crosslink does not occur at least once at the t-loop junction, t-loops would be resolved during the protocol enrichment. Given that psoralen crosslinking is limited by protein binding, it is possible that proteins that associate with the t-loop junction, might limit crosslinking and stabilization of t-loops (Wellinger and Sogo 1998). During the setting of the protocol for telomeres purification we tried to increase both the amount of psoralen and the cycles of crosslinking, but we observed that the digestions steps and the consequent levels of enrichment were negatively affected. We therefore proceeded in the analysis by electron microscopy of the telomere enriched samples, relative to the bulk DNA, in order to identify specific telomeric structures or intermediates.

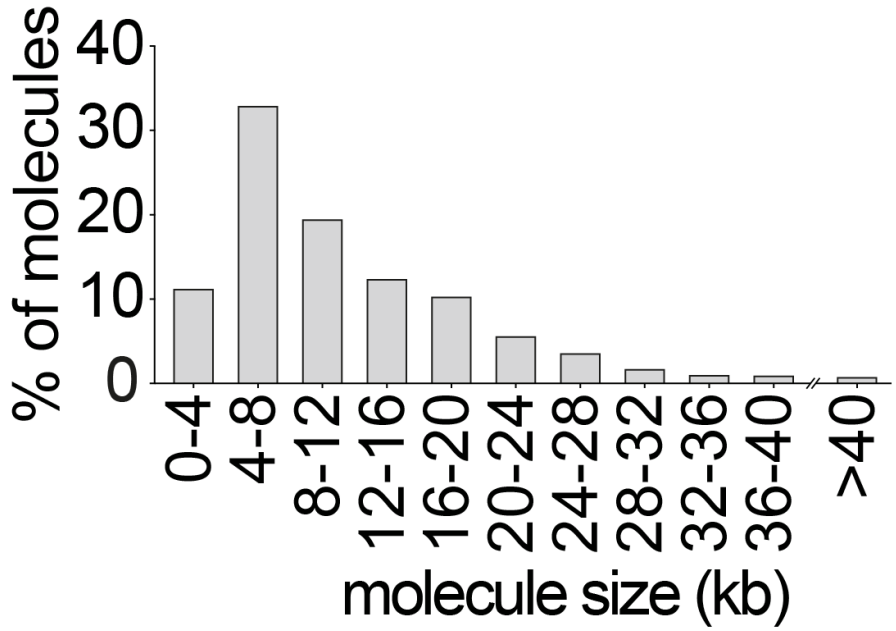

Figure 4. Molecule length distribution in telomere-enriched sample in electron microscopy.

Molecule length distribution of a representative telomere-enriched sample. N=1516 molecules.

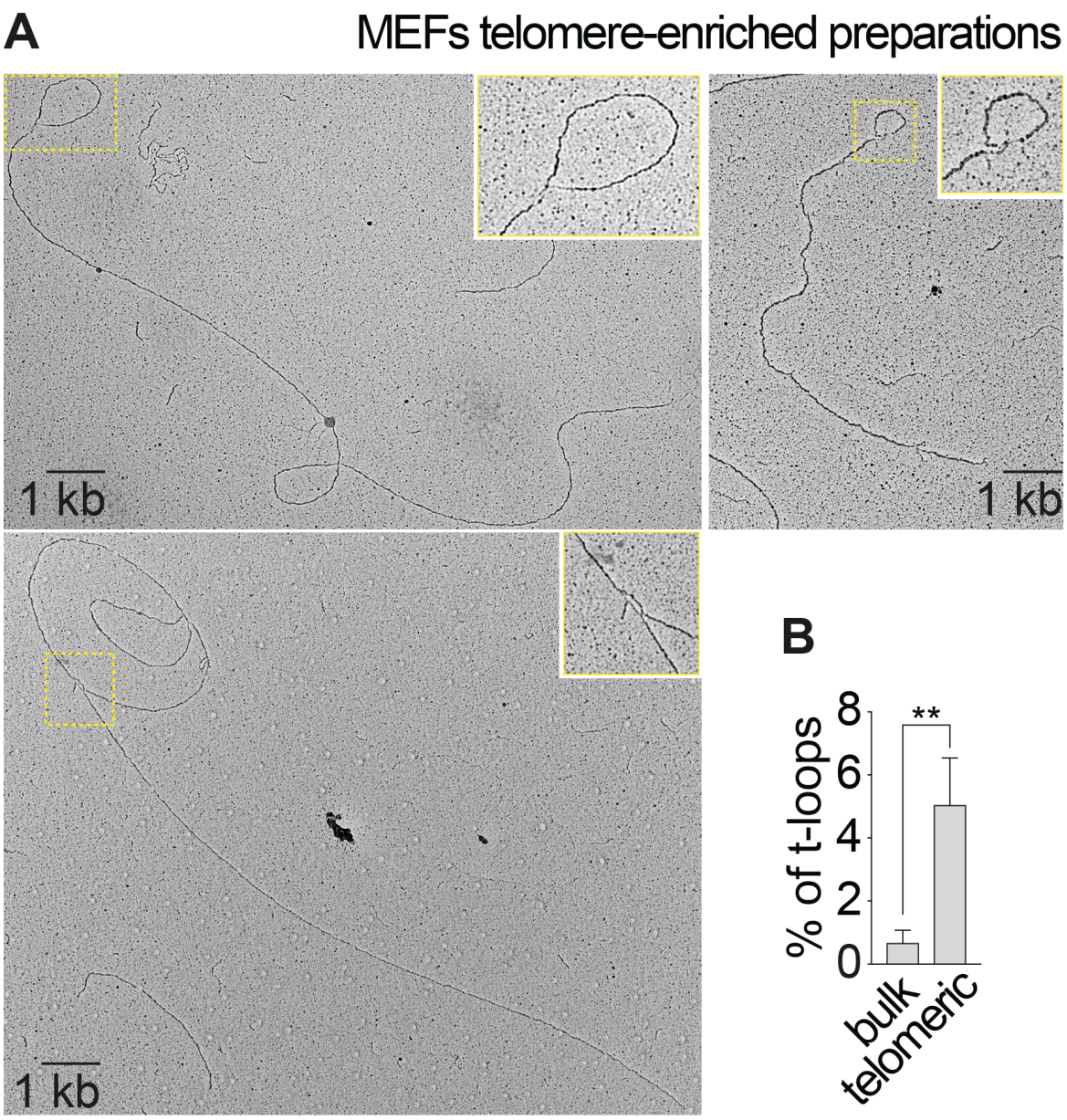

Figure 5. T-loops in telomere-enriched sample.

A. Examples of molecules with t-loops observed by EM in telomere-enriched samples. The area in yellow rectangles is showed enlarged two times in insets.

B. T-loops percentage in the bulk genomic DNA sample compared to the telomere-enriched sample. Bars represent the mean with the standard deviation.

Intramolecular loops enriched in telomeric DNA

Apart from the classical telomeric structures, we noticed that telomere-enriched samples had a high incidence of molecules containing internal loops (i-loops; Figure 6). These i-loops are distinct form t-loops since they do not appear to engage DNA ends but rather involved crossing of the internal regions of the DNA molecules. We considered the possibility that their formation could be due to random folding during the DNA preparation and spreading of the sample for the EM. To test this possibility, we decided to spread in parallel telomere-enriched DNA and is relative non-enriched genomic DNA control, which was fragmented at similar size by restriction enzyme digestion. The frequency of molecules with i-loops was analyzed in samples obtained from three independent experiments. SV40-LT MEFs telomere-enriched samples, resulted to contain around 14% of molecules with at least one internal loop, whereas in the fragmented genomic DNA they represent around the 3% (Figure 6B). We also test if this difference can be appreciated preparing telomere enriched sample using an alternative spreading method, the Kleinschmidt method (Kleinschmidt and Zahn 1959). Differently from the BAC method, where DNA is mixed with formamide and spread on a large water surface (hypophase), the Kleinschmidt method consists in the mix of the DNA with cytochrome C, a protein that will form a thick coating on the molecules, and incubated as droplet. Same preparations (both bulk DNA and telomere-enriched) were spread in parallel with the two methods and EM images where analyzed for the presence of molecules containing internal loops (Figures 7 and 8). Even in Kleinschmidt spreads, we detected molecules containing i-loops and their quantification reveal an accumulation of these molecules in telomere enriched samples compared to the bulk DNA, although the background level was higher than the BAC spreading (Figure 8), therefore we concluded that BAC method remains the more suitable for our investigation about the nature of these loops. Importantly, these data confirm that internal loops are not an artefact

caused by the EM spreading procedure but characterize telomere-enriched preparations. Furthermore, we considered the possibility that accumulation of i-loops could be a consequence of our telomere-enrichment procedure per se, rather than being a biological feature of telomeric repeats. To test this possibility, we performed a mock enrichment procedure, where genomic DNA from SV40-LT MEFs was subjected to all the steps of the protocol but omitting the restriction enzymes. The final sample was prepared for EM analysis where we found that internal loops occur on around the 5% of the counted molecules (N=927 molecules). From this experiment we concluded that the abundance of the i-loops at telomeric repeats cannot be simply attributed to the telomere enrichment procedure. Apart from mouse telomeres, we found molecules with internal loops also in human cells with long telomeres, Hela1.3, and similarly to what we observed in SV40-LT MEFs preparations, they accumulate in telomeric DNA enriched samples compared to genome wide (Figure 9). In both SV40-LT MEFs and Hela1.3, i-loops resulted to be variable in size: in SV40-LT MEFs ranged from 0.2 to 2.5 kb with a median size of 1.6 kb, similar size distribution was observed in the Hela 1.3 i-loops (Figure 10 A). In SV40-LT MEFs samples we also looked at i-loops distribution and in around of 55% of the molecules occur a single i-loop, whereas the remaining 25% is represented by molecules with two or more i-loops (Figure 10 B). The i-loop frequency reported above was estimated by analyzing large fields of EM grids acquired at low magnification (16500X) that is sufficient to identify the topology the molecules. In order to better visualize the fine structure of the i-loop junctions, we acquired single i-loops images at higher magnifications (8700X to 135kX) in SV40-LT MEFs telomere enriched samples (Figure 11). We noticed that often, at the level of i-loops junctions or in close proximity, there are single-stranded gaps, discernible from double-stranded DNA since appear as thinner tracts (Figure 11, red arrows). We counted the occurrence of this conditions and resulted that one in four i-loops

had single-stranded regions at the level of the junction whereas another 20% occurs close to gap, where sometimes is possible to observe a small flap of DNA (Figure 11, red asterixis). These observations, together with the consideration that telomeres are made of repetitive elements, lead us to hypothesized that i-loops could form in the presence of single-stranded DNA damage at telomeric repeats.

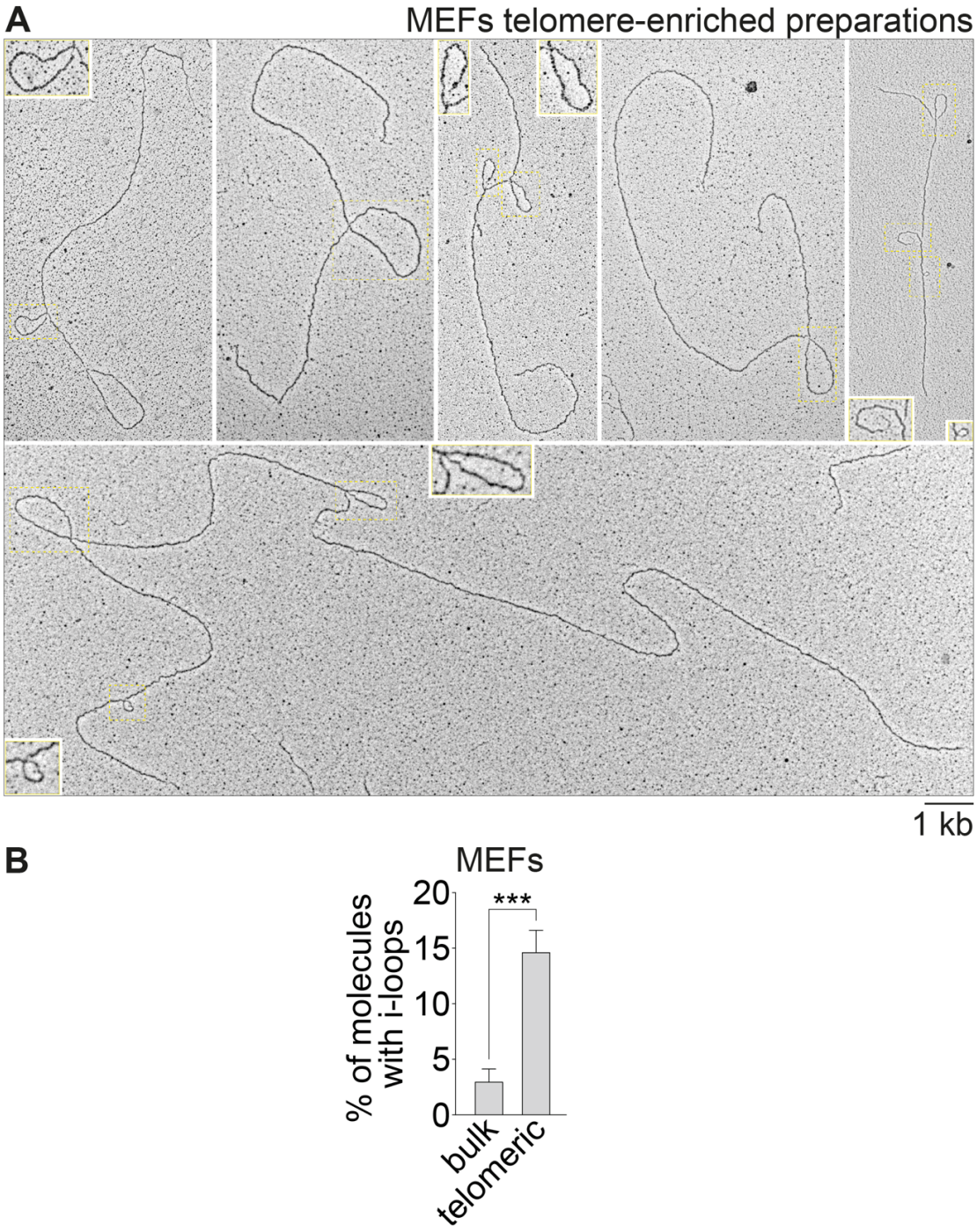

Figure 6. I-loops enriched at SV40-LT MEFs telomeric DNA.

A. Examples of molecules containing i-loops acquired in SV40-LT MEFs telomeric-enriched samples by EM, obtained with the procedure described in figure 1. Insets show 2X enlargement of i-loops contained in yellow rectangles.

B. I-loop quantification in bulk genomic DNA and telomere-enriched samples coming from EM analysis of three independent experiments. Bulk DNA was prepared digesting genomic DNA with KpnI that produce DNA fragments of 10 kb in average.

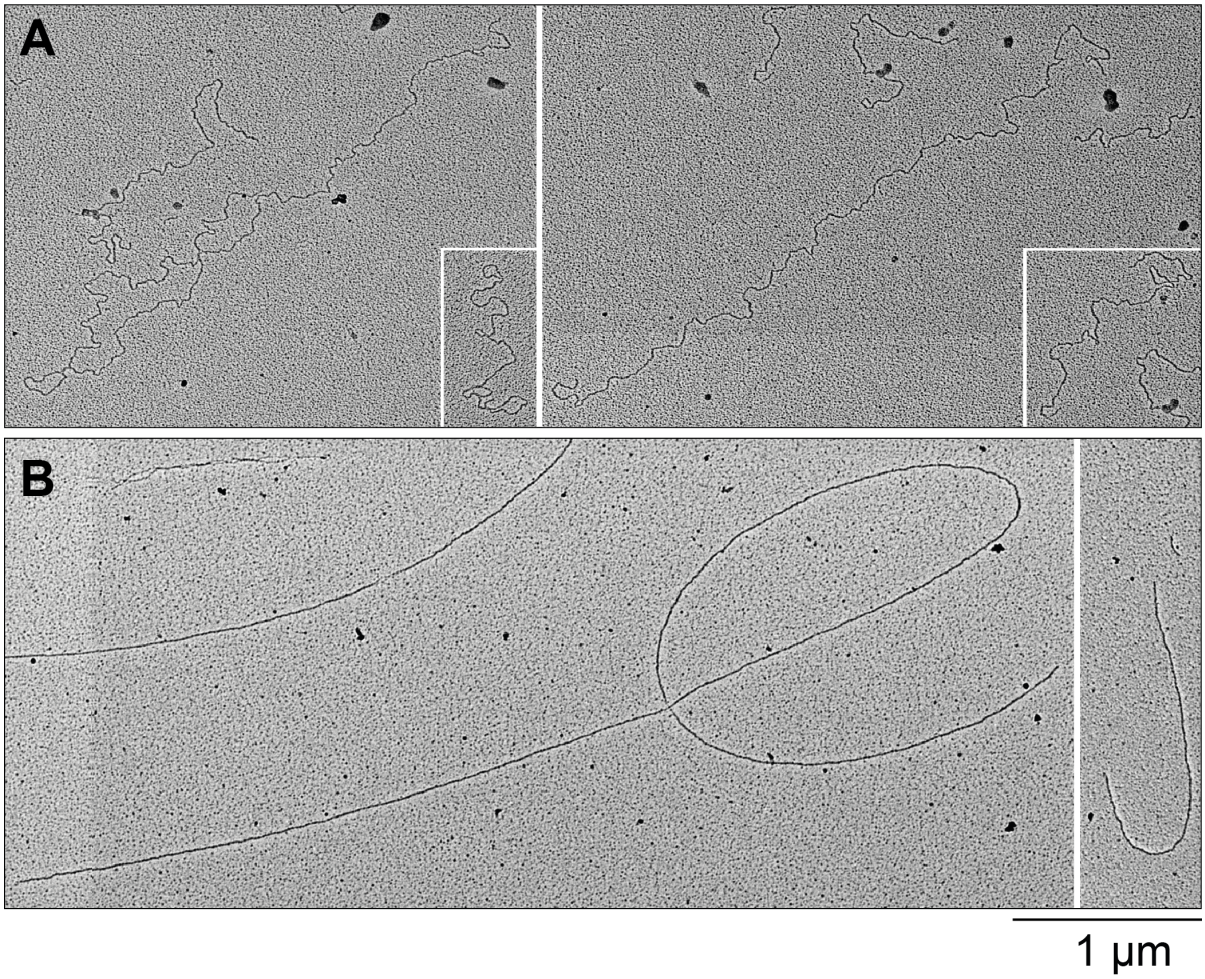

Figure 7. I-loops in Kleinschmidt and BAC EM spreading.

A-B. Mouse genomic DNA was fragmented by restriction digestion with KpnI and spread either with the Kleinschmidt method (A) or with the BAC method (B). Representative EM images of both linear and i-loop-containing molecules from the two spreading.

A

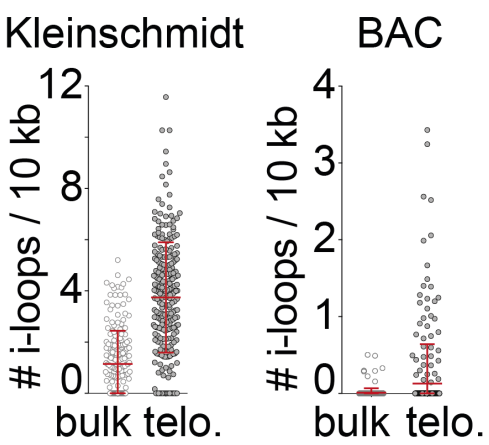

B

	Kleinschmidt		BAC	
	bulk	telo.	bulk	telo.
frequency (i-loops/10 kb)	0.92	3.21	0.04	0.10
% with i-loops	60.3	92.9	3.0	11.2
N (molecules)	194	253	265	384

Figure 8. Accumulation of molecules with internal loops in Kleinschmidt and BAC EM spreading.

A. I-loop density, calculated as number of i-loop each 10Kb in each sample. Each dot represents a molecule and bars represent the standard deviation. The number of molecules analyzed for each is reported in the last lane of table D.

B. I-loop occurrence in Kleinschmidt and BAC spreading of the KpnI-digested SV40-LT MEFs DNA. The first line reports the frequency of i-loop (i.e. the cumulative number of i-loops encountered/cumulative molecule length). The second lane reports the percentage of molecules containing at least one i-loop. The last row indicates the number of molecules analyzed for each sample.

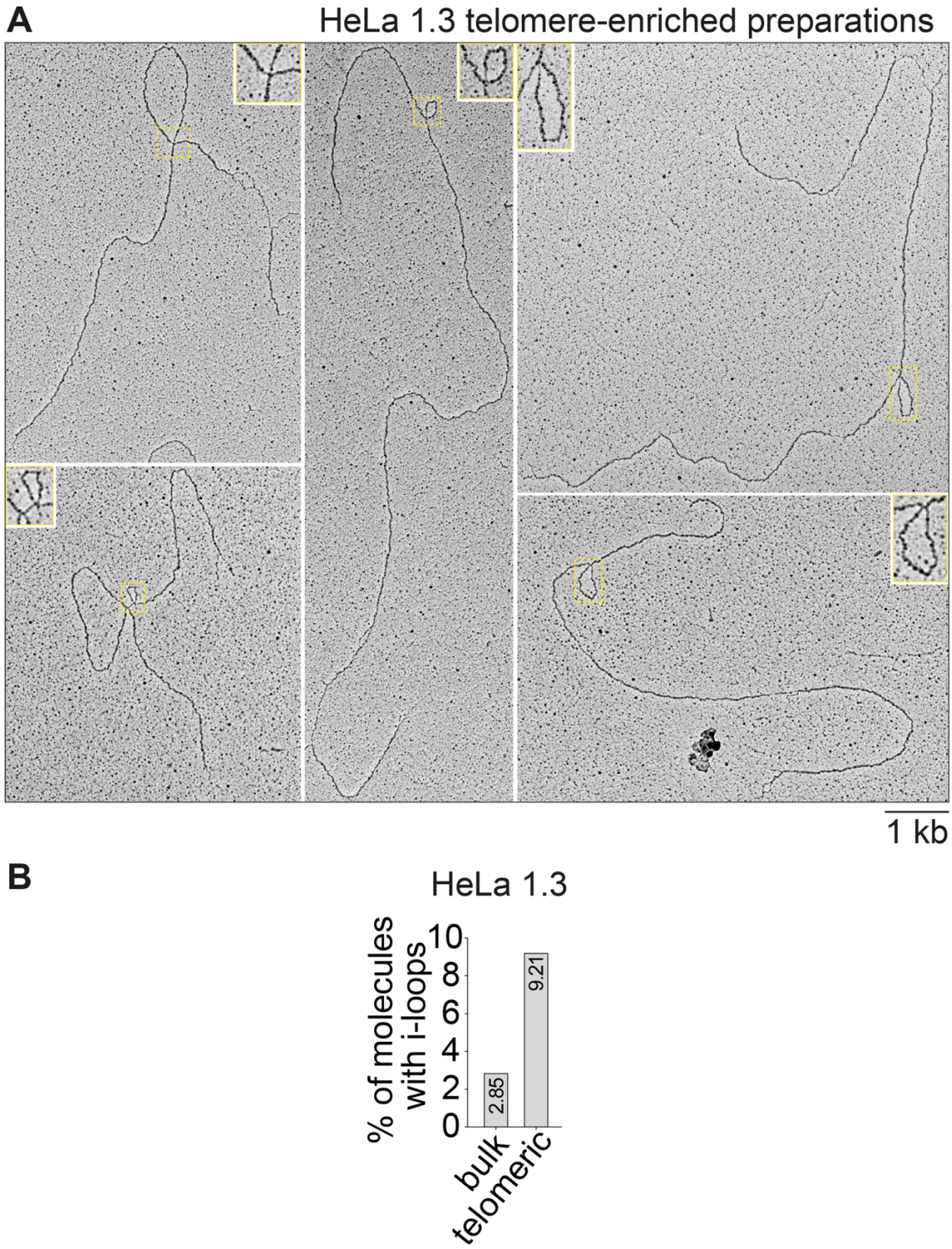

Figure 9. I-loops in Hela1.3 telomere-enriched sample.

A. Representative EM images of i-loops observed in telomere-enriched sample of Hela1.3. Insets show 2X enlargements of the area inside the yellow rectangles.

B. I-loop quantification in non-enriched genomic DNA and in telomere-enriched Hela1.3 samples. Bulk DNA N-1510, telomere enriched N= 239.

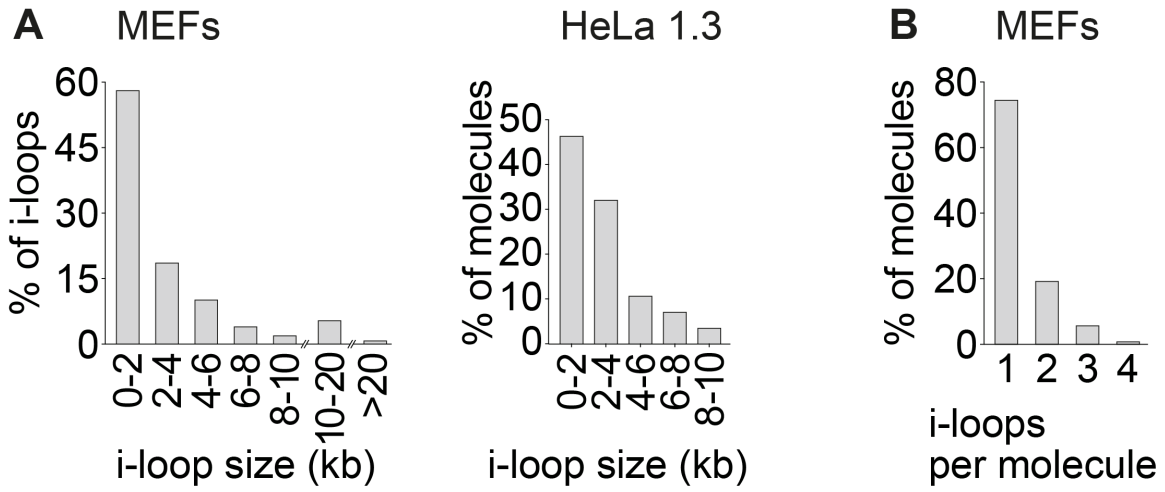

Figure 10. I-loops analysis in telomeric DNA of SV40-LT MEFs telomeric and Hela1.3.

A. I-loops size distribution in telomeric DNA of SV40-LT MEFs (N=342 i-loops) and Hela1.3 (N=28 i-loops).

B. Distribution of number i-loops/molecules in SV40-LT MEFs telomeric DNA. N= 266 molecules with i-loops.

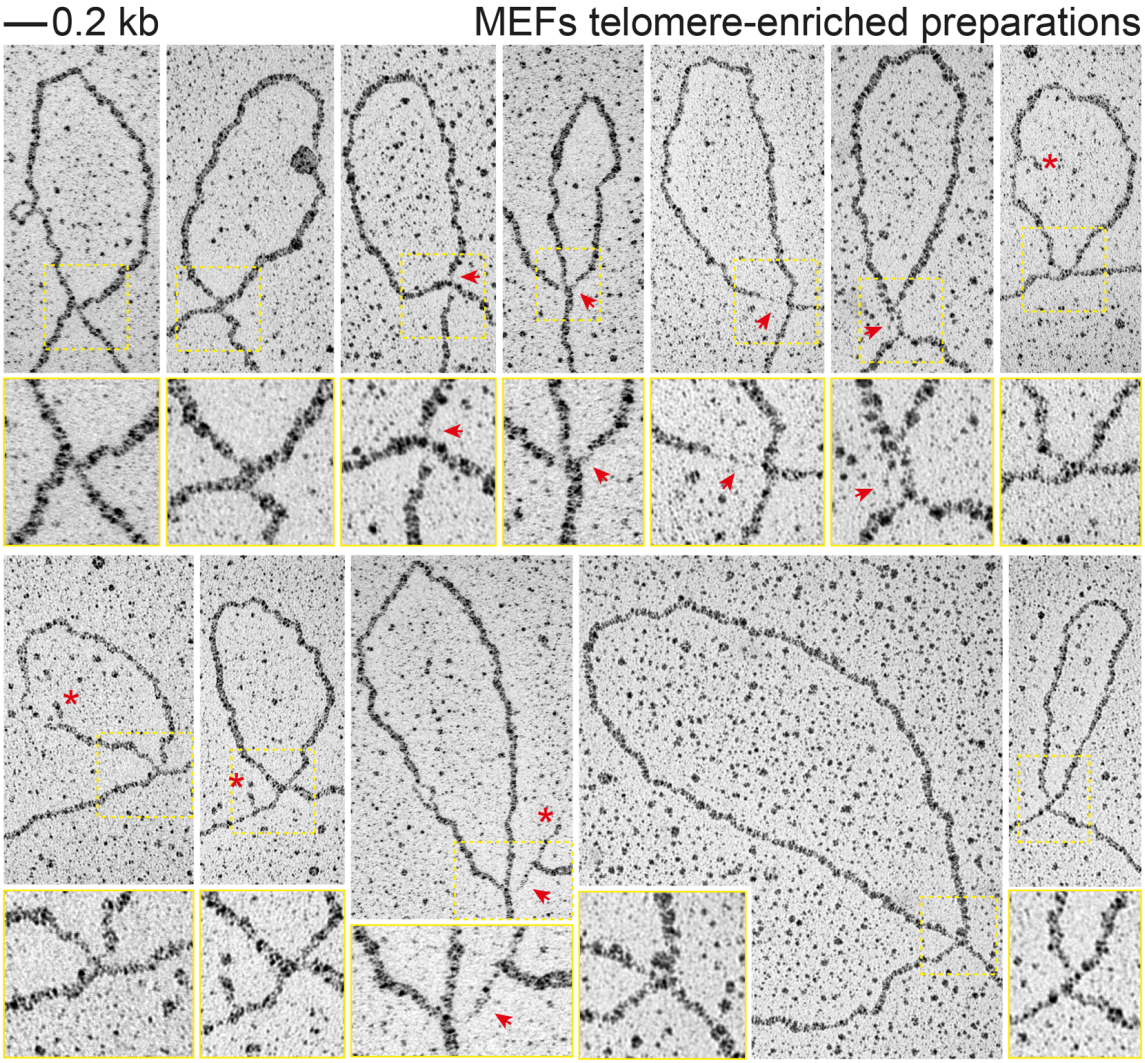

Figure 11. I-loops forms in proximity to single-stranded damage.

EM images at high magnification of i-loops observed in telomere-enriched sample. Insets shown 2X enlargement of i-loops junctions. Red arrows indicate regions of single-stranded DNA and asterisks point to DNA flaps.

I-loops represent the most frequent structures detected at ALT telomeres

The occurrence of i-loops next to tracts of single stranded DNA directed our attention to ALT cells, since it has been reported that they accumulate single-stranded damage at telomeric repeats, such as nicks and gaps (Nabetani and Ishikawa 2009; Wang, Smogorzewska, and de Lange 2004). ALT telomeres have been extensively studied in 2D-gel electrophoresis, where DNA is separated in a first dimension according to their size followed by a second run where DNA migration is influenced by the structure. ALT telomeres in 2D-gel reveal an unusual arc, named t-circle, initially described as open (containing nick) circular double stranded DNAs (Cesare and Griffith 2004; Wang, Smogorzewska, and de Lange 2004). However, upon close inspection, t-circle arc migration is close, but not exactly overlapping with the migration of open circular DNA markers (double-stranded circular DNA containing nick), suggesting that the molecules that generate the t-circle arc may not be simple open circular DNA species but a more complex one (Nabetani and Ishikawa 2009). Since i-loops include a circular shape that might be compatible with the migration in the t-circle arc, we decided to apply our procedure to purify the telomeres from the t-circle area in order to visualize their structure by EM. For this purpose, we performed a large-scale genomic DNA extraction from U2OS (ALT) cells and telomeric DNA was purified with the procedure described above except for the second round of enrichment where DNA, after the second round of digestion, was separated in 2D gel instead of a preparative agarose gel (Figure 12). This step allowed us to extract directly from the gel, and separately, the DNA accumulated in the t-circle area and the one migrated as linear. In order to verify the level of enrichment for telomeric DNA in this setting, we performed dot blot analysis using as representative of the second round 1ng of the linear sample since the amount DNA recovered from the t-circle area was too low. Our final samples resulted to be properly enriched for telomeric repeats therefore optimal for EM

analysis. As expected, the DNA from the t-circle area was enriched for structured molecules (Figure 13). Specifically, around 9% of the molecules of the t-circle arc are circular (Figure 13 and 14), and 28% of these show a single-stranded gap (Figure 14, red arrows) confirming previous observations about accumulation of double-stranded (t-circles) and partially single-stranded C-circles in ALT cells (Wang, Smogorzewska, and de Lange 2004; Cesare and Griffith 2004; Henson et al. 2009). However, over 40% of all the molecules recovered from the t-circle area were molecules containing one or more i-loops (Figure 13 and Figure 14), 4-fold more abundant than telomeric circles. I-loops were largely found in otherwise linear molecules, although some of them were found also in molecules having a t-loop at the end, or at branched molecules. Considering that about 40% of the molecules recovered were linear, i-loops represented overall ~80% of the structures detected in the t-circle arc. To note that the presence of linear molecules in the material purified from the t-circle area could be due to imperfect separation of large amounts of genomic DNA in agarose gel and in part to structure resolution during the isolation from 2D gel. It is not uncommon that in EM preparation of genomic DNA recovered from areas of 2D gels where should be only structures there are linear "contaminants". For example, a similar approach applied to study of meiotic recombination intermediates in yeast, yielded around 60%-80% of linear molecules isolated from an area of the gel where structured DNA migrates (Cromie et al. 2006). Interesting, focusing our attention on the analysis of the i-loops in t-circle sample, we observed that, similarly to what was seen in SV40-LT MEFs telomeres, ALT i-loops often occur in close proximity to strand damage (Figure 9 D, red arrows). These results provide direct evidence that different structures, including telomeric circles, t-loops and replication intermediates can populate the t-circle arc in ALT cells however, molecules containing one or more i-loops are the majority of DNA

structures detected in this arc. The frequent proximity of i-loops to single-stranded gap suggests that telomere damage is involved in the i-loop formation.

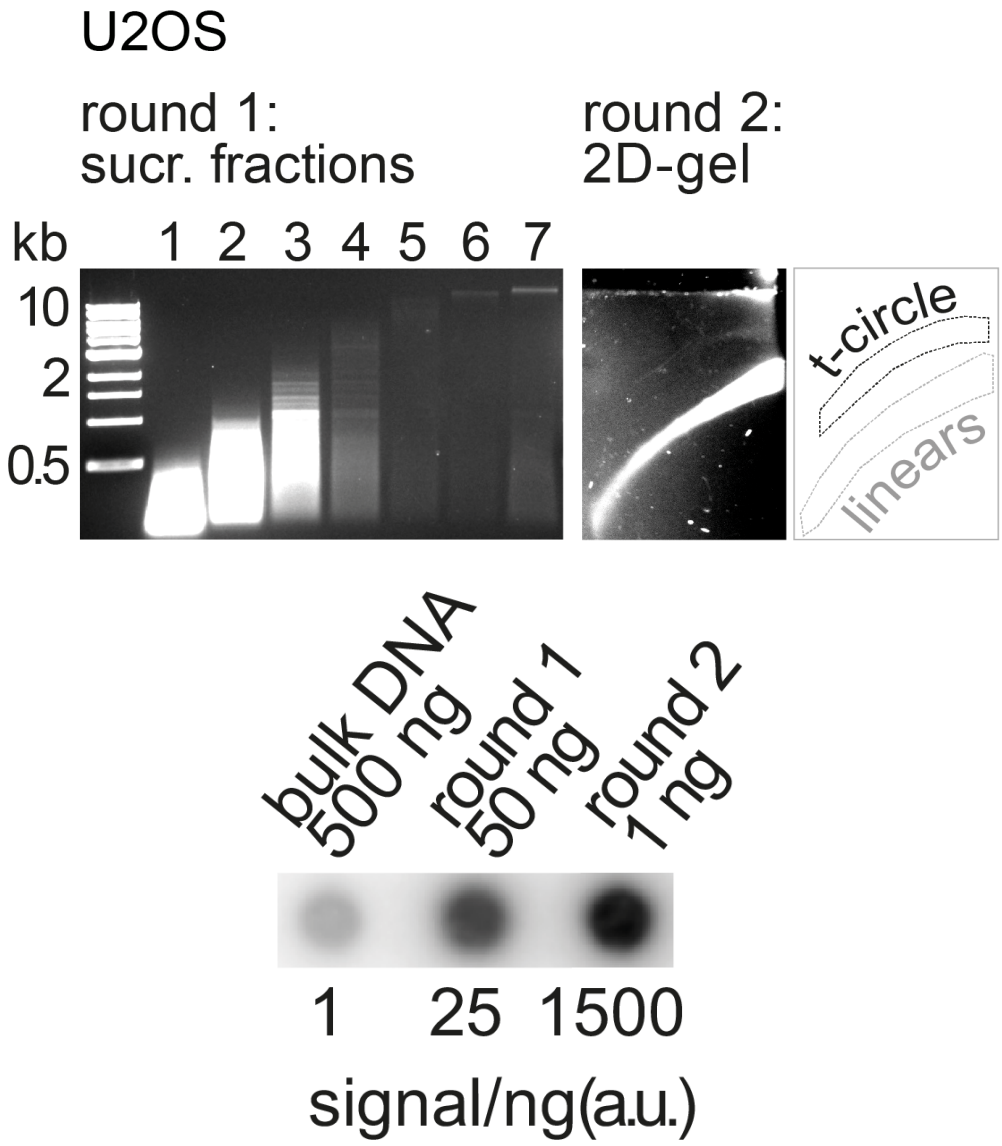

Figure 12. U2OS telomeric DNA purification from 2D gel.

Telomeric DNA from U2OS cells was purified using the protocol described in Figure 1, except for the separation in 2D gel instead of preparative agarose gel in the second round of enrichment. The area of the t-circle and of the linear signal were excised and DNA recovered for EM analysis. Dot blot analysis: indicated amounts from each step were spotted on membrane and hybridized with a probe recognizing TTAGGG repeats. The DNA used as second round spot is the linear sample. The level of enrichment is indicated as amount of signal/ng reported relative to the non-enriched DNA.

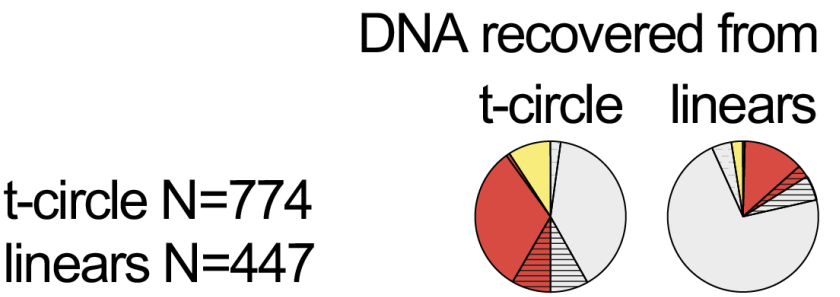

	t-circle	linears
circles	**9.2%**	**2.5%**
with i-loops	**40.8%**	**16.1%**
t-loops with i.loops	8.4%	2.7%
branched with i.loops	0.8%	0.4%
linear with i.loops	31.6%	13.0%
without i-loops	**50.0%**	**81.4%**
t-loops	8.4%	5.4%
branched	2.2%	4.2%
linear	39.4%	71.8%

Figure 13. I-loops are the most represented telomeric structures in ALT cells.
The pie chart showing the distribution of the molecules recovered from 2D gel. Percentage of the three major categories are highlighted, whereas in the table is reported the detailed sub-distribution of each category.

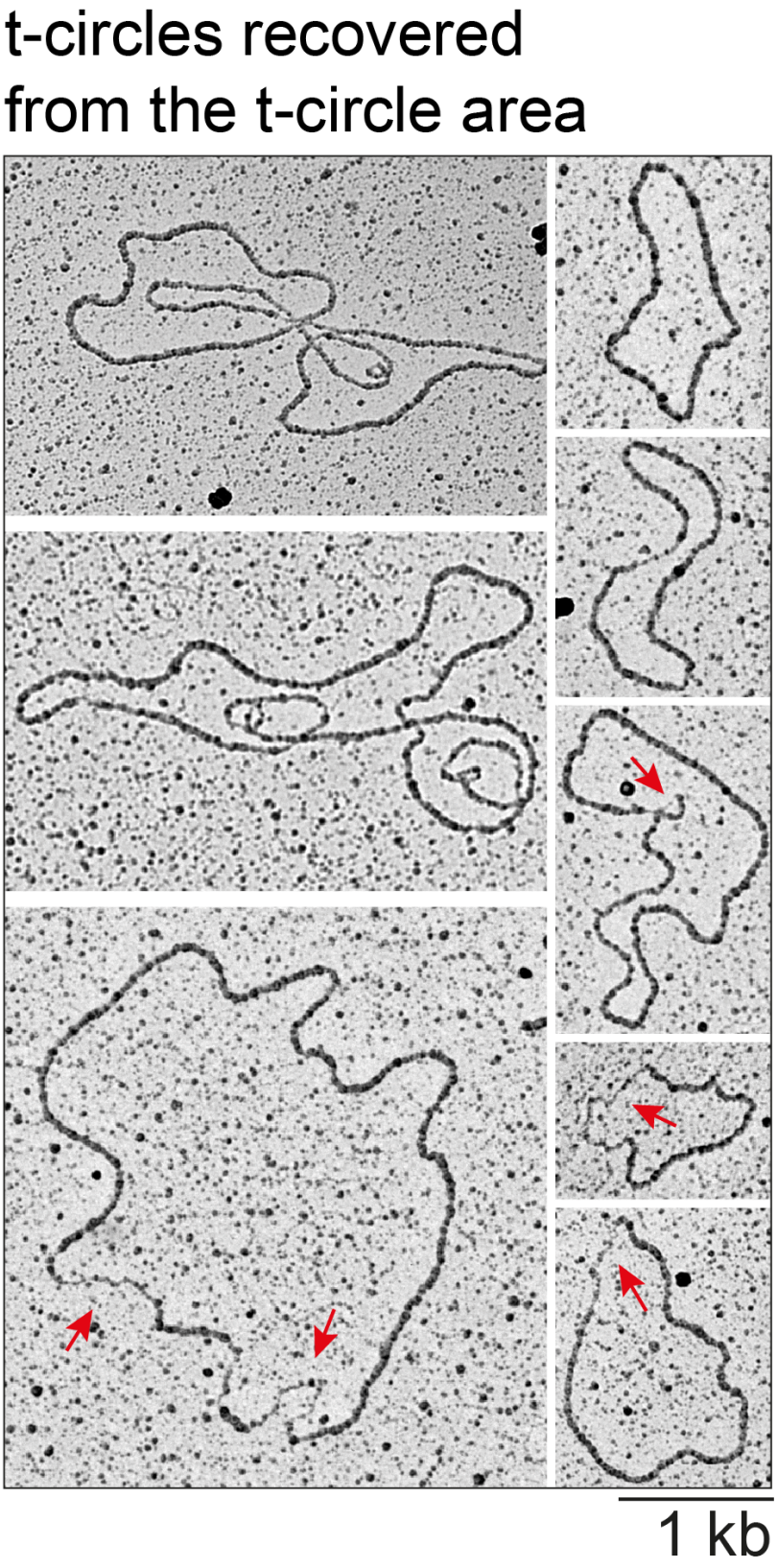

Figure 14. Telomeric structures from the t-circle area include telomeric-circle.
Examples of circular molecules visualized in the EM analysis of the DNA recovered from the t-circle area. Red arrows point to single-stranded regions.

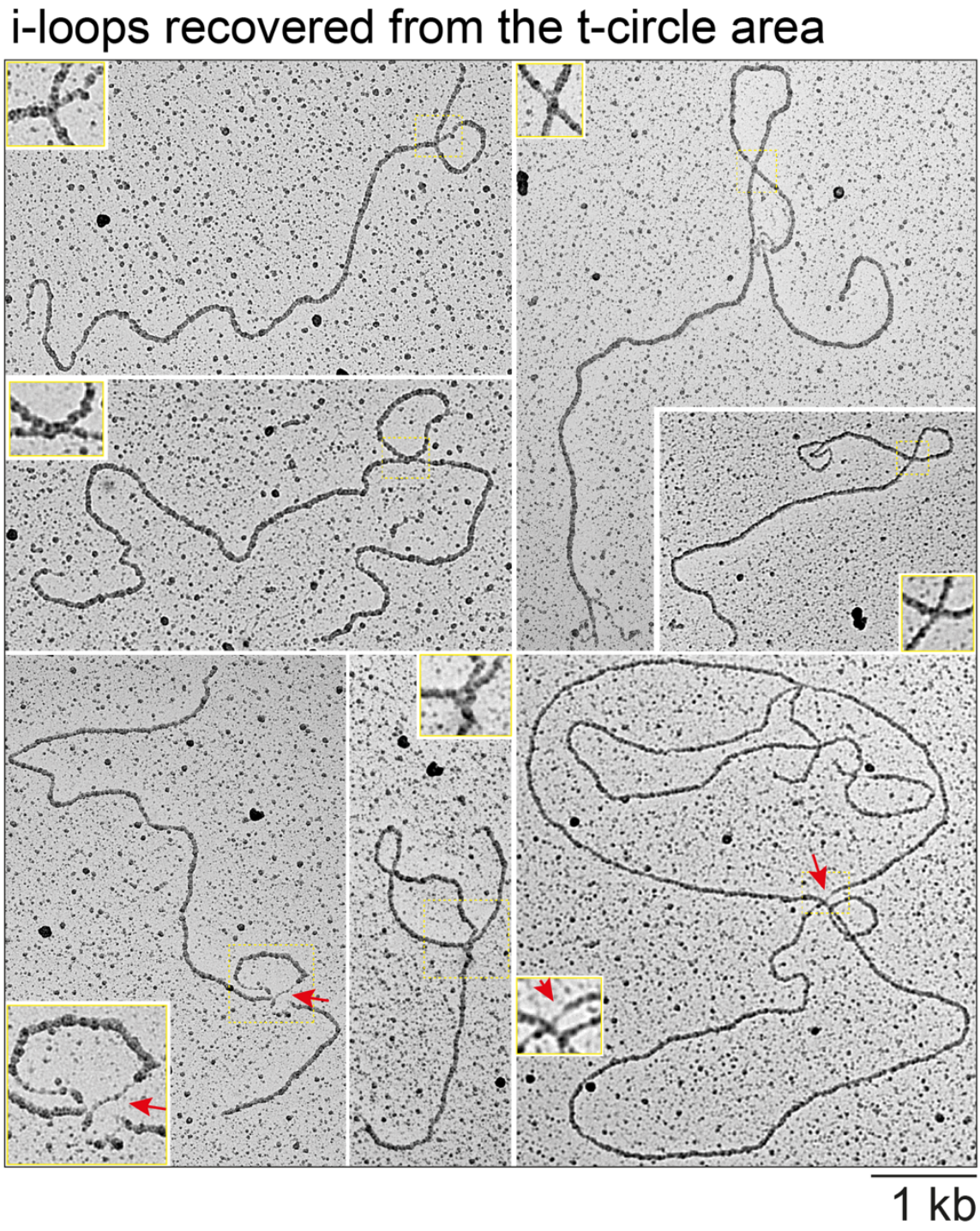

Figure 15. I-loops are the most represented telomeric structures in ALT cells.
Examples of molecules with i-loops found in the DNA purified from the t-circle arc. 2X enlargement of the area inside yellow rectangle in shown in the insets. Red arrows indicate single-stranded regions at the junctions.

I-loops formation is induced by single-strand damage at telomeric DNA

Based on the occurrence of i-loops close to single-stranded gaps and their abundance in the t-circle arc in ALT cells, we hypothesized that i-loops could be associated with telomere damage. Therefore, we asked if damaging telomeric DNA we can induce i-loop formation. To test this possibility, we set up experiments with the DNase I enzyme, which induces both nicks and gaps (Riley 1980). In order to monitor i-loops formation in a condition resembling in vivo situation, where DNA is still bound by proteins in chromatin state, we used SV40-LT MEFs nuclei. SV40-LT MEFs nuclei were incubated with increasing concentration of DNase I, the reaction was stopped, DNA was extracted and separated by 2D gel electrophoresis (Figure 16 A). The telomeric DNA coming from the mock treatment, as expected, resulted to be mainly linear (Figure 16 A, black arrow), whereas after the DNase I-treatment in addition to the linear arc, telomeres show an accumulation of the t-circle signal (Figure 16 A, yellow arrows). The increasing intensity of the t-circle arc with the treatment is confirmed by the ratio of the t-circle and the linear signal quantification relative to the untreated sample. We wanted then to verify if this structural transition, is specific for telomeric repeats or is a general feature of nicked DNA. Therefore, I performed a similar experiment where SV40-LT MEFs nuclei undergo to mock or a DNase I treatment and the recovered DNA was separated in duplicate in two 2D gels. After blotting, one membrane was hybridized with a telomeric probe, while the other with a probe recognizing the mouse L1 interspersed repeats (Figure 16 B). The telomeric DNA in the DNase I-treated sample generated the t-circle arc as observed previously, while the L1 repeats did not show the same structural transition remaining represented entirely by linear molecules. Moreover, representative ethidium bromide pictures coming from a single second-dimension gel (both were equal) has been reported as genome wide profile where DNA is made only by linear molecules both in the not treated condition and after DNaseI treatment. These

results underlined the peculiarity of the accumulation of the t-circle arc after DNaseI treatment for telomeres. In addition, we investigated if the same structural transition in response to DNaseI treatment occurs also in human (non-ALT) cells with different telomere length. For this purpose, we used Hela 204 with short telomeres (2-4 kb), HTC75 where telomeric DNA in average is around 4-8 Kb and Hela1.3 cell line with long telomeres (in average 20 kb long) (Figure 17 A). Nuclei of each cell line were treated with DNase I, similarly to what performed for SV40-LT MEFs and the recovered DNA was separated in 2D gels to monitor the presence of the t-circle arc (Figure 17 B). If in response to the mock treatment telomeres are all in the linear conformation, after the DNase I nicking the t-circle arc was visible in all the cell lines (Figure 17 B, yellow arrows). Interestingly, we observed a relation between the accumulation of the t-circle signal and telomere length where the induction of the arc strongly decreased in shorter telomeres. Since these results were obtained treating DNA in nuclei, we asked if the chromatin environment or any chromatin-associated factors are required for the generation of those telomere structures that migrates in the t-circle arc. To answer this question, I performed mild DNaseI treatment on isolated, protein-free, genomic DNA extracted from SV40-LT MEFs cells. As performed in nuclei, I used increasing amounts of DNaseI and after the inhibition of the reaction, the DNA of each condition was separated in 2D gel and hybridized with a telomeric specific probe (Figure 18 A). Surprisingly, the treatment on protein-free DNA induced a strong accumulation of the arc signal, similarly to what observed with the treatment in nuclei. Differently from the experiments performed in nuclei, also in the mock treatment there is a faint arc signal, probably due to telomere nicking during extraction and manipulation. However, the ratio between the arc and the linear signals of each samples compared with the mock treatment show that the t-circle arc is more than the double after DNaseI treatment. Then, starting from the same bulk of genomic DNA, I repeated this experiment with

double amounts, in order to split each sample in half and run two 2D gels. Each gel was transferred on a membrane, one hybridized with telomeric probe and the other with a probe recognizing the mouse L1 repeats. Similarly, to the result obtained with the DNaseI digestion in nuclei, also in this setting, the arc induction is not a general feature of nicked DNA, but occurs at telomeric repeats and not in L1 repeats or at bulk genomic DNA (Figure 18 B). These results demonstrated that t-circle arc can be generated even in absence of telomeric circles and, it may, represent an intrinsic ability of telomeric repeats to undergo structural transitions in the presence of damage. Having established that telomere damage is sufficient to promote the formation of the t-circle arc in 2D gels, we wanted to verify the nature of the telomere structures that accumulate in response to DNaseI nicks. For this purpose, I set up a large scale DNaseI treatment on SV40-LT MEFs nuclei in order to purify telomeric DNA and analyze it by EM. Around $500x10^6$ of SV40-LT MEFs nuclei were incubated with buffer (mock) or with DNaseI, DNA was extracted after psoralen crosslinking and processed for telomeric DNA purification following the procedure described in Figure 1. I obtained final samples represented by around the 50% of telomeric molecules (Figure 19 A) that were spread and analyzed in EM. Telomere damage induced by DNaseI lead to three-fold increase in i-loops formation compared to the mock treatment, whereas i-loops levels in the bulk genomic DNA after treatment remain basal (Figure 19 B,C). These experiments provide a clear evidence that telomere damage is sufficient to induce i-loops formation that are responsible for 2D-arc generation in 2D gel.

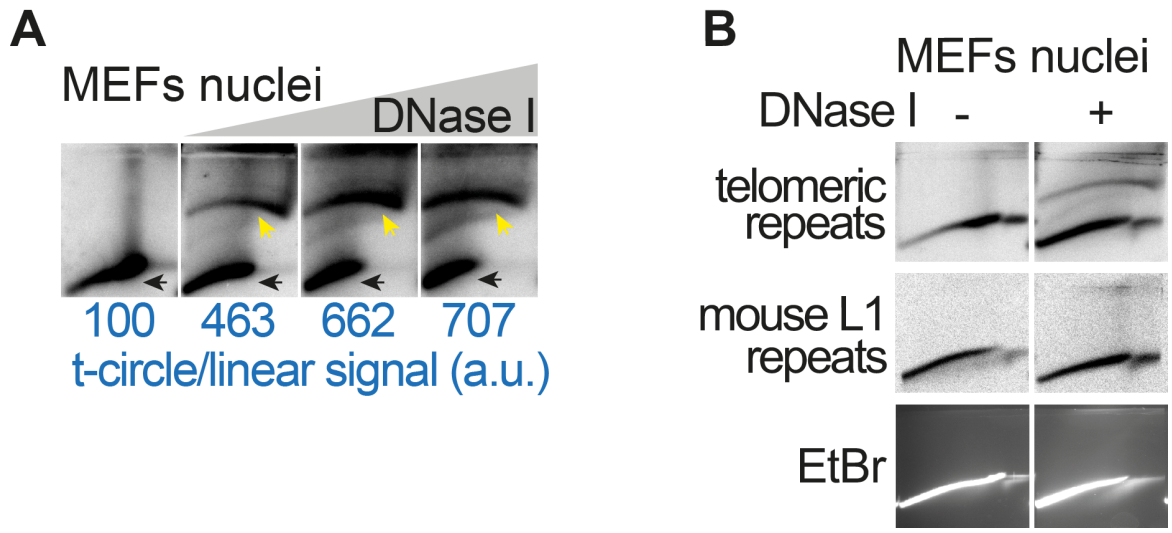

Figure 16. T-circle arc is induced by DNA damage in non-ALT cells.

A. 2D gels showing the strong induction of the t-circle arc (yellow arrows) at telomeres by nicks and gaps induced by DNaseI treatment of SV40-LT MEFs nuclei. The ratio between the t-circle arc and the linear signal (black arrow) is reported as relative to the untreated sample, arbitrarily set to 100.

B. 2D profile of SV40-LT MEFs DNA untreated or treated in nuclei with DNaseI for telomeric repeats, L1 mouse highly repeated sequence and genome wide (ethidium bromide). Ethidium bromide profiles were equally representative and only one is reported. t-circle arc is specifically induced at telomeric DNA.

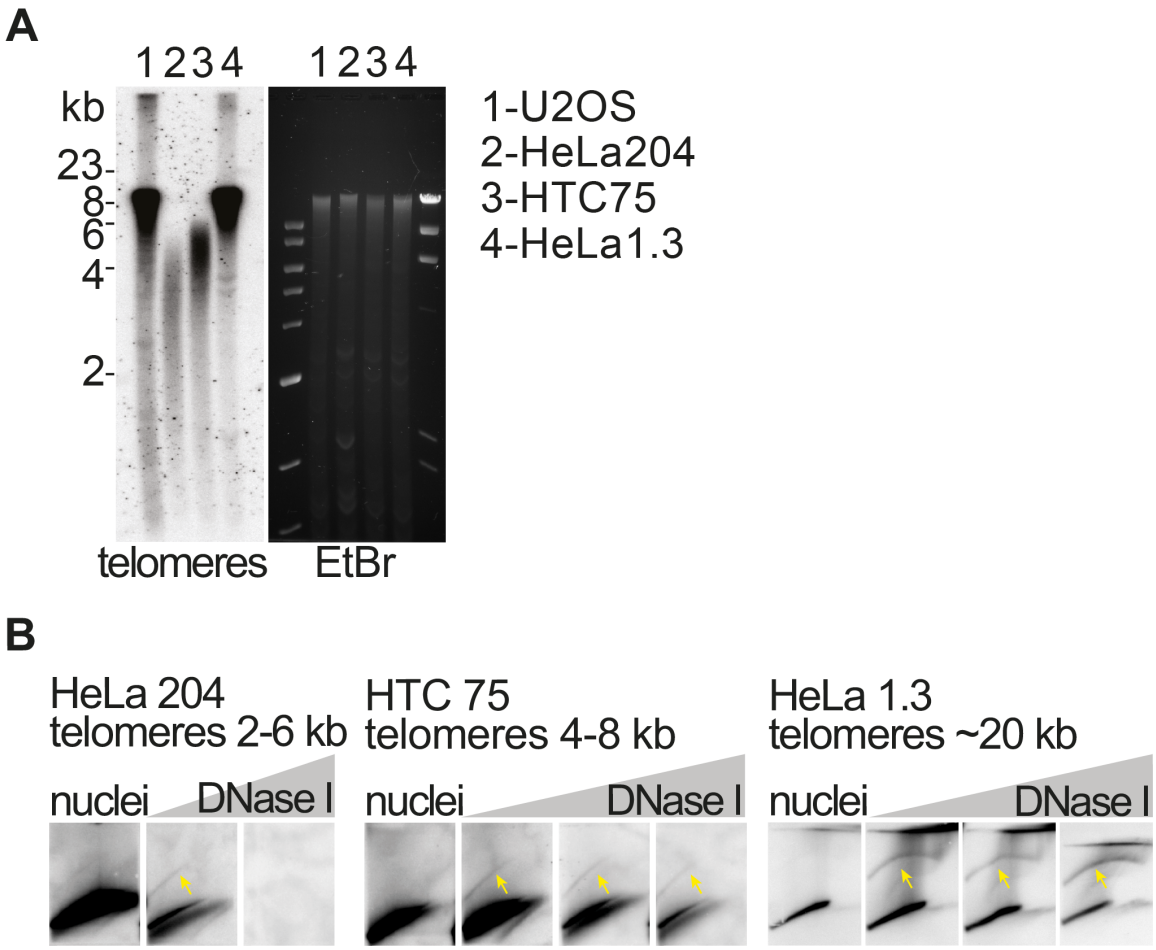

Figure 17. T-circle arc induction is related to telomere length in human non ALT cell lines.

A. Blot of AluI- and MboI-digested DNA showing telomere lengths for the indicated human cell lines.

B. T-circle arc induction (yellow arrows) by DNaseI treatment at human non ALT telomeres. Shorter are the telomeres, weaker is t-arc induction.

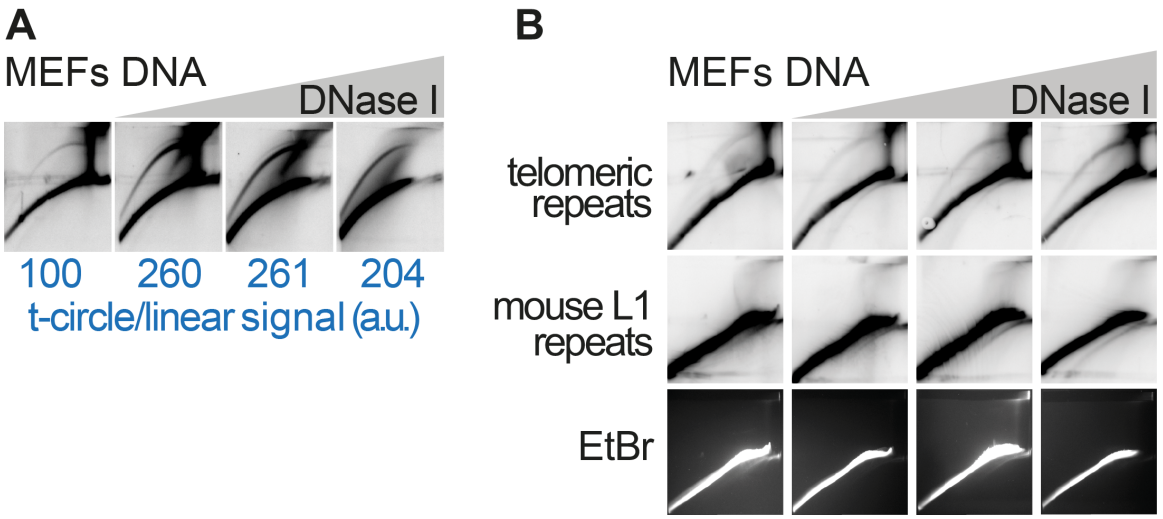

Figure 18. T-circle arc is induced also by DNA damage on purified DNA.

A. 2D gels showing the induction of the t-circle arc at telomeres by DNaseI treatment of SV40-LT MEFs extracted genomic DNA. T-circle arc can form spontaneously at telomeres. The ratio between the t-circle arc and the linear signal is reported as relative to the untreated sample, arbitrarily set to 100.

B. DNase I treatment on isolated DNA does not induce the t-circle arc in the bulk genomic DNA or at the L1 repeats. Ethidium bromide profiles were equally representative and only one is reported.

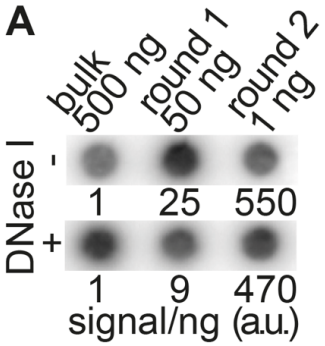

B

Sample	i-loops	N
Mock-treated, telomeric	10.6 %	490
DNase-I, telomeric	30.6 %	206
DNase-I, bulk DNA	2.6 %	310

Figure 19. I-loops are induced by telomere damage in non ALT cells.

A. Level of telomeric DNA enrichment after large-scale DNaseI treatment. Around 500x10^6 SV40-LT MEFs nuclei were treated either with 5 µg/ml of DNaseI or without for 8 minutes. The recovered DNA was processed to purify telomeric repeats with the procedure described in Figure 1. The reported amounts of DNA are spotted on membrane and hybridized either with a probe specific for telomeric repeats. The enrichment level was obtained as telomeric signal/ng of each sample with to the one of the bulk DNA.

B. I-loops accumulation observed by EM analysis in telomeric DNA, untreated or DNaseI-treated, and in genomic DNA digested with KpnI after DNaseI treatment (bulk).

C. Examples of molecules with i-loops observed in the DNaseI-large scale enrichment experiment described above. 2X enlargement of the area inside yellow rectangle in shown in the insets.

The formation of i-loops requires branch migration

Considering that single-stranded damage is sufficient to induce i-loop formation and that the damage resulted often to be at level of the i-loop junction or in close proximity, we hypothesized that these structures involve strand-annealing and branch migration at damage site, favored by the high level of homology of the telomeric repeats. To investigate this hypothesis, I applied the system normally used for EM analysis to prevent branch migration, the psoralen inter-strand crosslinking, before DNaseI treatment. If the formation of i-loops after DNaseI damage result to be sensitive to crosslinking, could confirm that events of strand invasion and branch migration are actually required. SV40-LT MEFs DNA was crosslinked in nuclei prior to DNaseI treatment. After DNA extraction, for each sample we monitor the telomeric 2D-gels profiles. While the non-crosslinked samples showed the expected induction of the t-circle arc, this signal was strongly inhibited in the crosslinked sample (Figure 20 A). This was also confirmed by the ratio of the t-circle and the linear signal quantification relative to the untreated sample. However, here the t-circle arc formed in response to DNA damage induced *in vitro* by DNase I treatment. In order to confirm that this induction occurs also in response to telomeric DNA damage present *in vivo* and not only in response to eventual nicking due to DNA manipulation, we applied the same approach to ALT cells, where we found that i-loops represent the main telomeric structures forming the t-circle arc. An equal number of U2OS cells were processed in parallel and one pool was crosslinked prior to cell lysis. Extracted DNA from both untreated and crosslinked samples was separated in 2D gel, and hybridized for telomeric DNA (Figure 20 B). The t-circle arc of U2OS is not affected by psoralen crosslinking, confirming that i-loops are present *in vivo* in ALT cells. We therefore conclude that i-loops are a telomeric structure that can spontaneously form at damaged sites and their formation is likely

driven by the extreme abundance of sequence homology which favor strand invasion and branch migration events.

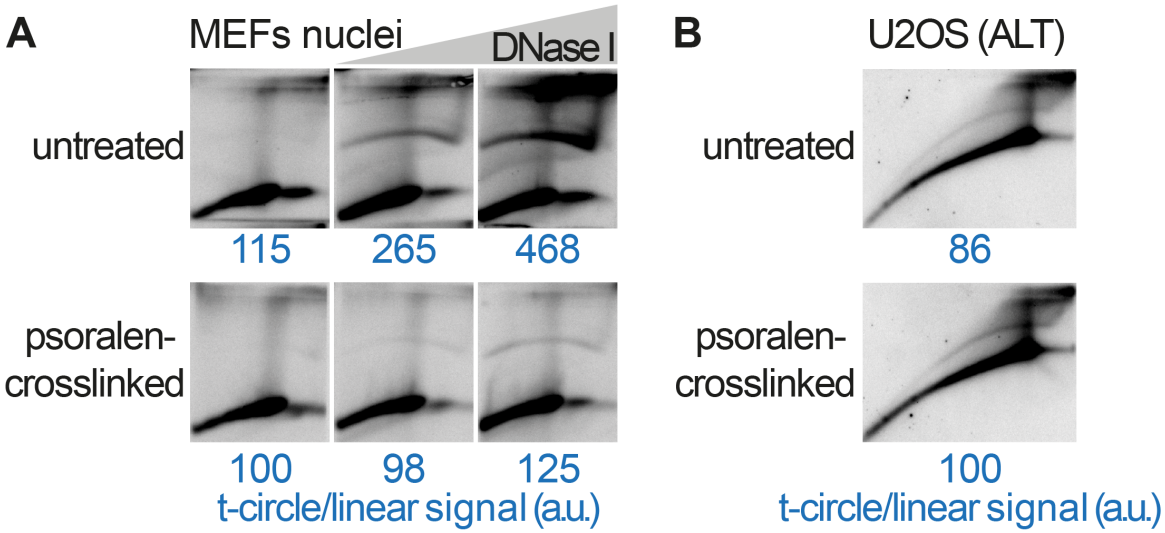

Figure 20. I-loops formation after DNA damage requires branch migration.

A. i-loops accumulation at SV40-LT MEFs telomeres is sensitive to crosslinking. A preparation of SV40-LT MEFs nuclei was equally split in two and one half undergo psoralen-crosslinking (that prevent branch migration). Both crosslinked and untreated sample were divided in three and two part of each treated with increasing concentrations of DNaseI. DNA from each sample was separated in 2D, transferred on membrane and hybridized with telomeric probe. The ratio between the t-circle arc and the linear signal is reported as relative to the sample not treated with DNaseI of each setting, arbitrarily set to 100.

B. i-loops accumulation at ATL telomeres is not affected by crosslinking. As for A, pool of U2OS cells were split in two where half experience psoralen crosslinking. Both genomic DNAs were extracted and processed for 2D-gel. The ratio between the t-circle arc and the linear signal is reported as relative to the crosslinked samples, arbitrarily set to 100.

I-loops are a substrate for the generation of telomeric circles

We showed that i-loops form in response to single-stranded DNA damage and that their formation requires events of strand invasion and branch migration. Telomeric DNA is made of short motif repeated in tandem for several kilobases providing a context with high level of sequence homology. Therefore, our hypothesis is that at telomeric repeats, any single-stranded gap could find a favorable contest for strand invasion or exchange at any other region of the telomere, promoting i-loop formation. Specifically, we propose two models that differs for the position of the starting single-stranded gaps (Figure 21). Two gaps occurring on opposite telomeric strand (i.e., one gap on the G-strand and one on the C-strand of the same telomere) can come in close proximity by looping of the molecule and base pairing could be favored by the complementarity of the sequence. Strand rotation can lead to plectonemic pairing (the pairing of single strands in a linear double-stranded tract) forming the junction of i-loops. The junction than could migrate as hemicatenane and generate a double Holliday junction simply by pairing of the opposite strands (Figure 21 A). Similarly, if two gaps occur on the same telomeric strand (i.e. both gaps on the G or on the C strand of the same telomere) and come in proximity by DNA looping, could undergo directly to strand exchange due to complementarity of the sequence, resulting in an i-loop with a single Holliday junction at the base (Figure 21 B) (Haider et al. 2018). These models are similar to the initial recombination model of Robin Holliday, where strand exchange was proposed to occur at level of single-stranded DNA tract expose in opposite homologous chromatids that can anneal or with the complementary strand form the other chromatid (Holliday 1964). T-loops are formed through strand invasion of the single-stranded 3' telomeric overhang into the double-stranded part of the telomere, forming a three-way junction at the base of the t-loop (see Figure 5B Introduction). Previous work has suggested that limited branch migration at level of the t-loop junction can generate Holliday

junction that, if not protected by TRF2, can be resolved by HJ resolvases leading to t-loop excision and telomere truncation (Wang, Smogorzewska, and de Lange 2004; Schmutz et al. 2017). Following our i-loop model and based on what was already suggested for unprotected t-loops, we hypothesized that also i-loops could be substrate for Holliday junction resolvases. If this is the case, then 50% of the events, when the i-loop junction resolution involved the cleavage on the horizontal axis (Figure 22 A, red arrows), would result in the generation of extrachromosomal telomeric circles and consequent telomere erosion (Figure 22 A). To note that the released circles would contain both a nick and one of the gaps that initially generated i-loop. To test if actually i-loops are a substrate for the generation of telomeric circles, we applied a biochemical approach where we provided genomic DNA containing i-loops to nuclear extracts. SV40-LT MEFs extracted genomic DNA was subjected to DNaseI treatment, that we previously demonstrate to be sufficient to generate i-loops, and after purification was incubated at 37˚C with Hela nuclear extract for 30 min. Since, among other enzymatic activities, also HJ resolvases requires availability of both ATP and Mg^{2+}, we include extra controls, performing the reactions depleting one or the other. The same procedure was applied in parallel to the same genomic DNA in native condition as negative control. The recovered DNA, after phenol-chloroform extraction, was subjected to C-circle assay (in absence of a telomeric primer) that allows to monitor the accumulation of telomeric circles containing nicks or small gaps (Henson et al. 2009) (Figure 22 B). C-circle assay consist in the rolling circle amplification of partially double-stranded telomeric circles by the Phi29 DNA polymerase which is auto-primed by the presence of nick or gap at telomeric circles and results in a long telomeric single-stranded DNA concatemers. The assay refers to C-circles since G-circles, even if specific for ALT cells as C-circles, are 100-fold less abundant (Henson et al. 2009) To define the specificity of the Phi29 amplification, the c-circle assay was performed in double,

where in one set the enzyme was omitted from the reaction. This control, moreover, allow to define the effective amount of DNA loaded on the membrane representing the basal signal of the sample. After nuclear extract incubation and rolling circle amplification, the DNA was blotted on membrane and hybridized in native condition with a telomeric probe in order to selectively detect single-stranded telomeric products. The accumulation of telomeric circles, represented by the increased intensity of the signal, occur only where DNA is both treated with DNaseI and incubated in nuclear extract whereas after the single treatments, amplification did not occur (Figure 22 C, D). Importantly, the no Phi29 control confirms that this increment of the signal is not dictated by a different amount of DNA of that specific sample. Moreover, this accumulation is dependent on the presence of both ATP and Mg^{2+}, consistent with the possible involvement of a Holliday junction resolvase (Figure 22 C). This result confirm that i-loops are a substrate for the generation of extrachromosomal telomeric circles which involves reactions resembling HJ resolution and define i-loops as potential intermediates of telomere damage, leading to extrachromosomal telomeric circle generation and in telomere deletion.

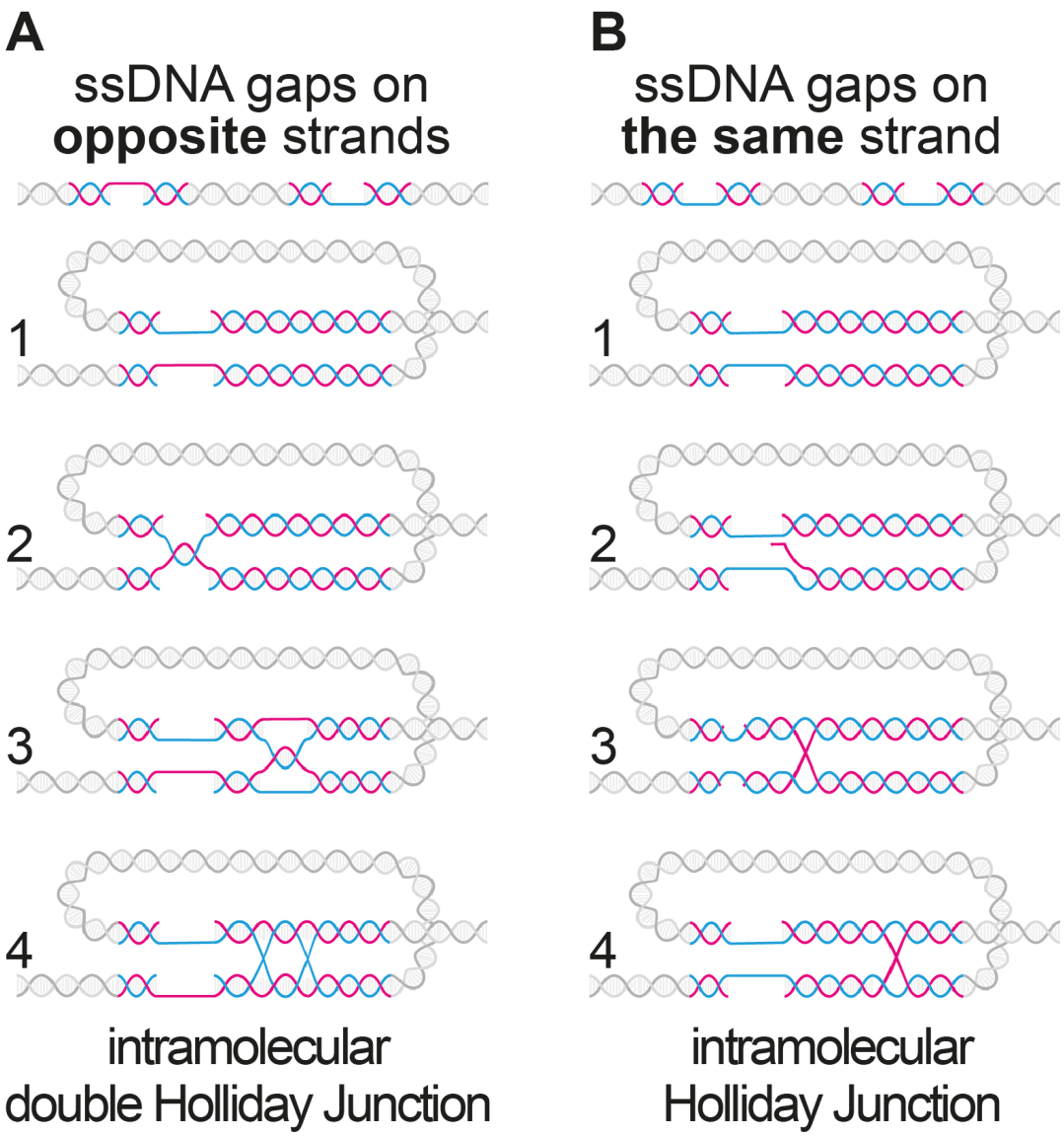

Figure 21. Model for i-loop formation starting from single-stranded damage.

A. Single-stranded damages on opposite strands. Step1: exposed complementary DNA come in close proximity by DNA looping. Step2: strand rotation promotes base pairing leading to i-loop formation. Step3: branch migration as hemicatenane DNA. Step4: pairing of the opposite strand and formation of double Holliday junction.

B. Single-stranded damages on the same strands. Step1: exposed complementary DNA come in close proximity by DNA looping. Step2: strand exchange is promoted by the complementarity of the exposed DNA. Step3: i-loop formation with a single Holliday junction. Step4: eventual branch migration.

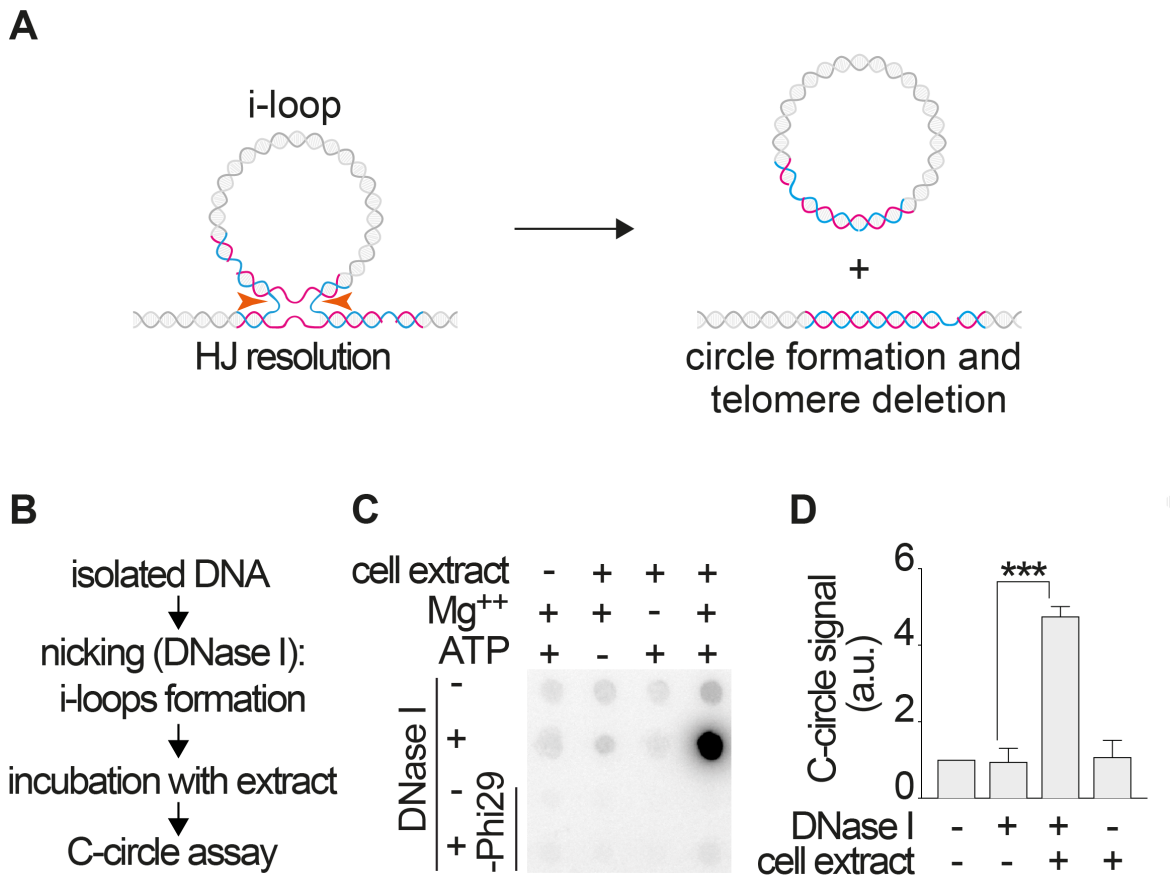

Figure 22. I-loops are a substrate for the generation of telomeric circles.

A. Model of i-loop excision by Holliday junction resolution: horizontal cleavage of i-loop junction (arrows) leads to the formation of telomeric circle containing a nick and one of the two original gap and the loss of telomeric repeats.

B. Experiment procedure used to test the model shown in (C). Protein-free isolated SV40-LT MEFs DNA was treated with DNaseI, in order to induce i-loops formation. After extraction, DNA was incubated with Hela nuclear extract at 37ºC for 30 minutes in order to allow Holliday junction resolution. The recovered DNA was subjected to rolling circle amplification.

C. Telomeric signal of C-circle assay products (D) in dot blot. After rolling circle amplification the DNA was blotted on membrane and hybridized with telomeric probe.

D. Telomeric signal quantification of C-circle products in dot blot of three independent experiments performed as described in (D). The quantification reported is relative to the untreated sample (no DNaseI, no extract), set to 1. Bar represent the mean with the standard deviation.

DISCUSSION

We developed a new protocol for the purification of telomeric DNA that allowed to investigate telomere structure using electron microscopy (EM). Our samples are characterized by the expected telomeric features, such as t-loops and molecules ending with a single-stranded tract whose length was consistent with that reported for the 3'-overhang, and by replication intermediates (replication forks). We identified then a new category of telomere structures, loops that occur at internal regions, the i-loops. They accumulate specifically at telomeric repeats and we make all the controls to exclude them as artefacts of the enrichment procedure or of EM sample preparation. Investigating about the nature of these structures, using EM at high magnification, we noticed that they often occur in proximity of single-stranded DNA tract, leading us to hypothesize that they could be involved in telomere damage. Actually, we showed that i-loops accumulate at telomeres of both mouse and human cells as consequence of induced single-stranded DNA damage. Moreover, i-loops represent the majority of telomere structures in ALT tumor cells, where telomeres experience endogenous telomere damage. Providing DNA containing i-loops to a nuclear extract, we demonstrated that i-loops are a substrate for the formation of telomeric circles. Based on these results, we developed a model in which i-loops form starting by strand exchange at level of DNA damage and after branch migration, Holliday junctions can form at the base of the loop that can be resolved leading to formation of extrachromosomal telomeric circles and shortened telomere.

I-loops in DNA damage-induced telomere erosion

I-loops are related to telomere damage that have important roles in telomere erosion. However, the molecular mechanisms that translate telomere damage in telomere shortening are not well understood (Petersen, Saretzki, and von Zglinicki 1998; von Zglinicki 2000). Telomere shortening occurs normally and gradually in

cells where telomerase activity is suppressed, as in somatic cells, due to the inability of the DNA replication machinery to fully replicate the lagging strand (end-replication problem) and the 5' end resection involved in 3' overhang formation (Huffman et al. 2000). The process occurs until the formation of critically-short telomeres, that losing their chromosome ends protective function activate the DNA damage response (DDR) leading to senescence or apoptosis. Telomere-induce senescence limits the tissue regeneration (ageing) and acts as a barrier against tumorigenesis (Greenberg et al. 1999; Rudolph et al. 1999; Qi et al. 2003; Feldser and Greider 2007). On the other end, dysfunctional telomeres can be source a of genome instability: when cell-cycle checkpoints are lost and consequently cells continue to proliferate in the presence of critically-short telomeres, a condition called telomere crisis, the number of unprotected telomeres increase increasing the probability they fuse with each other. With the progression of cell cycles, fused chromosomes undergo to a series of breakage and fusion (BFB cycle) leading to a wide spectrum of cancer-relevant genome alteration (Murnane 2006; Maciejowski and de Lange 2017). For all these reasons, the understanding of the processes that leads to loss of telomeric repeats is important to define causes of accumulation of genome instability and cancer transformation. In addition to the gradual erosion, telomere loss can occur suddenly and it could be caused by DNA damage. I-loops form as consequence of telomere damage and we showed that they are substrates for the formation of extrachromosomal telomeric circles, leading consequently to telomere shortening. Therefore, the formation of extrachromosomal telomeric circles is a process that contributes to telomere erosion. I-loops could link telomere damage to telomere erosion and extrachromosomal telomeric circles accumulation, providing a mechanism for telomeric circle formation.

I-loops as potential obstacle for telomere replication fork progression

Telomere replication could be another link between telomere damage and the loss of telomeric repeats, since telomere replication forks are terminal and their collapse at level of damaged sites would promote telomere loss in one division. Besides, telomeres behave as replication fragile sites, they repetitive nature make them hard to replicate and the presence of secondary structures, such as G quadruplex, the tightly bound proteins and the ongoing transcription (TERRA) can represent obstacles for the replication forks (Sfeir et al. 2009; Fouche et al. 2006). It has been reported that the deficiency of different helicases, such as RTEL1, WRN and BLM, as well as nucleases like SXL4 and Fanconi anemia complex increase telomere fragility and telomere loss (Vannier et al. 2012; Crabbe et al. 2004; Ding et al. 2004; Sarkar and Liu 2016; Joksic et al. 2012). These proteins being recruited at telomeres by shelterin components could be directed towards specific structures that otherwise could interfere with telomere replication causing collapse and loss of telomeric repeats. Frequent formation of i-loops could provide another challenge to replication fork progression at telomeric repeats contributing to telomere fragility and all the component cited before, might be involved in their resolution or excision as extrachromosomal circles in order to preserve telomere replication fork progression.

i-loops excision as sources of extrachromosomal telomeric DNA and telomere heterogeneity in ALT cells

ALT cells are characterized by extreme telomere length heterogeneity, single-stranded damage accumulation at telomeric repeats and constant presence of extrachromosomal telomeric circles (Wang, Smogorzewska, and de Lange 2004; Cesare and Griffith 2004; Henson et al. 2009; Bryan et al. 1995; Nabetani and Ishikawa 2009). The accumulation of telomeric circles in ALT cells has been also associated to the formation of a peculiar arc (t-circle) in 2D gel which is consistent

with the migration of circular-shaped molecules. We demonstrated that the telomeric arc in 2D gel can be induced also in non-ALT cells after DNA damage and, from the same condition, EM analysis revealed that the telomere-enriched samples accumulate molecules with i-loops three times more compared to the control and the bulk genomic DNA, where i-loops levels remain basal. These results indicate that the t-circle signal detected in 2D-gels can form also in absence of circular molecules. In order to investigate the different telomeric structures that accumulate in ALT cells, we analyzed by EM telomere-enriched DNA extracted from the ALT t-circle arc and we observed that the most represented structures are molecules with i-loops. Since i-loops can form telomeric circles and represent the vast majority of the telomeric structures in ALT cells probably due to endogenous telomeric DNA damage accumulation, our model could provide an explanation about the continuous generation of telomeric circles and, leading to stochastic deletions, partially explain the telomere length heterogeneity in these cell lines.

I-loops and telomere length

Telomeric circle accumulation and telomere heterogeneity was reported also in telomerase-positive human cells when telomeric DNA was artificially elongated and in stem cells suggesting that the generation of extrachromosomal telomeric circle could be a telomere trimming mechanism used to counteract telomere overextension (Pickett et al. 2009; Rivera et al. 2017). These data sustain the existence of a positive correlation between telomere length and accumulation of the telomeric circles. In agreement with this observation, we showed that inducing DNA damage in cell lines with different telomere length, the accumulation of i-loops strongly decrease with telomere length.

I-loops induction or prevention

The formation of the t-circle arc in 2D, therefore presumably i-loops, is reported also in an increasing list of mutants of genes involved in DNA metabolism and telomere maintenance like in human somatic cells depleted for Ku86 gene, involved in nonhomologous end joining (NHEJ) and in telomere maintenance and mutant for the origin recognition complex (ORC) which coordinates DNA replication at most chromosome sites but localizes at telomeres with TRF2 (Wang et al. 2009; Deng et al. 2007). Even if these mutants apparently seem to be unrelated, following our model the accumulation of telomeric damage could be the common feature that explains the formation of i-loops and consequently the appearance of the t-circle arc in 2D-gels. We demonstrated that i-loop formation requires events of strand exchange and branch migration, since it is inhibited introducing DNA inter-strand crosslinking, which prevents branch migration, before the induction of the DNA damage. In this view, conditions associated with chronic telomere (or DNA) damage, such as chemotherapeutics or replication stress, will promote telomere loss through the formation of telomeric circles whereas mechanisms that prevent i-loops formation at sites of damage, would counteract the accumulation of extrachromosomal telomeric circles. As mentioned before, specialize helicases with strong involvement in telomere metabolism, such as BLM, WRN and RTEL1 could have a role in counteracting i-loops formation by resolution of strand-exchange intermediates or by branch migration and dissolution, thereby reducing the probability of telomere loss due to i-loop excision (Ding et al. 2004; Crabbe et al. 2004; Vannier et al. 2012). These mechanisms could not be efficient in ALT cells due to the presence of non-canonical variant repeats that are interspersed throughout telomeres (Conomos et al. 2012). Apart from specialized factors involved in DNA metabolism like helicases and nucleases, i-loop formation could be significantly influenced by chromatin context and transcription. Telomeres are

known to contain heterochromatin marks like H3K9 trimethylation and HP1, which could limit DNA pairing and exchanges at sites of single-stranded damage (Blasco 2007). In this view it is possible that chromatin relaxation at sites of DNA damage could facilitate i-loop formation, and importantly i-loop formation could be more efficient during telomere replication when the DNA strands are more exposed to pairing and exchange (Hauer and Gasser 2017). Transcription of telomeric repeats could also have a profound impact on i-loop formation. The transient displacement loop formed during transcription could provide a pairing partner for a site of single-stranded break. This situation can be aggravated in conditions associated with the accumulation of stable R-loops. In this view it is important to notice that transcription or R-loops at telomeres will displace and expose the telomeric G-strand, therefore it can be predicted that R-loops could contribute to i-loop formation in the presence of single-strand damage on the G-strand (Figure 23).

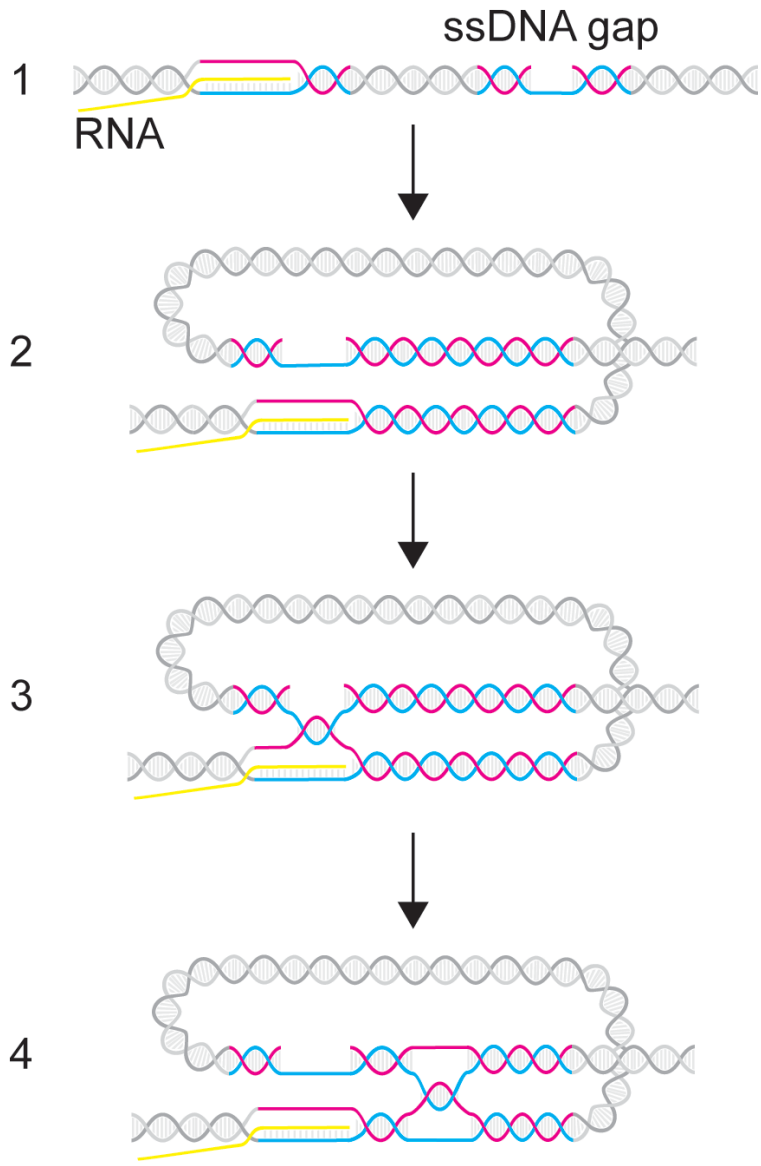

Figure 23. Model depicting i-loop formation mediated by R-loop.

Step1: telomere transcription leads to a transient displacement loop (in yellow, RNA molecule) exposing a single-stranded DNA portion can could be a pairing partner for a single-strand gap present along the telomeric DNA. Step2: as for the model proposed in Figure 21, a single-stranded gap at a different point of the telomeric DNA can come in close proximity to the displacement loop. Step3: strand rotation promotes base pairing. Step4: branch migration as hemicatenated DNA leads to i-loop formation.

Formation of i-loops at other repetitive sequences

The accumulation of circular DNAs containing highly-repetitive sequences has been observed from yeast to human (Cohen and Lavi 1996; Gaubatz and Flores 1990; Sinclair and Guarente 1997; Fujimoto et al. 1985). For examples, extrachromosomal DNA was reported to contain tandem repeats sequences like satellites, short or long interspersed sequences (i.e transposon-like sequences or B1 and L1 in mouse genome), or retroviral-like elements. We demonstrated that i-loops form also damaging deproteinated DNA, after cell extraction, suggesting that the presence of homology sequence is the main requirement to induce the rearrangement at site of damage. Similar to telomeric DNA, other classes of tandem repeats could provide a homology-rich context where i-loops might occur at level of single-stranded DNA tract exposed after DNA damage. Is important to consider that repetitive elements with shorter repeated motifs will be more likely to expose complementary sequences after DNA damage, leading to higher rate of i-loop formation. For this reason, it is reasonable that telomeric DNA with 6-nucleotides repetitive motif could be more prone to generate i-loops and consequently extrachromosomal circles compared to most other long repeated sequences.

In conclusion, our results suggest that the increase of telomere length increase the probability of the loss of telomeric repeats due to the generation of extrachromosomal telomeric circles derived from the excision of i-loops formed at level of stochastic telomeric damage. This could represent one of the mechanisms that explain telomere deletion as consequence of telomere damage, providing an important point for the understanding of the sources of dysfunctional telomeres and telomere heterogeneity that characterizes different organisms.

FUTURE PLANS

Study of the mechanisms of i-loop formation

Our model suggests that i-loops form as a consequence of annealing and strand exchange events at the damaged site where single-stranded telomeric DNA is exposed. Therefore, we expect that i-loop formation is sustained by pathways that promote Single-Stranded Annealing (SSA) and homologous recombination, whereas it is prevented by those pathways that counteract homology-directed repair. Based on this observation, we anticipate that specialized helicases with strong involvement in telomere metabolism, such as BLM, WRN and RTEL1 could also have a role in counteracting i-loops formation by resolution of strand-exchange intermediates or by branch migration and dissolution (Ding et al. 2004; Crabbe et al. 2004; Vannier et al. 2012). We are considering to use our telomeric DNA enrichment procedure to analyze by electron microscopy which telomere structures eventually accumulate in mutants for those kinds of activities in order to understand which steps characterize i-loops formation and which mechanisms leads to telomere dysfunction. To this aim, I can use 2D-gel electrophoresis as a readout for telomeric i-loop accumulation in different mutants in order to select proper candidate for telomeres enrichment and electron microscopy analysis. To make this approach more effective, I can also extract specifically structured-telomeric DNA from 2D gel after the procedure for telomere enrichment, as I performed for U2OS (ALT cells) in order to have a higher concentration of telomere structures to compare with the linear DNA of the same sample and among DNA coming from different conditions.

Investigation of molecular mechanism of i-loop excision and generation of t-circles

In addition to telomere structures analysis, that will allow us to understand the molecular steps that lead to i-loop formation, we want also to investigate which are

the factors involved in the excision of i-loops and the consequent generation of telomeric circles. Until now, the approach used to investigate these aspects was mainly based on the monitoring of telomeric circles accumulation in different genetics backgrounds. However, in this way it is hard to reveal on which molecular step certain factors are involved. Based on our model, we anticipated that the excision of i-loops to generate telomeric circles could involve the processing of the Holliday Junction at the i-loop junction. In mammals there are two major mechanism of HJ processing: dissolution and resolution. HJ dissolution, that occurs through the Blm-TopIII-Rmi1 (BTR) complex which leads exclusively to non-crossover product preventing sister chromatid exchange (Wu and Hickson 2003). HJ resolution involves two main activities, one dependent on Gen1 nuclease and the other dependent on the Mus81/Eme1 - Slx1/Slx4 complexes (West et al. 2015). There are contrasting evidences of the role of these pathways in the extrachromosomal telomeric circles accumulation (Sarkar et al. 2015; Pickett et al. 2011; Saint-Leger et al. 2014; Panier et al. 2019; Verma et al. 2019). In the TRF2$^{\Delta B}$ mutant, where TRF2 lacks the N-terminal basic domain, but is able to properly bind telomeric DNA, and in cells with long telomeres has been reported that XRCC3, factor involved in homologous recombination but also in HJ resolution, contributes in these contests to telomeric circles accumulation (Pickett et al. 2011; Wang, Smogorzewska, and de Lange 2004; Rivera et al. 2017). It has to be considered that all these structure-specific nucleases are involved in different levels of DNA metabolism, including replication, recombination and segregation, therefore is not easy to target one of their specific activities in the contest of the cell. We showed that providing DNA containing i-loops to a nuclear lysate results in accumulation of extrachromosomal telomeric circles and that this reaction requires both Mg++ and ATP, consistent with HJ resolution reaction requirement. Considering that this system can recapitulate the final step of telomeric circle formation in vivo, by providing different samples with

the same DNA substrate (with or without i-loops) we could separate the different steps of t-circle formation and provide a tool to investigate the activities necessary for the i-loop excision step and telomeric circle generation. In order to identify the factors involved in the i-loop excision reaction, we can incubate DNA containing i-loops in cellular extracts lacking for the activities of interest (i.e BLM, SLX4, GEN1). For this purpose, we can immunodeplete proteins from our stocks of nuclear extracts or directly prepare extract after deletion/knock-down of the gene of interest. However, we have to consider that HJ resolvases activity and cellular localization are tightly regulated by post-translational modification, therefore it could be necessary to produce cellular extracts starting from a synchronized cell population (West et al. 2015). This could also allow to figured out the temporal regulation of telomeric circles formation. An extract-based approach has been already used to explore for HJ resolution factors, but here we can specifically investigate their role in a defined contest and at the level of specific structures. Moreover, we can apply this approach also to ALT cells where telomeres are extremely heterogeneous in length and characterized by single-strand damage (nicks or gaps), extrachromosomal telomeric circles are abundant and provide a diagnostic marker (Bryan et al. 1995; Nabetani and Ishikawa 2009; Henson et al. 2009). Comparing ALT and non-ALT cells cellular extract with this assay, we could address if accumulation of telomeric circles is due to higher i-loop excision reactions or simply to do the fact that ALT telomeres contains higher amounts of telomere damage.

The extract-based assay of i-loop excision, combined with the rolling circle amplification of the excised telomeric circles, ultimately leads to a quantitative increase in the amount of telomeric signal that is dependent on the efficiency of i-loop excision. This setting will be exploited in the future for high-throughput screening of small molecules that could interfere with i-loop excision. In principle, the incubation of i-loop-containing DNA and cellular extract could be performed in a

multi-well plate. An aliquot of this reaction could then be used as a template for RCA amplification of circular DNA, which has been shown to generate a telomeric signal that increases in a linear fashion with the amount of telomeric circles (Henson et al. 2017). Fluorescent probes could be used to measure signal accumulation during RCA in real time (Cawthon 2002). High-throughput quantification of telomeric signal could be performed by qPCR, a procedure commonly-used to estimate telomere length in different settings (Sethi et al. 2021).This assay could identify potential candidate molecules that could stimulate or counteract the excision of i-loops as extrachromosomal circular DNA. Since telomeric circles have been shown to strongly correlate with ALT activity, this approach might deliver potential candidate drugs that counteract the growth of ALT-tumors.

EM analysis of telomeric replication intermediates

Electron microscopy have been widely used to uncover the fine architecture of DNA replication forks genome wide from bacteriophages to mammalian cells (Inciarte, Salas, and Sogo 1980; Lucchini and Sogo 1995; Sogo et al. 1986). Our procedure for telomeric DNA purification provides an important tool to perform the same kind of analysis at telomeres, whose proper replication is essential for genome stability. Most of the information we have about telomere replication derives from FISH analysis on metaphase spreads, 2D gels and in some instances from SMARD (single molecule analysis replicating DNA). Thanks to these cytological approaches were identified genes required for telomere replication. (Miller, Rog, and Cooper 2006) showed through 2D gel analysis in *Schizosaccharomyces pombe* that loss of Taz1 leads to stalled telomere replication forks and accumulation of aberrant telomeric structures. In mammals, it has been confirmed that in the absence of the Taz1 orthologue, the shelterin protein TRF1, telomere replication is impaired leading

to telomere aberration like fragility or sister chromatid association (Sfeir et al. 2009). Telomere fragility and telomere loss occurs in absence of RTEL1 helicase, which is proposed to dismantle secondary structures like t-loop or G-quartets ensuring proper telomeric replication fork progression (Vannier et al., 2012. Cell). WRN mutants exhibit deletion of telomeres from single sister chromatids at level of the lagging strand, suggesting it is necessary for efficient replication of the G-rich telomeric DNA (Crabbe et al. 2004). However, it is not known which structures accumulate in these mutants and which leads to the fragile phenotype observed in FISH analysis. With electron microscopy analysis after telomeric DNA purification, we can directly identify replication structures that accumulate at telomeres compared to those occurring genome-wide, but importantly at telomeric repeats of mutant for genes essential for telomere replication. For example, we can hypothesize to find accumulation of reversed forks at telomeric repeats compared to genome wide, since telomere are difficult to replicate and behave like replication fragile sites (Sfeir et al. 2009). These kinds of results could provide insight about how replication occurs also in other replication fragile sites of the genome. Therefore, our protocol is an important tool to identify telomere structures that could provide information about the molecular mechanisms that characterized telomere replication, an essential process to preserve genome stability and counteract tumorigenesis.

MATERIAL AND METHODS

Cell culture

SV40LT-immortalized MEFs were grown in D-MEM (Lonza, BE12-614F) supplemented with 10% fetal bovine serum (EuroClone, ECS0180L), 2 mM L-glutamine (EuroClone, LOBE17605F), 100 U/ml penicillin-0.1 µg/ml streptomycin (EuroClone, ECB3001L), 0.1mM non-essential amino acids (Microtech, X-0557). U2OS cells (ATCC) were grown in Mc Coy's 5 A w/Glutamax (Life Technologies, 36600-088) supplemented with 10% fetal bovine serum (EuroClone, ECS0180L). U2OS cells were authenticated using the GenePrint® 10 System (10-Locus STR System for Cell Line Authentication) by Promega CAT. NUM. B9510. HeLa 1.3, HeLa204 and HTC75 cells were grown in D-MEM (Lonza, BE12-614F) supplemented with 10% fetal bovine serum (EuroClone, ECS0180L), 2 mM L-glutamine (EuroClone, LOBE17605F), 100 U/ml penicillin-0.1 µg/ml streptomycin (EuroClone, ECB3001L). HeLa1,3, HeLa204, and HTC75 cell lines are a gift from Titia de Lange. All cell lines are tested for mycoplasma both upon arrival at IFOM and after a new stock of cells is made, and all of them resulted to be negative for mycoplasma contamination. Mycoplasma test is performed by the IFOM Cell Biology UNIT and consist of two independent tests: a PCR analysis (For detail protocol see36 and a biochemical test (MycoAlert Detection Kit, Lonza
Catalog #: LT07-418).

Enrichment of telomeric repeats

Around $500x10^6$ cells were harvested from 60-70 15cm dishes through trypsinization that after centrifugation are resuspended in 10 ml of ice-cold PBS complemented with $MgCl_2$ and $CaCl_2$. For psoralen crosslinking, the cell suspension was poured in a 10 cm dish and kept on ice while stirring, throughout the procedure. The suspension was first incubated with 30 µg/ml of 4, 5′, 8-trimethylpsoralen (Sigma, T6137, stock 2 mg/ml in DMSO, stored at -20˚C) for 5 minutes in the dark

and then exposed to 365 nm UV light for 8 minutes in a UV Stratalinker 1800 (Stratagene) at 2-3 cm from the light source. The incubation and irradiation steps were repeated for 4 cycles total. Cell suspension was recovered washing the plate with ice-cold PBS complemented with $MgCl_2$ and $CaCl_2$. After centrifugation, cells pellet was resuspended in TNE buffer (Tris 10 mM pH8.0, NaCl 100 mM, EDTA 10 mM) and lysed adding 1 volume of TNES buffer (Tris 10 mM pH8.0, NaCl 100 mM, EDTA 10 mM; 0.5% SDS) containing 50 µg/ml RNaseA (Sigma, R500) followed by incubation for 60 min at 37˚C. Then 100 µg/ml of Proteinase K (Roche, 3115887001) were added and the suspension was incubated again at 37˚C overnight. The DNA was extracted with Phenol Chloroform Isoamyl alcohol 25:24:1 (Sigma, P2069) followed by an extraction with Chloroform (VWR, 22711) and precipitation with isopropanol. The DNA was resuspended in around 5 ml of Tris 10mM pH8 and let homogenize few hours at room temperature under gentle shaking before quantification and separation of 1 µl on agarose gel to check its integrity. Around 2.5 mg of DNA was digested overnight at 37ºC with 750 units of HinfI and MspI (NEB) in 20 ml of CutSmart (NEB) 1X buffer. The digestion mix was poured in two tubes for the JS13.1 rotor, precipitated with isopropanol and DNA resuspended in final volume of 4.5 ml of TE1X. The digested DNA was loaded in 3 tubes of sucrose gradient (1.5 ml each), each containing 10%-20%-30% gradient. Each sucrose solution was prepared in TNE buffer and the gradient was made deposit slowly 8 ml of each solution starting from the densest. After DNA loading on the top, the gradients were centrifugated in SW32-Ti rotor (Beckman) at 30100 rpm (111265 g) for 16 hours. Different volumes (fractions) from each tube were slowly collected and an aliquot of each separated in agarose gel in order to verify fragment distribution. The DNA from the agarose gel was transferred by Southern blot to membrane and hybridized with radioactive telomeric probe. For Southern blotting, the gel was first incubated 2 x 30 min with the depurination solution (HCl 0.25N) 2 x 30 min with

denaturing solution (NaOH 0.5M, NaCl 1.5 M), 2 x 30 min with neutralizing solution (Tris 0.5M pH 7.5, NaCl 3M). The DNA was then transferred by capillarity in SSC 20X onto an Amersham Hybond-X membrane (GE healthcare RPN203). For TTAGGG repeats probe the 800 bp EcoRI fragment of the Sty11 plasmid (a gift from Titia de Lange) (de Lange, 1992. EMBO J) was used. The fractions containing high molecular weight fragments, where telomeric repeats deposit, were collected, concentrated and washed twice with Tris 10mM pH 8.0 in Amicon Ultra-15 Ultracel-PL PLTK, 30 kDa MWCO (Millipore/MERCK UFC903024) filters. The DNA was then digested overnight with 50 units each of RsaI, AluI, MboI, HinfI, MspI, HphI, MnlI (NEB) and then separated on a 0.7% low-melting agarose gel (SeaPlaque Agarose, Lonza, 50100). Fragments migrating above the 5 kb band of the marker were extracted with electroelution or Silica beads (see above) and quantified using Qubit dsDNA HS assay kit (Invitrogen, Q32854). In the telomere enrichment of U2OS, after the digestion with the seven restriction enzymes, the DNA was separated in 2D gel and the DNA extracted with Silica beads.

DNA extraction from agarose gel

Preparative agarose gel:

DNA was separated in a low melting agarose (SeaPlaque LONZA 50101) gel at low percentage (0.7%) without ethidium bromide in TBE 0.5X or TAE 1X. The run was conducted at low voltage the time sufficient just to separate high molecular weight molecules (up to 5 kb) from the smaller fragments produced by the restriction digestion (i.e., 0.8-1 V/cm for 15-12 hours), since we need to minimize the agarose gel portion containing HMW DNA. DNA ladder was loaded leaving at least one well empty from the sample. The marker lane was cut after separation, stained in ethidium bromide for 30 minutes and acquired with UV transilluminator close to a ruler, in order to define at which distance from the well to cut the sample slice.

2D gel for DNA extraction:

DNA was separated as first dimension in 0.4% agarose gel in TAE1X without ethidium bromide with a run of 0.8V/cm for 10 hours. In parallel to the sample was separated DNA ladder, loaded leaving at least one empty well from the sample. The marker lane was cut and stained in ethidium bromide for 1 hour and the band separation was acquired close to a ruler in order to define at which level from the well to cut the sample slices, without expose the DNA to UV light. The sample slice was cut including DNA longer than 3Kb to the well and trap in 0.7% low melting agarose gel (SeaPlaque LONZA 50101) containing ethidium bromide (check amount) in TAE 1X. The second dimension was run at 3V/cm for 8 hours. The gel was layered on transilluminator and exposing the shorter time possible, was cut at the level of the linear and of the arc signal. The slices were then transferred in clean and separated tubes in order to extract DNA with the Silica beads DNA extraction kit (see below).

Electroelution

The Whatman® Elutrap electroelution system consists in a chamber where agarose gel slice is placed in a compartment close to a trap made of two membranes where the sample migrates thanks an electric field (Figure 1). The complete chamber was place into horizontal gel electrophoresis systems and we applied an electric field of 100V for 10-12 hours. The DNA pass through a first membrane (BT2) that blocks agarose and other particulates and remains trapped thank to another membrane (BT1) that allows sample concentration but contaminants smaller than 3-5 KDa to pass off.

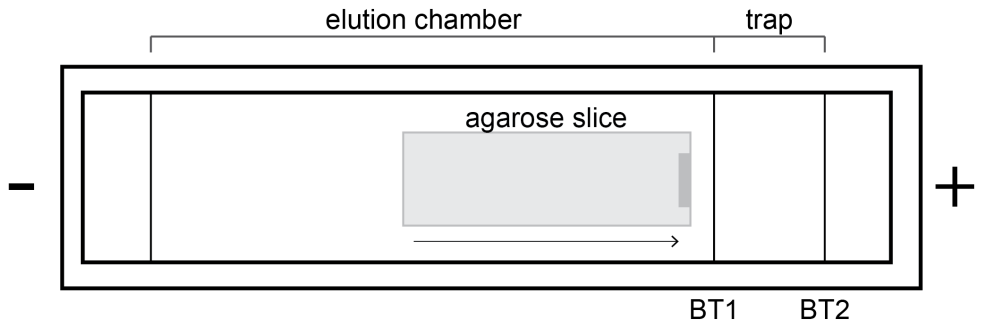

Figure 1. Electroelution chamber.

Representative scheme of the agarose gel slice palced in the electroelution chamber. The HMW DNA is positionated toward the trap and the arrow indicates the migration of the DNA under electric field.

Before sample collection, we applied 20 seconds of inverted field at 100V. The volume whithin the trap (~ 800 µl/ 1 ml) was recovered, washing twice with fresh buffer and concentrated to a final volume of ~ 180 µl using Amicon columns 0.5 ml (MWCO 30K, UFC 503096 Millipore) washing twice with water. Eventual traces of agarose were digested with beta-Agarase (NEB), adding 20µl of beta- agarase buffer 10X and 2 µl of beta agarase (M0392 NEB). The reaction was incubated for 1 hour at 42˚C. DNA was then extracted with 1 volume of phenol-chloroform-isoamyl alcohol, successively precipitate with isopropanol and resuspended in 25µl of filtered TE 1X buffer.

Silica Beads DNA gel extraction kit

We used silica bead DNA gel extraction kit (Thermo Fisher Scientific, K0513) following the manufacturer's instructions with few exceptions. Briefly, agarose gel slice was excised with a clean scalpel and transferred in a pre-weighted 15ml-falcon tube in order to record the weight of the slice. The gel was dissolved in the binding buffer in a 3:1 ratio volume : weight, incubating at 50ºC for 5 minutes. The proper amount of Silica powder suspension was added to the DNA/binding buffer mixture and incubated at 50ºC for 15 minutes to allow DNA binding to the silica matrix, gently inverting every 5 minutes to keep silica powder in suspension. The suspension is

transferred in 1.5 ml tube in different rounds, each spinning down the beads, removing the supernatant and adding other solution until all the volume is transferred and all the beads collected. Starting from now, the beads were not resuspended to avoid mechanical shearing of the DNA interacting with the matrix. The beads were washed three times with 1 ml of ice-cold ethanol-containing wash buffer was gently added without resuspending. The DNA was eluted adding 25-30 µl of TE1X, resuspending the beads by flicking and incubated @ 50ºC for 5 minutes. After rapid spin, the supernatant was recovered in a new tube, avoiding to perturb the pellet, and elution was repeated a second time. In order to verify any residues of silica powder, the elution tubes were spin for 30" at 16000g and eventually the supernatant transferred in a new tube.

Single molecule analysis of telomeric enrichment

Around 10 ng of bulk genomic DNA or telomere-enriched DNA was combed on silanized coverslips (Genomic Vision, COV-002) using the DNA Fiber Comb apparatus (Genomic Vision, version 3 REF: MSC-001). The coverslips with the attached DNA were baked for 2-3 hours at 60˚C, denatured in 0.5 M NaOH, 1M NaCl for 8 min, washed twice with PBS and undergo dehydration step in ethanol series (70%; 90%; 100%, 1 min each). Blocking with 5% BSA in PBS for 1 hour at 37˚C and incubation with an anti single-stranded DNA antibody (Sigma, MAB3034) diluted 1:80 in 5% BSA in PBS, for 2 hours at RT, followed by three washes with PBS-0.05% Tween 20. Incubation with Alexa488-labeled anti-mouse secondary antibody (Invitrogen, A1101) diluted 1:400 in 5% BSA in PBS, followed by three washes with PBS-0.05% Tween 20 and dehydration in ethanol series (70%; 90%; 100%, 1 min each). Incubation with a Cy3-labeled $TTAGGG_3$ PNA probe (PNA Bio, F1006), 50 nM in 70% formamide (Thermo Scientific, 17899) 0.5% Blocking reagent (Roche 11096176001) and 10 mM Tris, pH 7.4, for 3 min at 80˚C and then 2 hours

at RT, followed by 2 x15 min washes in formamide 70%, 10 mM Tris, pH 7.4 and three washes with PBS-0.05% Tween 20. The coverslips were mounted using ProLong Gold (Invitrogen, P36930). Large overlapping areas were acquired and stitched in a DeltaVison microscope.

Electron microscopy analysis

BAC spreading

EM analysis was performed as described in (Lopes 2009). Typically, 5 µl of telomere-enriched DNA corresponding to 5-20 ng were used for each spread. For non-enriched controls, 30 ng of KpnI-digested genomic DNA was spread using the same method. Briefly, EM grids previously coated with a carbon layer, are activated by contact with an ethidium bromide solution 33 µg/ml in TE1X for 30 to 45 minutes at room temperature. The DNA was mixed with 5 µl of formamide (Thermo Scientific, 17899) and 0.4 µl of benzalkonium chloride (BAC, Sigma B6285) 0.02% in TE. (BAC stock solution 0.2% in formamide was diluted 1:10 in TE 1X before use). After mixing, the mix was immediately spread on a water surface in a 15 cm dish containing 50 ml of distilled water, using a freshly-cleaved mica sheet (Ted pella inc, product no: 52-6) as a ramp. The monomolecular layer was gently touched with pre-activated EM grids. The DNA recovered from the linear and t-circle arc of 2D-gels, was spread using the droplet method as in (Fouche et al. 2006). Briefly, 1 ng of DNA in 28 µl of TE 1X, was mixed with 30 µl of Formamide (Thermo Scientific, 17899) and 2 µl of benzyldimethyl-alkylammonium chloride (BAC) 0.08%. The droplet was incubated for 5 min at RT and the surface was gently touched with a carbon-coated EM grid, previously activated by contact with an ethidium bromide. The grids were then processed for staining with Uranyl Acetate and rotary shadowing as described in (Lopes 2009).

Kleinschmidt spreading

Kleinschmidt spreading was performed according to (Griffith et al. 1999) with minor modifications. Briefly, 50 ng of DNA in TRIS 10mMpH 8.0 was mixed with ammonium acetate (pH 7.8, 0.25M final concentration). Cytochrome C (Sigma) was added to 4 µg/ml final concentration and the droplet (50 µl) was placed on parafilm for 90 s. A carbon-coated EM grid was touched to the drop and then dehydrated through two washes of 30 s in 75% and 90% ethanol, followed by air drying and rotary shadowing with platinum.

TEM acquisition

TEM pictures were taken using a FEI Tecnai12 Bio twin microscope operated at 120 KV and equipped with a side-mounted GATAN Orius SC-1000 camera controlled by the Digital Micrograph software. Images in DM3 format were analyzed using the ImageJ software. In these conditions 0.36 µm correspond to 1 kb of double-stranded DNA. Images in DM3 format were analyzed in FIJI/ImageJ software v2.0.0-rc-69/1.52p. In these conditions, in BAC spreads, a length of 0.36 µm corresponds to 1 kb of double-stranded DNA. Data annotation and storage during the analysis was performed with an Image J macro.

DNase I treatment on isolated nuclei.

MEF nuclei were isolated as described previously (Pipkin and Lichtenheld 2006). Briefly, cells were collected by trypsinization, washed with ice-cold PBS, and resuspended in ice-cold fibroblast lysis buffer (12.5 mM Tris pH 7.4, 5 mM KCl, 0.1 mM spermine, 0.25 mM spermidine, 175 mM sucrose, supplemented with protease inhibitor cocktail (Roche, 11836170001) at a concentration of 8 x 10^6 cells/ml). After 10 min of incubation on ice, 0.02 vol 10% NP-40 was added and cells were

incubated for 5 min on ice. Nuclei were collected by centrifugation at 1000g for 5 min at 4˚C and washed once with ice-cold Nuclei Wash Buffer (NWB) (10 mM Tris-HCl pH 7.4, 15 mM NaCl, 60 mM KCl, 5 mM $MgCl_2$, 300 mM sucrose) and resuspended in NWB. When indicated, psoralen crosslinking was performed on the nuclei suspension in NWB, as described above for cell suspensions. For the DNase I treatment, 1 volume of nuclei suspension was mixed with 1 volume of DNase I cocktail (NWB supplemented with $CaCl_2$ 2 mM, BSA 100 µg/ml, and twice the indicated concentration of DNase I (Roche 10104159001) and incubated for 8 minutes at RT. The reactions were stopped with 0.5 vol of ice-cold stop buffer (50 mM EDTA, 10 mM EGTA). The nuclei were then processed for genomic DNA extraction as described above for cells.

DNase I treatment on isolated DNA.

Genomic DNA, extracted as described above, was incubated with DNase I (Roche 10104159001) in 10 mM Tris-HCl pH 7.4, 15 mM NaCl, 60 mM KCl, 5 mM $MgCl_2$, 10 mM $CaCl_2$, for 8 min at RT. The reaction was stopped by adding 0.2 vol of EDTA-EGTA 0.25 M each, extracted with 1 volume of phenol-cholorform-isoamylalcohol and precipitated in isopropanol.

2D-gels

10 µg of genomic DNA was digested overnight with 20 units of AluI and MboI (NEB) and then precipitated with isopropanol. For the analysis of the mouse BamHI repeats, the DNA was digested either with BglI or with KpnI as indicated. The first dimension was run in 0.35% agarose (US-biological, A1015) in TBE 0.5X, without ethidium bromide for 12-24 hours at 1 V/cm. The gel was stained with 0.3 µg/ml ethidium bromide in TBE 0.5X and lanes were excised above 5 kb for mouse, U2OS and HeLa 1.3 telomeres and above 2 kb for HeLa 204 and HTC75 telomeres. The

second dimension was run in 0.7% agarose in TBE 0.5X with 0.3 µg/ml ethidium bromide at 3-5 Volts/cm at 4˚C. When necessary, psoralen crosslinking was reversed before southern blotting by exposing the gel to 254 nm UV for 10 min in a stratalinker (UVP CL1000 Ultraviolet crosslinker). For Southern blotting, the gel was first incubated 2 x 30 min with the depurination solution (HCl 0.25N) 2 x 30 min with denaturing solution (NaOH 0.5M, NaCl 1.5 M), 2 x 30 min with neutralizing solution (Tris 0.5M pH 7.5, NaCl 3M). The DNA was then transferred by capillarity in SSC 20X onto an Amersham Hybond-X membrane (GE healthcare RPN203). For TTAGGG repeats probe the 800 bp EcoRI fragment of the Sty11 plasmid (a gift from Titia de Lange) (de Lange 1992) was used. For the BamHI repeats probe a 1 kb EcoRV fragment, containing mouse BamHI dispersed repeats cloned in pBlue was used (Fanning 1983). Radioactive signal was captured on phosphor screens (FUJIFILM Storage Phosphor screen MS3543 E), read on a Typhon Trio (GE) and analyzed on ImageJ.

Telomere blots

10 µg of genomic DNA was digested overnight with 20 units of AluI and MboI (NEB) and then precipitated with isopropanol. The DNA was separated in a 0.7% agarose gel (US-biological, A1015) in TBE 0.5X, with 0.3 µg/ml ethidium bromide for 21 h at 1.6 V/cm. The gel was then processed for Southern blotting and hybridization with a telomeric probe as described above.

Incubation with HeLa extracts

1 µg of genomic DNA was incubated with 60 µg of HeLa nuclear extract (6 mg/ml) (IPRACELL, CC012010) in 50mM Tris HCl pH8, 150 mM NaCl, 5 mM MgCl2, 2 mM ATP, 1mM DTT for 35 minutes at 37˚C in 20 µl final volume. The reaction was

stopped with 0.1 vol of EDTA-EGTA 0.25 M each, extracted with 1 volume of phenol-cholorform isoamylalcohol and precipitated in isopropanol.

C-circle assay

Was performed according to (Henson et al. 2009). Briefly, 25 ng of genomic DNA, digested with AluI and MboI, were incubated for 12 hours at 30˚C with 7.5 Units of Phi29 polymerase (NEB M0269) in Phi29 NEB buffer 1X, supplemented with dNTPs 0,37 mM each, in a final volume of 20 µl. The enzyme was inactivated by heating to 65˚C for 20 minutes and the reaction was blotted onto a Hybond-X membrane. Telomeric repeats were detected using the TTAGGG repeats probe described above.

REFERENCES

Abdallah, P., P. Luciano, K. W. Runge, M. Lisby, V. Geli, E. Gilson, and M. T. Teixeira. 2009. 'A two-step model for senescence triggered by a single critically short telomere', *Nat Cell Biol*, 11: 988-93.

Amiard, S., M. Doudeau, S. Pinte, A. Poulet, C. Lenain, C. Faivre-Moskalenko, D. Angelov, N. Hug, A. Vindigni, P. Bouvet, J. Paoletti, E. Gilson, and M. J. Giraud-Panis. 2007. 'A topological mechanism for TRF2-enhanced strand invasion', *Nat Struct Mol Biol*, 14: 147-54.

Andersen, S. L., D. T. Bergstralh, K. P. Kohl, J. R. LaRocque, C. B. Moore, and J. Sekelsky. 2009. 'Drosophila MUS312 and the vertebrate ortholog BTBD12 interact with DNA structure-specific endonucleases in DNA repair and recombination', *Mol Cell*, 35: 128-35.

Anisimova, V. E., D. V. Rebrikov, P. A. Zhulidov, D. B. Staroverov, S. A. Lukyanov, and A. S. Shcheglov. 2006. 'Renaturation, activation, and practical use of recombinant duplex-specific nuclease from Kamchatka crab', *Biochemistry (Mosc)*, 71: 513-9.

Armanios, M., J. K. Alder, E. M. Parry, B. Karim, M. A. Strong, and C. W. Greider. 2009. 'Short telomeres are sufficient to cause the degenerative defects associated with aging', *Am J Hum Genet*, 85: 823-32.

Artandi, S. E., S. Chang, S. L. Lee, S. Alson, G. J. Gottlieb, L. Chin, and R. A. DePinho. 2000. 'Telomere dysfunction promotes non-reciprocal translocations and epithelial cancers in mice', *Nature*, 406: 641-5.

Artandi, S. E., and R. A. DePinho. 2010. 'Telomeres and telomerase in cancer', *Carcinogenesis*, 31: 9-18.

Bailey, S. M., E. H. Goodwin, and M. N. Cornforth. 2004. 'Strand-specific fluorescence in situ hybridization: the CO-FISH family', *Cytogenet Genome Res*, 107: 14-7.

Baird, D. M., J. Rowson, D. Wynford-Thomas, and D. Kipling. 2003. 'Extensive allelic variation and ultrashort telomeres in senescent human cells', *Nat Genet*, 33: 203-7.

Baumann, P., and T. R. Cech. 2001. 'Pot1, the putative telomere end-binding protein in fission yeast and humans', *Science*, 292: 1171-5.

Bechter, O. E., J. W. Shay, and W. E. Wright. 2004. 'The frequency of homologous recombination in human ALT cells', *Cell Cycle*, 3: 547-9.

Bell, L., and B. Byers. 1983. 'Separation of branched from linear DNA by two-dimensional gel electrophoresis', *Anal Biochem*, 130: 527-35.

Bermudez, V. P., L. A. Lindsey-Boltz, A. J. Cesare, Y. Maniwa, J. D. Griffith, J. Hurwitz, and A. Sancar. 2003. 'Loading of the human 9-1-1 checkpoint complex onto DNA by the checkpoint clamp loader hRad17-replication factor C complex in vitro', *Proc Natl Acad Sci U S A*, 100: 1633-8.

Bianchi, A., R. M. Stansel, L. Fairall, J. D. Griffith, D. Rhodes, and T. de Lange. 1999. 'TRF1 binds a bipartite telomeric site with extreme spatial flexibility', *EMBO J*, 18: 5735-44.

Bilaud, T., C. Brun, K. Ancelin, C. E. Koering, T. Laroche, and E. Gilson. 1997. 'Telomeric localization of TRF2, a novel human telobox protein', *Nat Genet*, 17: 236-9.

Blanco, L., and M. Salas. 1996. 'Relating structure to function in phi29 DNA polymerase', *J Biol Chem*, 271: 8509-12.

Blasco, M. A. 2007. 'The epigenetic regulation of mammalian telomeres', *Nat Rev Genet*, 8: 299-309.

Blasco, M. A., H. W. Lee, M. P. Hande, E. Samper, P. M. Lansdorp, R. A. DePinho, and C. W. Greider. 1997. 'Telomere shortening and tumor formation by mouse cells lacking telomerase RNA', *Cell*, 91: 25-34.

Bonner, W. M., C. E. Redon, J. S. Dickey, A. J. Nakamura, O. A. Sedelnikova, S. Solier, and Y. Pommier. 2008. 'GammaH2AX and cancer', *Nat Rev Cancer*, 8: 957-67.

Bothmer, A., D. F. Robbiani, M. Di Virgilio, S. F. Bunting, I. A. Klein, N. Feldhahn, J. Barlow, H. T. Chen, D. Bosque, E. Callen, A. Nussenzweig, and M. C. Nussenzweig. 2011. 'Regulation of DNA end joining, resection, and immunoglobulin class switch recombination by 53BP1', *Mol Cell*, 42: 319-29.

Bothmer, A., D. F. Robbiani, N. Feldhahn, A. Gazumyan, A. Nussenzweig, and M. C. Nussenzweig. 2010. '53BP1 regulates DNA resection and the choice between classical and alternative end joining during class switch recombination', *J Exp Med*, 207: 855-65.

Brenneman, D. E., J. M. Hauser, C. Spong, and T. M. Phillips. 2002. 'Chemokine release is associated with the protective action of PACAP-38 against HIV envelope protein neurotoxicity', *Neuropeptides*, 36: 271-80.

Brewer, B. J., and W. L. Fangman. 1987. 'The localization of replication origins on ARS plasmids in S. cerevisiae', *Cell*, 51: 463-71.

Broccoli, D., A. Smogorzewska, L. Chong, and T. de Lange. 1997. 'Human telomeres contain two distinct Myb-related proteins, TRF1 and TRF2', *Nat Genet*, 17: 231-5.

Bryan, T. M., A. Englezou, L. Dalla-Pozza, M. A. Dunham, and R. R. Reddel. 1997. 'Evidence for an alternative mechanism for maintaining telomere length in human tumors and tumor-derived cell lines', *Nat Med*, 3: 1271-4.

Bryan, T. M., A. Englezou, J. Gupta, S. Bacchetti, and R. R. Reddel. 1995. 'Telomere elongation in immortal human cells without detectable telomerase activity', *EMBO J*, 14: 4240-8.

Bucholc, M., Y. Park, and A. J. Lustig. 2001. 'Intrachromatid excision of telomeric DNA as a mechanism for telomere size control in Saccharomyces cerevisiae', *Mol Cell Biol*, 21: 6559-73.

Burma, S., B. P. Chen, M. Murphy, A. Kurimasa, and D. J. Chen. 2001. 'ATM phosphorylates histone H2AX in response to DNA double-strand breaks', *J Biol Chem*, 276: 42462-7.

Castor, D., N. Nair, A. C. Declais, C. Lachaud, R. Toth, T. J. Macartney, D. M. Lilley, J. S. Arthur, and J. Rouse. 2013. 'Cooperative control of holliday junction resolution and DNA repair by the SLX1 and MUS81-EME1 nucleases', *Mol Cell*, 52: 221-33.

Cawthon, R. M. 2002. 'Telomere measurement by quantitative PCR', *Nucleic Acids Res*, 30: e47.

Celli, G. B., and T. de Lange. 2005. 'DNA processing is not required for ATM-mediated telomere damage response after TRF2 deletion', *Nat Cell Biol*, 7: 712-8.

Cesare, A. J., and J. D. Griffith. 2004. 'Telomeric DNA in ALT cells is characterized by free telomeric circles and heterogeneous t-loops', *Mol Cell Biol*, 24: 9948-57.

Cesare, A. J., C. Groff-Vindman, S. A. Compton, M. J. McEachern, and J. D. Griffith. 2008. 'Telomere loops and homologous recombination-dependent telomeric circles in a Kluyveromyces lactis telomere mutant strain', *Mol Cell Biol*, 28: 20-9.

Cesare, A. J., N. Quinney, S. Willcox, D. Subramanian, and J. D. Griffith. 2003. 'Telomere looping in P. sativum (common garden pea)', *Plant J*, 36: 271-9.

Cesare, A. J., and R. R. Reddel. 2010. 'Alternative lengthening of telomeres: models, mechanisms and implications', *Nat Rev Genet*, 11: 319-30.

Chiruvella, KK, Z Liang, and TE Wilson. 2013. 'Repair of double-strand breaks by end joining.', *Cold Spring Harb Perspect Biol*, 5: a012757.

Chong, L., B. van Steensel, D. Broccoli, H. Erdjument-Bromage, J. Hanish, P. Tempst, and T. de Lange. 1995. 'A human telomeric protein', *Science*, 270: 1663-7.

Choudhury, A. R., Z. Ju, M. W. Djojosubroto, A. Schienke, A. Lechel, S. Schaetzlein, H. Jiang, A. Stepczynska, C. Wang, J. Buer, H. W. Lee, T. von Zglinicki, A. Ganser, P. Schirmacher, H. Nakauchi, and K. L. Rudolph. 2007. 'Cdkn1a deletion improves stem cell function and lifespan of mice with dysfunctional telomeres without accelerating cancer formation', *Nat Genet*, 39: 99-105.

Cohen, S., and S. Lavi. 1996. 'Induction of circles of heterogeneous sizes in carcinogen-treated cells: two-dimensional gel analysis of circular DNA molecules', *Mol Cell Biol*, 16: 2002-14.

Cohen, S., and M. Mechali. 2002. 'Formation of extrachromosomal circles from telomeric DNA in Xenopus laevis', *EMBO Rep*, 3: 1168-74.

Conomos, D., M. D. Stutz, M. Hills, A. A. Neumann, T. M. Bryan, R. R. Reddel, and H. A. Pickett. 2012. 'Variant repeats are interspersed throughout the telomeres and recruit nuclear receptors in ALT cells', *J Cell Biol*, 199: 893-906.

Cortez, D., S. Guntuku, J. Qin, and S. J. Elledge. 2001. 'ATR and ATRIP: partners in checkpoint signaling', *Science*, 294: 1713-6.

Costa, A., M. G. Daidone, L. Daprai, R. Villa, S. Cantu, S. Pilotti, L. Mariani, A. Gronchi, J. D. Henson, R. R. Reddel, and N. Zaffaroni. 2006. 'Telomere maintenance mechanisms in liposarcomas: association with histologic subtypes and disease progression', *Cancer Res*, 66: 8918-24.

Crabbe, L., R. E. Verdun, C. I. Haggblom, and J. Karlseder. 2004. 'Defective telomere lagging strand synthesis in cells lacking WRN helicase activity', *Science*, 306: 1951-3.

Cromie, G. A., R. W. Hyppa, A. F. Taylor, K. Zakharyevich, N. Hunter, and G. R. Smith. 2006. 'Single Holliday junctions are intermediates of meiotic recombination', *Cell*, 127: 1167-78.

d'Adda di Fagagna, F., P. M. Reaper, L. Clay-Farrace, H. Fiegler, P. Carr, T. Von Zglinicki, G. Saretzki, N. P. Carter, and S. P. Jackson. 2003. 'A DNA damage checkpoint response in telomere-initiated senescence', *Nature*, 426: 194-8.

Dai, X., C. Huang, A. Bhusari, S. Sampathi, K. Schubert, and W. Chai. 2010. 'Molecular steps of G-overhang generation at human telomeres and its function in chromosome end protection', *EMBO J*, 29: 2788-801.

de Jager, M., J. van Noort, D. C. van Gent, C. Dekker, R. Kanaar, and C. Wyman. 2001. 'Human Rad50/Mre11 is a flexible complex that can tether DNA ends', *Mol Cell*, 8: 1129-35.

de Lange, T. 1992. 'Human telomeres are attached to the nuclear matrix', *EMBO J*, 11: 717-24.

———. 2005a. 'Shelterin: the protein complex that shapes and safeguards human telomeres', *Genes Dev*, 19: 2100-10.

———. 2005b. 'Telomere-related genome instability in cancer', *Cold Spring Harb Symp Quant Biol*, 70: 197-204.

———. 2018. 'Shelterin-Mediated Telomere Protection', *Annu Rev Genet*, 52: 223-47.

de Lange, T., L. Shiue, R. M. Myers, D. R. Cox, S. L. Naylor, A. M. Killery, and H. E. Varmus. 1990. 'Structure and variability of human chromosome ends', *Mol Cell Biol*, 10: 518-27.

Dean, F. B., J. R. Nelson, T. L. Giesler, and R. S. Lasken. 2001. 'Rapid amplification of plasmid and phage DNA using Phi 29 DNA polymerase and multiply-primed rolling circle amplification', *Genome Res*, 11: 1095-9.

Delacroix, S., J. M. Wagner, M. Kobayashi, K. Yamamoto, and L. M. Karnitz. 2007. 'The Rad9-Hus1-Rad1 (9-1-1) clamp activates checkpoint signaling via TopBP1', *Genes Dev*, 21: 1472-7.
Denchi, E. L., and T. de Lange. 2007. 'Protection of telomeres through independent control of ATM and ATR by TRF2 and POT1', *Nature*, 448: 1068-71.
Deng, Z., J. Dheekollu, D. Broccoli, A. Dutta, and P. M. Lieberman. 2007. 'The origin recognition complex localizes to telomere repeats and prevents telomere-circle formation', *Curr Biol*, 17: 1989-95.
Deriano, L., and D. B. Roth. 2013. 'Modernizing the nonhomologous end-joining repertoire: alternative and classical NHEJ share the stage', *Annu Rev Genet*, 47: 433-55.
Dilley, R. L., and R. A. Greenberg. 2015. 'ALTernative Telomere Maintenance and Cancer', *Trends Cancer*, 1: 145-56.
Ding, H., M. Schertzer, X. Wu, M. Gertsenstein, S. Selig, M. Kammori, R. Pourvali, S. Poon, I. Vulto, E. Chavez, P. P. Tam, A. Nagy, and P. M. Lansdorp. 2004. 'Regulation of murine telomere length by Rtel: an essential gene encoding a helicase-like protein', *Cell*, 117: 873-86.
Doksani, Y. 2019. 'The Response to DNA Damage at Telomeric Repeats and Its Consequences for Telomere Function', *Genes (Basel)*, 10.
Doksani, Y., and T. de Lange. 2014. 'The role of double-strand break repair pathways at functional and dysfunctional telomeres', *Cold Spring Harb Perspect Biol*, 6: a016576.
Doksani, Y., J. Y. Wu, T. de Lange, and X. Zhuang. 2013. 'Super-resolution fluorescence imaging of telomeres reveals TRF2-dependent T-loop formation', *Cell*, 155: 345-56.
Dunham, M. A., A. A. Neumann, C. L. Fasching, and R. R. Reddel. 2000. 'Telomere maintenance by recombination in human cells', *Nat Genet*, 26: 447-50.
Fairall, L., L. Chapman, H. Moss, T. de Lange, and D. Rhodes. 2001. 'Structure of the TRFH dimerization domain of the human telomeric proteins TRF1 and TRF2', *Mol Cell*, 8: 351-61.
Fanning, T. G. 1983. 'Size and structure of the highly repetitive BAM HI element in mice', *Nucleic Acids Res*, 11: 5073-91.
Fekairi, S., S. Scaglione, C. Chahwan, E. R. Taylor, A. Tissier, S. Coulon, M. Q. Dong, C. Ruse, J. R. Yates, 3rd, P. Russell, R. P. Fuchs, C. H. McGowan, and P. H. L. Gaillard. 2009. 'Human SLX4 is a Holliday junction resolvase subunit that binds multiple DNA repair/recombination endonucleases', *Cell*, 138: 78-89.
Feldser, D. M., and C. W. Greider. 2007. 'Short telomeres limit tumor progression in vivo by inducing senescence', *Cancer Cell*, 11: 461-9.
Ferreira, M. G., and J. P. Cooper. 2001. 'The fission yeast Taz1 protein protects chromosomes from Ku-dependent end-to-end fusions', *Mol Cell*, 7: 55-63.
Fouche, N., S. Ozgur, D. Roy, and J. D. Griffith. 2006. 'Replication fork regression in repetitive DNAs', *Nucleic Acids Res*, 34: 6044-50.
Friedman, K. L., and B. J. Brewer. 1995. 'Analysis of replication intermediates by two-dimensional agarose gel electrophoresis', *Methods Enzymol*, 262: 613-27.
Frit, P, N Barboule, Y Yuan, D Gomez, and P Calsou. 2014. 'Alternative end-joining pathway(s): bricolage at DNA breaks.', *DNA Repair (Amst)*, 17: 81-97.
Fujimoto, S., T. Tsuda, M. Toda, and H. Yamagishi. 1985. 'Transposon-like sequences in extrachromosomal circular DNA from mouse thymocytes', *Proc Natl Acad Sci U S A*, 82: 2072-6.
Garner, E., Y. Kim, F. P. Lach, M. C. Kottemann, and A. Smogorzewska. 2013. 'Human GEN1 and the SLX4-associated nucleases MUS81 and SLX1 are

essential for the resolution of replication-induced Holliday junctions', *Cell Rep*, 5: 207-15.
Gaubatz, J. W., and S. C. Flores. 1990. 'Tissue-specific and age-related variations in repetitive sequences of mouse extrachromosomal circular DNAs', *Mutat Res*, 237: 29-36.
Gisselsson, D., L. Pettersson, M. Hoglund, M. Heidenblad, L. Gorunova, J. Wiegant, F. Mertens, P. Dal Cin, F. Mitelman, and N. Mandahl. 2000. 'Chromosomal breakage-fusion-bridge events cause genetic intratumor heterogeneity', *Proc Natl Acad Sci U S A*, 97: 5357-62.
Grawunder, U., M. Wilm, X. Wu, P. Kulesza, T. E. Wilson, M. Mann, and M. R. Lieber. 1997. 'Activity of DNA ligase IV stimulated by complex formation with XRCC4 protein in mammalian cells', *Nature*, 388: 492-5.
Greenberg, R. A., L. Chin, A. Femino, K. H. Lee, G. J. Gottlieb, R. H. Singer, C. W. Greider, and R. A. DePinho. 1999. 'Short dysfunctional telomeres impair tumorigenesis in the INK4a(delta2/3) cancer-prone mouse', *Cell*, 97: 515-25.
Griffith, J. D., L. Comeau, S. Rosenfield, R. M. Stansel, A. Bianchi, H. Moss, and T. de Lange. 1999. 'Mammalian telomeres end in a large duplex loop', *Cell*, 97: 503-14.
Grobelny, J. V., A. K. Godwin, and D. Broccoli. 2000. 'ALT-associated PML bodies are present in viable cells and are enriched in cells in the G(2)/M phase of the cell cycle', *J Cell Sci*, 113 Pt 24: 4577-85.
Groff-Vindman, C., A. J. Cesare, S. Natarajan, J. D. Griffith, and M. J. McEachern. 2005. 'Recombination at long mutant telomeres produces tiny single- and double-stranded telomeric circles', *Mol Cell Biol*, 25: 4406-12.
Gu, P., J. N. Min, Y. Wang, C. Huang, T. Peng, W. Chai, and S. Chang. 2012. 'CTC1 deletion results in defective telomere replication, leading to catastrophic telomere loss and stem cell exhaustion', *EMBO J*, 31: 2309-21.
Haider, S., P. Li, S. Khiali, D. Munnur, A. Ramanathan, and G. N. Parkinson. 2018. 'Holliday Junctions Formed from Human Telomeric DNA', *J Am Chem Soc*, 140: 15366-74.
Harley, C. B., A. B. Futcher, and C. W. Greider. 1990. 'Telomeres shorten during ageing of human fibroblasts', *Nature*, 345: 458-60.
Hauer, M. H., and S. M. Gasser. 2017. 'Chromatin and nucleosome dynamics in DNA damage and repair', *Genes Dev*, 31: 2204-21.
Heaphy, C. M., R. F. de Wilde, Y. Jiao, A. P. Klein, B. H. Edil, C. Shi, C. Bettegowda, F. J. Rodriguez, C. G. Eberhart, S. Hebbar, G. J. Offerhaus, R. McLendon, B. A. Rasheed, Y. He, H. Yan, D. D. Bigner, S. M. Oba-Shinjo, S. K. Marie, G. J. Riggins, K. W. Kinzler, B. Vogelstein, R. H. Hruban, A. Maitra, N. Papadopoulos, and A. K. Meeker. 2011. 'Altered telomeres in tumors with ATRX and DAXX mutations', *Science*, 333: 425.
Helton, E. S., and X. Chen. 2007. 'p53 modulation of the DNA damage response', *J Cell Biochem*, 100: 883-96.
Hemann, M. T., M. A. Strong, L. Y. Hao, and C. W. Greider. 2001. 'The shortest telomere, not average telomere length, is critical for cell viability and chromosome stability', *Cell*, 107: 67-77.
Henle, E. S., and S. Linn. 1997. 'Formation, prevention, and repair of DNA damage by iron/hydrogen peroxide', *J Biol Chem*, 272: 19095-8.
Henson, J. D., Y. Cao, L. I. Huschtscha, A. C. Chang, A. Y. Au, H. A. Pickett, and R. R. Reddel. 2009. 'DNA C-circles are specific and quantifiable markers of alternative-lengthening-of-telomeres activity', *Nat Biotechnol*, 27: 1181-5.
Henson, J. D., J. A. Hannay, S. W. McCarthy, J. A. Royds, T. R. Yeager, R. A. Robinson, S. B. Wharton, D. A. Jellinek, S. M. Arbuckle, J. Yoo, B. G. Robinson, D. L. Learoyd, P. D. Stalley, S. F. Bonar, D. Yu, R. E. Pollock, and

R. R. Reddel. 2005. 'A robust assay for alternative lengthening of telomeres in tumors shows the significance of alternative lengthening of telomeres in sarcomas and astrocytomas', *Clin Cancer Res*, 11: 217-25.
Henson, J. D., L. M. Lau, S. Koch, N. Martin La Rotta, R. A. Dagg, and R. R. Reddel. 2017. 'The C-Circle Assay for alternative-lengthening-of-telomeres activity', *Methods*, 114: 74-84.
Henson, J. D., A. A. Neumann, T. R. Yeager, and R. R. Reddel. 2002. 'Alternative lengthening of telomeres in mammalian cells', *Oncogene*, 21: 598-610.
Henson, J. D., and R. R. Reddel. 2010. 'Assaying and investigating Alternative Lengthening of Telomeres activity in human cells and cancers', *FEBS Lett*, 584: 3800-11.
Herbig, U., W. A. Jobling, B. P. Chen, D. J. Chen, and J. M. Sedivy. 2004. 'Telomere shortening triggers senescence of human cells through a pathway involving ATM, p53, and p21(CIP1), but not p16(INK4a)', *Mol Cell*, 14: 501-13.
Hockemeyer, D., J. P. Daniels, H. Takai, and T. de Lange. 2006. 'Recent expansion of the telomeric complex in rodents: Two distinct POT1 proteins protect mouse telomeres', *Cell*, 126: 63-77.
Hockemeyer, D., A. J. Sfeir, J. W. Shay, W. E. Wright, and T. de Lange. 2005. 'POT1 protects telomeres from a transient DNA damage response and determines how human chromosomes end', *EMBO J*, 24: 2667-78.
Holliday, R. 1964. 'The Induction of Mitotic Recombination by Mitomycin C in Ustilago and Saccharomyces', *Genetics*, 50: 323-35.
Hopfner, K. P., L. Craig, G. Moncalian, R. A. Zinkel, T. Usui, B. A. Owen, A. Karcher, B. Henderson, J. L. Bodmer, C. T. McMurray, J. P. Carney, J. H. Petrini, and J. A. Tainer. 2002. 'The Rad50 zinc-hook is a structure joining Mre11 complexes in DNA recombination and repair', *Nature*, 418: 562-6.
Hsu, H. L., D. Gilley, E. H. Blackburn, and D. J. Chen. 1999. 'Ku is associated with the telomere in mammals', *Proc Natl Acad Sci U S A*, 96: 12454-8.
Hsu, H. L., D. Gilley, S. A. Galande, M. P. Hande, B. Allen, S. H. Kim, G. C. Li, J. Campisi, T. Kohwi-Shigematsu, and D. J. Chen. 2000. 'Ku acts in a unique way at the mammalian telomere to prevent end joining', *Genes Dev*, 14: 2807-12.
Huffman, K. E., S. D. Levene, V. M. Tesmer, J. W. Shay, and W. E. Wright. 2000. 'Telomere shortening is proportional to the size of the G-rich telomeric 3'-overhang', *J Biol Chem*, 275: 19719-22.
Inciarte, M. R., M. Salas, and J. M. Sogo. 1980. 'Structure of replicating DNA molecules of Bacillus subtilis bacteriophage phi 29', *J Virol*, 34: 187-99.
Ip, S. C., U. Rass, M. G. Blanco, H. R. Flynn, J. M. Skehel, and S. C. West. 2008. 'Identification of Holliday junction resolvases from humans and yeast', *Nature*, 456: 357-61.
Ira, G., A. Pellicioli, A. Balijja, X. Wang, S. Fiorani, W. Carotenuto, G. Liberi, D. Bressan, L. Wan, N. M. Hollingsworth, J. E. Haber, and M. Foiani. 2004. 'DNA end resection, homologous recombination and DNA damage checkpoint activation require CDK1', *Nature*, 431: 1011-7.
Iwano, T., M. Tachibana, M. Reth, and Y. Shinkai. 2004. 'Importance of TRF1 for functional telomere structure', *J Biol Chem*, 279: 1442-8.
Jazayeri, A., J. Falck, C. Lukas, J. Bartek, G. C. Smith, J. Lukas, and S. P. Jackson. 2006. 'ATM- and cell cycle-dependent regulation of ATR in response to DNA double-strand breaks', *Nat Cell Biol*, 8: 37-45.
Jiang, W. Q., Z. H. Zhong, J. D. Henson, A. A. Neumann, A. C. Chang, and R. R. Reddel. 2005. 'Suppression of alternative lengthening of telomeres by Sp100-mediated sequestration of the MRE11/RAD50/NBS1 complex', *Mol Cell Biol*, 25: 2708-21.

Johnson, R. D., and M. Jasin. 2001. 'Double-strand-break-induced homologous recombination in mammalian cells', *Biochem Soc Trans*, 29: 196-201.
Joksic, I., D. Vujic, M. Guc-Scekic, A. Leskovac, S. Petrovic, M. Ojani, J. P. Trujillo, J. Surralles, M. Zivkovic, A. Stankovic, P. Slijepcevic, and G. Joksic. 2012. 'Dysfunctional telomeres in primary cells from Fanconi anemia FANCD2 patients', *Genome Integr*, 3: 6.
Karlseder, J., D. Broccoli, Y. Dai, S. Hardy, and T. de Lange. 1999. 'p53- and ATM-dependent apoptosis induced by telomeres lacking TRF2', *Science*, 283: 1321-5.
Kim, S. H., P. Kaminker, and J. Campisi. 1999. 'TIN2, a new regulator of telomere length in human cells', *Nat Genet*, 23: 405-12.
Kipling, D., and H. J. Cooke. 1990. 'Hypervariable ultra-long telomeres in mice', *Nature*, 347: 400-2.
Kleinschmidt, AK, and RK Zahn. 1959. 'Uber desoxyribonucleinsauremolekuln in protein mischfilmen', *Z Naturforsch B 14*: 770–79.
Konishi, A., and T. de Lange. 2008. 'Cell cycle control of telomere protection and NHEJ revealed by a ts mutation in the DNA-binding domain of TRF2', *Genes Dev*, 22: 1221-30.
Kosa, P., M. Valach, L. Tomaska, K. H. Wolfe, and J. Nosek. 2006. 'Complete DNA sequences of the mitochondrial genomes of the pathogenic yeasts Candida orthopsilosis and Candida metapsilosis: insight into the evolution of linear DNA genomes from mitochondrial telomere mutants', *Nucleic Acids Res*, 34: 2472-81.
Kovac, L., J. Lazowska, and P. P. Slonimski. 1984. 'A yeast with linear molecules of mitochondrial DNA', *Mol Gen Genet*, 197: 420-4.
Kumagai, A., J. Lee, H. Y. Yoo, and W. G. Dunphy. 2006. 'TopBP1 activates the ATR-ATRIP complex', *Cell*, 124: 943-55.
Lee, H. W., M. A. Blasco, G. J. Gottlieb, J. W. Horner, 2nd, C. W. Greider, and R. A. DePinho. 1998. 'Essential role of mouse telomerase in highly proliferative organs', *Nature*, 392: 569-74.
Lee, J. H., and T. T. Paull. 2005. 'ATM activation by DNA double-strand breaks through the Mre11-Rad50-Nbs1 complex', *Science*, 308: 551-4.
Lee-Theilen, M., A. J. Matthews, D. Kelly, S. Zheng, and J. Chaudhuri. 2011. 'CtIP promotes microhomology-mediated alternative end joining during class-switch recombination', *Nat Struct Mol Biol*, 18: 75-9.
Lenain, C., S. Bauwens, S. Amiard, M. Brunori, M. J. Giraud-Panis, and E. Gilson. 2006. 'The Apollo 5' exonuclease functions together with TRF2 to protect telomeres from DNA repair', *Curr Biol*, 16: 1303-10.
Li, B., and A. J. Lustig. 1996. 'A novel mechanism for telomere size control in Saccharomyces cerevisiae', *Genes Dev*, 10: 1310-26.
Li, B., S. Oestreich, and T. de Lange. 2000. 'Identification of human Rap1: implications for telomere evolution', *Cell*, 101: 471-83.
Li, J. S., J. Miralles Fuste, T. Simavorian, C. Bartocci, J. Tsai, J. Karlseder, and E. Lazzerini Denchi. 2017. 'TZAP: A telomere-associated protein involved in telomere length control', *Science*, 355: 638-41.
Liu, Y., J. Y. Masson, R. Shah, P. O'Regan, and S. C. West. 2004. 'RAD51C is required for Holliday junction processing in mammalian cells', *Science*, 303: 243-6.
Londono-Vallejo, J. A., H. Der-Sarkissian, L. Cazes, S. Bacchetti, and R. R. Reddel. 2004. 'Alternative lengthening of telomeres is characterized by high rates of telomeric exchange', *Cancer Res*, 64: 2324-7.
Lopes, M. 2009. 'Electron microscopy methods for studying in vivo DNA replication intermediates', *Methods Mol Biol*, 521: 605-31.

Lopes, M., C. Cotta-Ramusino, A. Pellicioli, G. Liberi, P. Plevani, M. Muzi-Falconi, C. S. Newlon, and M. Foiani. 2001. 'The DNA replication checkpoint response stabilizes stalled replication forks', *Nature*, 412: 557-61.

Lovejoy, C. A., W. Li, S. Reisenweber, S. Thongthip, J. Bruno, T. de Lange, S. De, J. H. Petrini, P. A. Sung, M. Jasin, J. Rosenbluh, Y. Zwang, B. A. Weir, C. Hatton, E. Ivanova, L. Macconaill, M. Hanna, W. C. Hahn, N. F. Lue, R. R. Reddel, Y. Jiao, K. Kinzler, B. Vogelstein, N. Papadopoulos, A. K. Meeker, and A. L. T. Starr Cancer Consortium. 2012. 'Loss of ATRX, genome instability, and an altered DNA damage response are hallmarks of the alternative lengthening of telomeres pathway', *PLoS Genet*, 8: e1002772.

Lucchini, R., and J. M. Sogo. 1995. 'Replication of transcriptionally active chromatin', *Nature*, 374: 276-80.

Lundblad, V., and E. H. Blackburn. 1993. 'An alternative pathway for yeast telomere maintenance rescues est1- senescence', *Cell*, 73: 347-60.

Lundblad, V., and J. W. Szostak. 1989. 'A mutant with a defect in telomere elongation leads to senescence in yeast', *Cell*, 57: 633-43.

Lustig, A. J. 2003. 'Clues to catastrophic telomere loss in mammals from yeast telomere rapid deletion', *Nat Rev Genet*, 4: 916-23.

Maciejowski, J., and T. de Lange. 2017. 'Telomeres in cancer: tumour suppression and genome instability', *Nat Rev Mol Cell Biol*, 18: 175-86.

Maciejowski, J., Y. Li, N. Bosco, P. J. Campbell, and T. de Lange. 2015. 'Chromothripsis and Kataegis Induced by Telomere Crisis', *Cell*, 163: 1641-54.

Malkova, A., E. L. Ivanov, and J. E. Haber. 1996. 'Double-strand break repair in the absence of RAD51 in yeast: a possible role for break-induced DNA replication', *Proc Natl Acad Sci U S A*, 93: 7131-6.

Margalef, P., P. Kotsantis, V. Borel, R. Bellelli, S. Panier, and S. J. Boulton. 2018. 'Stabilization of Reversed Replication Forks by Telomerase Drives Telomere Catastrophe', *Cell*, 172: 439-53 e14.

Martinez, P., M. Thanasoula, P. Munoz, C. Liao, A. Tejera, C. McNees, J. M. Flores, O. Fernandez-Capetillo, M. Tarsounas, and M. A. Blasco. 2009. 'Increased telomere fragility and fusions resulting from TRF1 deficiency lead to degenerative pathologies and increased cancer in mice', *Genes Dev*, 23: 2060-75.

Matsuoka, S., B. A. Ballif, A. Smogorzewska, E. R. McDonald, 3rd, K. E. Hurov, J. Luo, C. E. Bakalarski, Z. Zhao, N. Solimini, Y. Lerenthal, Y. Shiloh, S. P. Gygi, and S. J. Elledge. 2007. 'ATM and ATR substrate analysis reveals extensive protein networks responsive to DNA damage', *Science*, 316: 1160-6.

Matsuoka, S., M. Huang, and S. J. Elledge. 1998. 'Linkage of ATM to cell cycle regulation by the Chk2 protein kinase', *Science*, 282: 1893-7.

Mazzucco, G., A. Huda, M. Galli, D. Piccini, M. Giannattasio, F. Pessina, and Y. Doksani. 2020. 'Telomere damage induces internal loops that generate telomeric circles', *Nat Commun*, 11: 5297.

McClintock, B. 1939. 'The Behavior in Successive Nuclear Divisions of a Chromosome Broken at Meiosis', *Proc Natl Acad Sci U S A*, 25: 405-16.

———. 1941. 'The Stability of Broken Ends of Chromosomes in Zea Mays', *Genetics*, 26: 234-82.

Miller, K. M., O. Rog, and J. P. Cooper. 2006. 'Semi-conservative DNA replication through telomeres requires Taz1', *Nature*, 440: 824-8.

Min, J., W. E. Wright, and J. W. Shay. 2017. 'Alternative Lengthening of Telomeres Mediated by Mitotic DNA Synthesis Engages Break-Induced Replication Processes', *Mol Cell Biol*, 37.

Munoz, I. M., K. Hain, A. C. Declais, M. Gardiner, G. W. Toh, L. Sanchez-Pulido, J. M. Heuckmann, R. Toth, T. Macartney, B. Eppink, R. Kanaar, C. P. Ponting, D. M. Lilley, and J. Rouse. 2009. 'Coordination of structure-specific nucleases by human SLX4/BTBD12 is required for DNA repair', *Mol Cell*, 35: 116-27.

Munoz-Jordan, J. L., G. A. Cross, T. de Lange, and J. D. Griffith. 2001. 't-loops at trypanosome telomeres', *EMBO J*, 20: 579-88.

Munro, J., K. Steeghs, V. Morrison, H. Ireland, and E. K. Parkinson. 2001. 'Human fibroblast replicative senescence can occur in the absence of extensive cell division and short telomeres', *Oncogene*, 20: 3541-52.

Muntoni, A., A. A. Neumann, M. Hills, and R. R. Reddel. 2009. 'Telomere elongation involves intra-molecular DNA replication in cells utilizing alternative lengthening of telomeres', *Hum Mol Genet*, 18: 1017-27.

Murnane, J. P. 2006. 'Telomeres and chromosome instability', *DNA Repair (Amst)*, 5: 1082-92.

Murnane, J. P., L. Sabatier, B. A. Marder, and W. F. Morgan. 1994. 'Telomere dynamics in an immortal human cell line', *EMBO J*, 13: 4953-62.

Murti, K. G., and D. M. Prescott. 1999. 'Telomeres of polytene chromosomes in a ciliated protozoan terminate in duplex DNA loops', *Proc Natl Acad Sci U S A*, 96: 14436-9.

Nabetani, A., and F. Ishikawa. 2009. 'Unusual telomeric DNAs in human telomerase-negative immortalized cells', *Mol Cell Biol*, 29: 703-13.

Napier, C. E., L. I. Huschtscha, A. Harvey, K. Bower, J. R. Noble, E. A. Hendrickson, and R. R. Reddel. 2015. 'ATRX represses alternative lengthening of telomeres', *Oncotarget*, 6: 16543-58.

Nassif, N., J. Penney, S. Pal, W. R. Engels, and G. B. Gloor. 1994. 'Efficient copying of nonhomologous sequences from ectopic sites via P-element-induced gap repair', *Mol Cell Biol*, 14: 1613-25.

Natarajan, S., C. Groff-Vindman, and M. J. McEachern. 2003. 'Factors influencing the recombinational expansion and spread of telomeric tandem arrays in Kluyveromyces lactis', *Eukaryot Cell*, 2: 1115-27.

Natarajan, S., and M. J. McEachern. 2002. 'Recombinational telomere elongation promoted by DNA circles', *Mol Cell Biol*, 22: 4512-21.

Nawotka, K. A., and J. A. Huberman. 1988. 'Two-dimensional gel electrophoretic method for mapping DNA replicons', *Mol Cell Biol*, 8: 1408-13.

Neal, J. A., and K. Meek. 2011. 'Choosing the right path: does DNA-PK help make the decision?', *Mutat Res*, 711: 73-86.

Nikitina, T., and C. L. Woodcock. 2004. 'Closed chromatin loops at the ends of chromosomes', *J Cell Biol*, 166: 161-5.

Nosek, J., N. Dinouel, L. Kovac, and H. Fukuhara. 1995. 'Linear mitochondrial DNAs from yeasts: telomeres with large tandem repetitions', *Mol Gen Genet*, 247: 61-72.

Nosek, J., A. Rycovska, A. M. Makhov, J. D. Griffith, and L. Tomaska. 2005. 'Amplification of telomeric arrays via rolling-circle mechanism', *J Biol Chem*, 280: 10840-5.

O'Sullivan, R. J., N. Arnoult, D. H. Lackner, L. Oganesian, C. Haggblom, A. Corpet, G. Almouzni, and J. Karlseder. 2014. 'Rapid induction of alternative lengthening of telomeres by depletion of the histone chaperone ASF1', *Nat Struct Mol Biol*, 21: 167-74.

Oppenheim, A. 1981. 'Separation of closed circular DNA from linear DNA by electrophoresis in two dimensions in agarose gels', *Nucleic Acids Res*, 9: 6805-12.

Opresko, P. L., C. von Kobbe, J. P. Laine, J. Harrigan, I. D. Hickson, and V. A. Bohr. 2002. 'Telomere-binding protein TRF2 binds to and stimulates the Werner and Bloom syndrome helicases', *J Biol Chem*, 277: 41110-9.

Paddock, M. N., A. T. Bauman, R. Higdon, E. Kolker, S. Takeda, and A. M. Scharenberg. 2011. 'Competition between PARP-1 and Ku70 control the decision between high-fidelity and mutagenic DNA repair', *DNA Repair (Amst)*, 10: 338-43.

Palm, W., and T. de Lange. 2008. 'How shelterin protects mammalian telomeres', *Annu Rev Genet*, 42: 301-34.

Panier, S., M. Maric, G. Hewitt, E. Mason-Osann, H. Gali, A. Dai, A. Labadorf, J. H. Guervilly, P. Ruis, S. Segura-Bayona, O. Belan, P. Marzec, P. L. Gaillard, R. L. Flynn, and S. J. Boulton. 2019. 'SLX4IP Antagonizes Promiscuous BLM Activity during ALT Maintenance', *Mol Cell*, 76: 27-43 e11.

Petersen, S., G. Saretzki, and T. von Zglinicki. 1998. 'Preferential accumulation of single-stranded regions in telomeres of human fibroblasts', *Exp Cell Res*, 239: 152-60.

Pickett, H. A., A. J. Cesare, R. L. Johnston, A. A. Neumann, and R. R. Reddel. 2009. 'Control of telomere length by a trimming mechanism that involves generation of t-circles', *EMBO J*, 28: 799-809.

Pickett, H. A., J. D. Henson, A. Y. Au, A. A. Neumann, and R. R. Reddel. 2011. 'Normal mammalian cells negatively regulate telomere length by telomere trimming', *Hum Mol Genet*, 20: 4684-92.

Pierce, A. J., R. D. Johnson, L. H. Thompson, and M. Jasin. 1999. 'XRCC3 promotes homology-directed repair of DNA damage in mammalian cells', *Genes Dev*, 13: 2633-8.

Pipkin, M. E., and M. G. Lichtenheld. 2006. 'A reliable method to display authentic DNase I hypersensitive sites at long-ranges in single-copy genes from large genomes', *Nucleic Acids Res*, 34: e34.

Potts, P. R., and H. Yu. 2007. 'The SMC5/6 complex maintains telomere length in ALT cancer cells through SUMOylation of telomere-binding proteins', *Nat Struct Mol Biol*, 14: 581-90.

Qi, L., M. A. Strong, B. O. Karim, M. Armanios, D. L. Huso, and C. W. Greider. 2003. 'Short telomeres and ataxia-telangiectasia mutated deficiency cooperatively increase telomere dysfunction and suppress tumorigenesis', *Cancer Res*, 63: 8188-96.

Raices, M., R. E. Verdun, S. A. Compton, C. I. Haggblom, J. D. Griffith, A. Dillin, and J. Karlseder. 2008. 'C. elegans telomeres contain G-strand and C-strand overhangs that are bound by distinct proteins', *Cell*, 132: 745-57.

Rass, E., A. Grabarz, I. Plo, J. Gautier, P. Bertrand, and B. S. Lopez. 2009. 'Role of Mre11 in chromosomal nonhomologous end joining in mammalian cells', *Nat Struct Mol Biol*, 16: 819-24.

Rass, U., S. A. Compton, J. Matos, M. R. Singleton, S. C. Ip, M. G. Blanco, J. D. Griffith, and S. C. West. 2010. 'Mechanism of Holliday junction resolution by the human GEN1 protein', *Genes Dev*, 24: 1559-69.

Reddel, R. R. 2000. 'The role of senescence and immortalization in carcinogenesis', *Carcinogenesis*, 21: 477-84.

Regev, A., S. Cohen, E. Cohen, I. Bar-Am, and S. Lavi. 1998. 'Telomeric repeats on small polydisperse circular DNA (spcDNA) and genomic instability', *Oncogene*, 17: 3455-61.

Riballo, E., L. Woodbine, T. Stiff, S. A. Walker, A. A. Goodarzi, and P. A. Jeggo. 2009. 'XLF-Cernunnos promotes DNA ligase IV-XRCC4 re-adenylation following ligation', *Nucleic Acids Res*, 37: 482-92.

Riley, D. E. 1980. 'Deoxyribonuclease I generates single-stranded gaps in chromatin deoxyribonucleic acid', *Biochemistry*, 19: 2977-92.
Rivera, T., C. Haggblom, S. Cosconati, and J. Karlseder. 2017. 'A balance between elongation and trimming regulates telomere stability in stem cells', *Nat Struct Mol Biol*, 24: 30-39.
Rodier, F., J. P. Coppe, C. K. Patil, W. A. Hoeijmakers, D. P. Munoz, S. R. Raza, A. Freund, E. Campeau, A. R. Davalos, and J. Campisi. 2009. 'Persistent DNA damage signalling triggers senescence-associated inflammatory cytokine secretion', *Nat Cell Biol*, 11: 973-9.
Rodier, F., D. P. Munoz, R. Teachenor, V. Chu, O. Le, D. Bhaumik, J. P. Coppe, E. Campeau, C. M. Beausejour, S. H. Kim, A. R. Davalos, and J. Campisi. 2011. 'DNA-SCARS: distinct nuclear structures that sustain damage-induced senescence growth arrest and inflammatory cytokine secretion', *J Cell Sci*, 124: 68-81.
Rogakou, E. P., D. R. Pilch, A. H. Orr, V. S. Ivanova, and W. M. Bonner. 1998. 'DNA double-stranded breaks induce histone H2AX phosphorylation on serine 139', *J Biol Chem*, 273: 5858-68.
Rogan, E. M., T. M. Bryan, B. Hukku, K. Maclean, A. C. Chang, E. L. Moy, A. Englezou, S. G. Warneford, L. Dalla-Pozza, and R. R. Reddel. 1995. 'Alterations in p53 and p16INK4 expression and telomere length during spontaneous immortalization of Li-Fraumeni syndrome fibroblasts', *Mol Cell Biol*, 15: 4745-53.
Rothkamm, K., I. Kruger, L. H. Thompson, and M. Lobrich. 2003. 'Pathways of DNA double-strand break repair during the mammalian cell cycle', *Mol Cell Biol*, 23: 5706-15.
Rudolph, K. L., S. Chang, H. W. Lee, M. Blasco, G. J. Gottlieb, C. Greider, and R. A. DePinho. 1999. 'Longevity, stress response, and cancer in aging telomerase-deficient mice', *Cell*, 96: 701-12.
Rycovska, A., M. Valach, L. Tomaska, M. Bolotin-Fukuhara, and J. Nosek. 2004. 'Linear versus circular mitochondrial genomes: intraspecies variability of mitochondrial genome architecture in Candida parapsilosis', *Microbiology (Reading)*, 150: 1571-80.
Saint-Leger, A., M. Koelblen, L. Civitelli, A. Bah, N. Djerbi, M. J. Giraud-Panis, A. Londono-Vallejo, F. Ascenzioni, and E. Gilson. 2014. 'The basic N-terminal domain of TRF2 limits recombination endonuclease action at human telomeres', *Cell Cycle*, 13: 2469-74.
Sanchez, Y., C. Wong, R. S. Thoma, R. Richman, Z. Wu, H. Piwnica-Worms, and S. J. Elledge. 1997. 'Conservation of the Chk1 checkpoint pathway in mammals: linkage of DNA damage to Cdk regulation through Cdc25', *Science*, 277: 1497-501.
Sarek, G., J. B. Vannier, S. Panier, J. H. Petrini, and S. J. Boulton. 2015. 'TRF2 recruits RTEL1 to telomeres in S phase to promote t-loop unwinding', *Mol Cell*, 57: 622-35.
Sarkar, J., and Y. Liu. 2016. 'Fanconi anemia proteins in telomere maintenance', *DNA Repair (Amst)*, 43: 107-12.
Sarkar, J., B. Wan, J. Yin, H. Vallabhaneni, K. Horvath, T. Kulikowicz, V. A. Bohr, Y. Zhang, M. Lei, and Y. Liu. 2015. 'SLX4 contributes to telomere preservation and regulated processing of telomeric joint molecule intermediates', *Nucleic Acids Res*, 43: 5912-23.
Schmutz, I., L. Timashev, W. Xie, D. J. Patel, and T. de Lange. 2017. 'TRF2 binds branched DNA to safeguard telomere integrity', *Nat Struct Mol Biol*, 24: 734-42.

Seifert, F. U., K. Lammens, G. Stoehr, B. Kessler, and K. P. Hopfner. 2016. 'Structural mechanism of ATP-dependent DNA binding and DNA end bridging by eukaryotic Rad50', *EMBO J*, 35: 759-72.
Sethi, I., G. R. Bhat, R. Kumar, E. Rai, and S. Sharma. 2021. 'Dual labeled fluorescence probe based qPCR assay to measure the telomere length', *Gene*, 767: 145178.
Sfeir, A, and T de Lange. 2012. 'Removal of shelterin reveals the telomere end-protection problem.', *Science*, 336: 593-7.
Sfeir, A. J., W. Chai, J. W. Shay, and W. E. Wright. 2005. 'Telomere-end processing the terminal nucleotides of human chromosomes', *Mol Cell*, 18: 131-8.
Sfeir, A., S. T. Kosiyatrakul, D. Hockemeyer, S. L. MacRae, J. Karlseder, C. L. Schildkraut, and T. de Lange. 2009. 'Mammalian telomeres resemble fragile sites and require TRF1 for efficient replication', *Cell*, 138: 90-103.
Shay, J. W., and S. Bacchetti. 1997. 'A survey of telomerase activity in human cancer', *Eur J Cancer*, 33: 787-91.
Shieh, S. Y., J. Ahn, K. Tamai, Y. Taya, and C. Prives. 2000. 'The human homologs of checkpoint kinases Chk1 and Cds1 (Chk2) phosphorylate p53 at multiple DNA damage-inducible sites', *Genes Dev*, 14: 289-300.
Simsek, D., E. Brunet, S. Y. Wong, S. Katyal, Y. Gao, P. J. McKinnon, J. Lou, L. Zhang, J. Li, E. J. Rebar, P. D. Gregory, M. C. Holmes, and M. Jasin. 2011. 'DNA ligase III promotes alternative nonhomologous end-joining during chromosomal translocation formation', *PLoS Genet*, 7: e1002080.
Simsek, D., and M. Jasin. 2010. 'Alternative end-joining is suppressed by the canonical NHEJ component Xrcc4-ligase IV during chromosomal translocation formation', *Nat Struct Mol Biol*, 17: 410-6.
Sinclair, D. A., and L. Guarente. 1997. 'Extrachromosomal rDNA circles--a cause of aging in yeast', *Cell*, 91: 1033-42.
Sitte, N., G. Saretzki, and T. von Zglinicki. 1998. 'Accelerated telomere shortening in fibroblasts after extended periods of confluency', *Free Radic Biol Med*, 24: 885-93.
Smith, J. R., and R. G. Whitney. 1980. 'Intraclonal variation in proliferative potential of human diploid fibroblasts: stochastic mechanism for cellular aging', *Science*, 207: 82-4.
Smogorzewska, A., J. Karlseder, H. Holtgreve-Grez, A. Jauch, and T. de Lange. 2002. 'DNA ligase IV-dependent NHEJ of deprotected mammalian telomeres in G1 and G2', *Curr Biol*, 12: 1635-44.
Sogo, J. M., H. Stahl, T. Koller, and R. Knippers. 1986. 'Structure of replicating simian virus 40 minichromosomes. The replication fork, core histone segregation and terminal structures', *J Mol Biol*, 189: 189-204.
Stansel, R. M., T. de Lange, and J. D. Griffith. 2001. 'T-loop assembly in vitro involves binding of TRF2 near the 3' telomeric overhang', *EMBO J*, 20: 5532-40.
Stewart, G. S., R. S. Maser, T. Stankovic, D. A. Bressan, M. I. Kaplan, N. G. Jaspers, A. Raams, P. J. Byrd, J. H. Petrini, and A. M. Taylor. 1999. 'The DNA double-strand break repair gene hMRE11 is mutated in individuals with an ataxia-telangiectasia-like disorder', *Cell*, 99: 577-87.
Svendsen, J. M., A. Smogorzewska, M. E. Sowa, B. C. O'Connell, S. P. Gygi, S. J. Elledge, and J. W. Harper. 2009. 'Mammalian BTBD12/SLX4 assembles a Holliday junction resolvase and is required for DNA repair', *Cell*, 138: 63-77.
Szostak, J. W., T. L. Orr-Weaver, R. J. Rothstein, and F. W. Stahl. 1983. 'The double-strand-break repair model for recombination', *Cell*, 33: 25-35.
Takai, H., A. Smogorzewska, and T. de Lange. 2003. 'DNA damage foci at dysfunctional telomeres', *Curr Biol*, 13: 1549-56.

Takai, K. K., S. Hooper, S. Blackwood, R. Gandhi, and T. de Lange. 2010. 'In vivo stoichiometry of shelterin components', *J Biol Chem*, 285: 1457-67.
Tercero, J. A., and J. F. Diffley. 2001. 'Regulation of DNA replication fork progression through damaged DNA by the Mec1/Rad53 checkpoint', *Nature*, 412: 553-7.
Tibbetts, R. S., K. M. Brumbaugh, J. M. Williams, J. N. Sarkaria, W. A. Cliby, S. Y. Shieh, Y. Taya, C. Prives, and R. T. Abraham. 1999. 'A role for ATR in the DNA damage-induced phosphorylation of p53', *Genes Dev*, 13: 152-7.
Timashev, L. A., and T. De Lange. 2020. 'Characterization of t-loop formation by TRF2', *Nucleus*, 11: 164-77.
Tomaska, L., J. Nosek, and H. Fukuhara. 1997. 'Identification of a putative mitochondrial telomere-binding protein of the yeast Candida parapsilosis', *J Biol Chem*, 272: 3049-56.
Tomaska, L., J. Nosek, J. Kramara, and J. D. Griffith. 2009. 'Telomeric circles: universal players in telomere maintenance?', *Nat Struct Mol Biol*, 16: 1010-5.
Tomaska, L., J. Nosek, A. M. Makhov, A. Pastorakova, and J. D. Griffith. 2000. 'Extragenomic double-stranded DNA circles in yeast with linear mitochondrial genomes: potential involvement in telomere maintenance', *Nucleic Acids Res*, 28: 4479-87.
Uziel, T., Y. Lerenthal, L. Moyal, Y. Andegeko, L. Mittelman, and Y. Shiloh. 2003. 'Requirement of the MRN complex for ATM activation by DNA damage', *EMBO J*, 22: 5612-21.
van Overbeek, M., and T. de Lange. 2006. 'Apollo, an Artemis-related nuclease, interacts with TRF2 and protects human telomeres in S phase', *Curr Biol*, 16: 1295-302.
van Steensel, B, A Smogorzewska, and T de Lange. 1998. 'TRF2 protects human telomeres from end-to-end fusions', *Cell*, 92: 401-13.
Vannier, J. B., V. Pavicic-Kaltenbrunner, M. I. Petalcorin, H. Ding, and S. J. Boulton. 2012. 'RTEL1 dismantles T loops and counteracts telomeric G4-DNA to maintain telomere integrity', *Cell*, 149: 795-806.
Varley, H., H. A. Pickett, J. L. Foxon, R. R. Reddel, and N. J. Royle. 2002. 'Molecular characterization of inter-telomere and intra-telomere mutations in human ALT cells', *Nat Genet*, 30: 301-5.
Verma, P., R. L. Dilley, T. Zhang, M. T. Gyparaki, Y. Li, and R. A. Greenberg. 2019. 'RAD52 and SLX4 act nonepistatically to ensure telomere stability during alternative telomere lengthening', *Genes Dev*, 33: 221-35.
Villwock, S. K., and O. M. Aparicio. 2014. 'Two-dimensional agarose gel electrophoresis for analysis of DNA replication', *Methods Mol Biol*, 1205: 329-40.
von Zglinicki, T. 2000. 'Role of oxidative stress in telomere length regulation and replicative senescence', *Ann N Y Acad Sci*, 908: 99-110.
———. 2002. 'Oxidative stress shortens telomeres', *Trends Biochem Sci*, 27: 339-44.
von Zglinicki, T., G. Saretzki, W. Docke, and C. Lotze. 1995. 'Mild hyperoxia shortens telomeres and inhibits proliferation of fibroblasts: a model for senescence?', *Exp Cell Res*, 220: 186-93.
Vousden, K. H., and D. P. Lane. 2007. 'p53 in health and disease', *Nat Rev Mol Cell Biol*, 8: 275-83.
Wang, F., J. A. Stewart, C. Kasbek, Y. Zhao, W. E. Wright, and C. M. Price. 2012. 'Human CST has independent functions during telomere duplex replication and C-strand fill-in', *Cell Rep*, 2: 1096-103.

Wang, P. Y., N. Neretti, R. Whitaker, S. Hosier, C. Chang, D. Lu, B. Rogina, and S. L. Helfand. 2009. 'Long-lived Indy and calorie restriction interact to extend life span', *Proc Natl Acad Sci U S A*, 106: 9262-7.

Wang, R. C., A. Smogorzewska, and T. de Lange. 2004. 'Homologous recombination generates T-loop-sized deletions at human telomeres', *Cell*, 119: 355-68.

Weis, J. H., and T. Quertermous. 2001. 'Size fractionation using sucrose gradients', *Curr Protoc Mol Biol*, Chapter 5: Unit5 3.

Wellinger, R. E., and J. M. Sogo. 1998. 'In vivo mapping of nucleosomes using psoralen-DNA crosslinking and primer extension', *Nucleic Acids Res*, 26: 1544-5.

West, S. C., M. G. Blanco, Y. W. Chan, J. Matos, S. Sarbajna, and H. D. Wyatt. 2015. 'Resolution of Recombination Intermediates: Mechanisms and Regulation', *Cold Spring Harb Symp Quant Biol*, 80: 103-9.

Williams, G. J., S. P. Lees-Miller, and J. A. Tainer. 2010. 'Mre11-Rad50-Nbs1 conformations and the control of sensing, signaling, and effector responses at DNA double-strand breaks', *DNA Repair (Amst)*, 9: 1299-306.

Wu, L., and I. D. Hickson. 2003. 'The Bloom's syndrome helicase suppresses crossing over during homologous recombination', *Nature*, 426: 870-4.

Wu, L., A. S. Multani, H. He, W. Cosme-Blanco, Y. Deng, J. M. Deng, O. Bachilo, S. Pathak, H. Tahara, S. M. Bailey, Y. Deng, R. R. Behringer, and S. Chang. 2006. 'Pot1 deficiency initiates DNA damage checkpoint activation and aberrant homologous recombination at telomeres', *Cell*, 126: 49-62.

Wu, P., H. Takai, and T. de Lange. 2012. 'Telomeric 3' overhangs derive from resection by Exo1 and Apollo and fill-in by POT1b-associated CST', *Cell*, 150: 39-52.

Wu, P., M. van Overbeek, S. Rooney, and T. de Lange. 2010. 'Apollo contributes to G overhang maintenance and protects leading-end telomeres', *Mol Cell*, 39: 606-17.

Wyatt, H. D., S. Sarbajna, J. Matos, and S. C. West. 2013. 'Coordinated actions of SLX1-SLX4 and MUS81-EME1 for Holliday junction resolution in human cells', *Mol Cell*, 52: 234-47.

Xie, A., A. Kwok, and R. Scully. 2009. 'Role of mammalian Mre11 in classical and alternative nonhomologous end joining', *Nat Struct Mol Biol*, 16: 814-8.

Ye, J. Z., J. R. Donigian, M. van Overbeek, D. Loayza, Y. Luo, A. N. Krutchinsky, B. T. Chait, and T. de Lange. 2004. 'TIN2 binds TRF1 and TRF2 simultaneously and stabilizes the TRF2 complex on telomeres', *J Biol Chem*, 279: 47264-71.

Yeager, T. R., A. A. Neumann, A. Englezou, L. I. Huschtscha, J. R. Noble, and R. R. Reddel. 1999. 'Telomerase-negative immortalized human cells contain a novel type of promyelocytic leukemia (PML) body', *Cancer Res*, 59: 4175-9.

Zellinger, B., S. Akimcheva, J. Puizina, M. Schirato, and K. Riha. 2007. 'Ku suppresses formation of telomeric circles and alternative telomere lengthening in Arabidopsis', *Mol Cell*, 27: 163-9.

Zhang, J. M., T. Yadav, J. Ouyang, L. Lan, and L. Zou. 2019. 'Alternative Lengthening of Telomeres through Two Distinct Break-Induced Replication Pathways', *Cell Rep*, 26: 955-68 e3.

Zhao, Y., H. Hoshiyama, J. W. Shay, and W. E. Wright. 2008. 'Quantitative telomeric overhang determination using a double-strand specific nuclease', *Nucleic Acids Res*, 36: e14.

Zhong, Z., L. Shiue, S. Kaplan, and T. de Lange. 1992. 'A mammalian factor that binds telomeric TTAGGG repeats in vitro', *Mol Cell Biol*, 12: 4834-43.

Zhu, X. D., B. Kuster, M. Mann, J. H. Petrini, and T. de Lange. 2000. 'Cell-cycle-regulated association of RAD50/MRE11/NBS1 with TRF2 and human telomeres', *Nat Genet*, 25: 347-52.

Zimmermann, M., T. Kibe, S. Kabir, and T. de Lange. 2014. 'TRF1 negotiates TTAGGG repeat-associated replication problems by recruiting the BLM helicase and the TPP1/POT1 repressor of ATR signaling', *Genes Dev*, 28: 2477-91.

Zou, L., and S. J. Elledge. 2003. 'Sensing DNA damage through ATRIP recognition of RPA-ssDNA complexes', *Science*, 300: 1542-8.